NASA
Technical
Paper
1848

1987

Three-Step Labyrinth Seal for High-Performance Turbomachines

Robert C. Hendricks

Lewis Research Center
Cleveland, Ohio

NASA

National Aeronautics
and Space Administration

Scientific and Technical
Information Office

Contents

Summary

A three-step labyrinth seal with 12, 11, and 10 labyrinth teeth per step, respectively, at nominal diameters of 8.077, 7.976, and 7.874 cm (3.180, 3.140, and 3.100 in.) was tested. The configuration represented the seal for a high-performance turbopump (e.g., the space shuttle main engine fuel pump). All tests were conducted under *static* (*nonrotating*) conditions. The test data included critical mass flux and pressure profiles over a wide range of fluid conditions at concentric, partially eccentric, and fully eccentric positions.[1]

The seal mass fluxes for the various positions differed by at most 5 percent and for all practical purposes can be treated as unaltered by eccentric positioning. This was also found to be the case for straight and three-step cylindrical seals in similar configurations.

The pressure profiles of the three-step labyrinth seal differed significantly from those of the cylindrical seals. Although the circumferential pressure drop showed positive stiffness at the first tooth of each step, as expected, this was completely reversed (i.e., negative stiffness) by the time the flow reached the reservoirs between steps. Such crossovers in the axial pressure distribution can provide little if any positive direct stiffness, which is required for stability in this or any other seal configuration. Circumferential pressure drop in the expansion cavity of the first tooth of each step generally increased with eccentricity and inlet stagnation pressure, although magnitudes at eccentricities of one-third and less were difficult to measure because of the small differences, the limits of the instrumentation, and difficulties with geometric alignment.

The method of corresponding states was applied to the helium mass flux data, which were found to have a pressure dependency, part of which can be attributed to the simplicity of the normalized flow relation and part to nonlinear effects of expanding fluid helium. Data for helium followed the parahydrogen and nitrogen results provided that the normalized pressure dependency was divided by an empirical constant of 10.

The leakage-rate characteristics for the labyrinth seal are quite good, but seal response to dynamic conditions for stabilizing a turbomachine would be quite poor unless some preconditioning such as antiswirl were introduced.

[1]All of the data and information obtained from these tests was released for general use in May 1977.

Introduction

In the early phases of the space shuttle main engine program excessive leakage and vibration engendered catastrophic turbomachine failures that in many cases destroyed the entire apparatus. From the accident investigations it was postulated that the excessive vibrations were caused by the seals. However, the seal geometry and fluid conditions leading to such unstable operations were unknown. A low-leakage seal with good dynamic response, low power consumption, and low heat dissipation during a rub should be the goal of every high-performance seal design. Accordingly a program was begun to evaluate seals for the space shuttle main engine fuel turbopumps.

One of the early shuttle-turbopump seal designs centered around a three-step labyrinth flow-path configuration that looked much like a set of deep-cut serrations. The three steps had 12, 11, and 10 labyrinth teeth per step, respectively, in the direction of flow at nominal diameters of 8.077, 7.976, and 7.874 cm (3.180, 3.140, and 3.100 in.). Two such seals were instrumented early in the program in order to investigate leakage and pressure profiles in a *nonrotating*, or *static*, configuration. One (called used) had been run in a turbopump and exhibited significant evidence of rubbing. The second (called newly machined) may have been installed, but there was no evidence of rubbing and its operating history is unknown.

Although the used-labyrinth-seal configuration was well instrumented, subsequent measurements revealed several geometric malformations, particularly in clearance, that indicated that the leakage rates for choked flows were beyond the capability of the test facility. Several test runs were made with fluid nitrogen and hydrogen. These runs demonstrated that hydrogen leakage was significantly higher than 0.3 kg/s (2/3 lbm/s) and that the pressure drop was insufficient to choke the flow. The used and newly machined labyrinth seal configurations are described in the appendix.

As a result of these preliminary tests interest centered on straight and three-step cylindrical seals, which are discussed in detail in references 1 and 2. The three-step labyrinth seal was thought to be of only academic interest. It was not investigated further until the end of the program, when the newly machined seal housing was modified to adapt it to the facility.

The modified three-step labyrinth seal configuration was investigated to determine the mass flux and pressure profiles, with special attention given to pressure profiles with the seal placed in offset, or eccentric, positions. The pressure profile differences due to eccentricity reflect the direct stiffness of a labyrinth flow-path seal and could be compared with profiles for the straight and three-step cylindrical seals (refs. 1 and 2). This comparison, however, is beyond the scope of this report.

Symbols

A	area, cm^2 ($in.^2$)
C	equivalent flow coefficient (constant)
C_f	flow coefficient, $G_R/G_{R,v}$
c	clearance, cm (in.)
D	diameter, cm (in.)
G	mass flux, g/cm^2 s ($lbm/in.^2$ s)
G_R	reduced mass flux, $G/G^*(1 + \psi_Q)$
G^*	flow-normalizing parameter (6010 g/cm^2 s (85.5 $lbm/in.^2$ s) for nitrogen), $\sqrt{P_c \rho_c / Z_c}$
L	length, cm (in.)
M	molecular weight
N	number of orifices
P	pressure, MPa (psi)
R	gas constant, MPa cm^3/g K (psi $in.^3$/lbm °R)
R_H	housing radius, cm (in.)
R_p	alignment pin radius, cm (in.)
R_1	seal centerbody radius, cm (in.)
T	temperature, K (°R)
t	thickness, cm (in.)
V	volume, cm^3 ($in.^3$)
$\dot{w}$	mass flow rate, g/s (lbm/s)
Z	compressibility, PV/RT
α,β	rake angles, deg (rad)
ϵ	clearance fraction, or eccentricity
θ	angular position, deg (rad)
ρ	density, g/cm^3 ($lbm/in.^3$)
ψ_Q	quantum correction factor

Subscripts:

B	backpressure
c	thermodynamic critical value
e	exit
h	hydraulic
i	arbitrary axial position
o	inlet stagnation conditions
R	reduced by corresponding-states parameter
v	venturi
0°	reference position
180°	180° to reference position

Apparatus and Instrumentation

The basic facility (figs. 1 and 2), of the blowdown type,[2] was the same as that used for testing the straight and three-step cylindrical seals (refs. 1 and 2) and will not be described further herein.

Although the used-labyrinth-seal system as originally installed could not be choked because the clearances were too large, a new housing was machined to provide a 0.0127-cm (0.0050-in.) clearance. The results could then be compared with those for the straight cylindrical seal (ref. 1) and the three-step cylindrical seal (ref. 2), which had the same nominal clearance.

Dimensional details of the labyrinth surface and the pressure tap installation are given in figure 3(a). The pressure taps were located at 0° and 180°, and the configuration geometry was symmetric about the centerline. Each labyrinth tooth was 0.0254 cm (0.0100 in.) wide and had an expansion cavity 0.089 cm (0.035 in.) deep by 0.091 cm (0.036 in.) wide. This gave a length-to-clearance ratio L/c of 2 and a length-to-hydraulic-diameter ratio L/D_h of 1. The basic labyrinth tooth was sharp edged. The sharpness of the leading edge is a key factor in leakage rates and dynamic stability. A practical, that is, rub-resistant, sharp-edge labyrinth seal tooth geometry is illustrated in the following sketch, where the rake angles α and β are greatly exaggerated (standard, forward- and rear-facing, and proposed tooth configurations are illustrated for comparison):

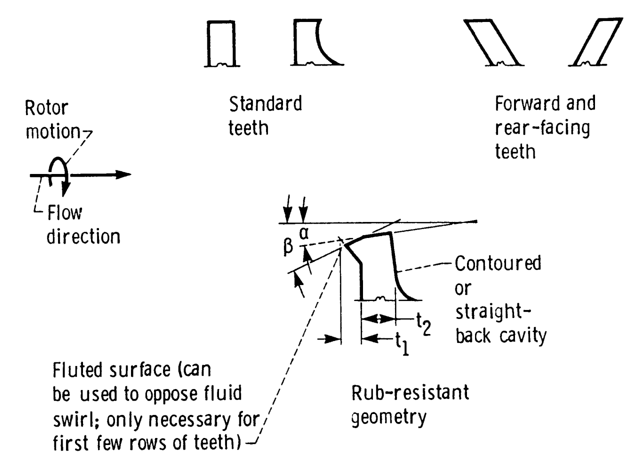

CD-86-23412

[2]The tank is filled with fluid, pressurized, and then exhausted to the atmosphere through vent piping. Fluid refers to a thermodynamic state independent of temperature, pressure, or density. The use of the terms liquid and gaseous is redundant but convenient for many readers. In this sense the fluid enters the test section nominally in the liquid state except for gaseous runs. And in most cases two-phase flow can and probably does occur within the test section much of the time.

Generally α and β are less than 1° depending on thicknesses t_1 and t_2, seal diameter, and fluid conditions. The flow path and rake angles α for the three steps are illustrated in figure 3(b). A photograph of the three-step labyrinth seal (fig. 4) shows the diametrically opposite sets of pressure taps and the newly machined and used geometries. The geometries are discussed in the appendix.

The nominal geometry (diameter by length) for the three steps of 12, 11, and 10 labyrinth teeth was 8.077 by 1.285 cm (3.180 by 0.506 in.), 7.976 by 1.168 cm (3.140 by 0.460 in.), and 7.874 by 1.052 cm (3.100 by 0.414 in.), respectively, with a clearance of 0.0127 cm (0.0050 in.). Because the geometry is complex, manufacturing can be a problem. However, the multiplicity of teeth and cavities provides the necessary loss coefficients associated with low leakage. Each step (figs. 3 and 4) empties into a pocket cavity, which serves as an inlet reservoir for the next step, with the last step (the 10-tooth step) emptying to the exit plane.

Flow tests of the installed newly machined labyrinth seal revealed higher than expected leakage rates and a small axial pressure profile response, similar to those associated with the used labyrinth seal. Changes in flow rate, pressure level, and inlet temperature all revealed minor profile variations at larger than expected flow rates. Because of a conviction that these flow rates were not characteristic of such a seal and that the leakage rates were too high (see refs. 1 to 3), another examination of the actual seal was undertaken. The newly machined seal was found to be shorter than specifications. It was short enough to bottom out at the inlet, so that some of the flow was diverted through the seal passage and the remainder along the splines of the simulated seal configuration (fig. 4), where it effectively bypassed the seal itself. Had the simulated shaft also been splined, such a leak could have easily gone undetected. Such leaks in an unfamiliar configuration are not readily detected and can result in consistent, reproducible, *but erroneous* mass flux and pressure profiles.[3] A flat, soft aluminum gasket was installed to correct the problem, and subsequent initial gaseous mass flux data fell within the anticipated range.

Alignment of the seal was difficult, especially for eccentric positioning, and several methods were used, including indicating in a lathe.[4] However, the best method was the careful and methodical use of alignment pins. A set of pins was carefully machined to fit between the simulated shaft and the housing for each of the four seal positions (eccentricity $\epsilon = 0$, 1/3, 2/3, and 1). The diameters of these pins were varied according to the following formula:

$$R_H + R_p = \epsilon^2 + (R_1 - R_p)^2 - 2\epsilon(R_1 - R_p)\cos\theta$$

where R_1 is the seal centerbody (shaft) radius, R_H is the housing radius, R_p is the pin radius, θ is the angle with respect to the shaft and the position of eccentricity, and ϵ is the clearance fraction, or eccentricity, where $0 < \epsilon < 1$. Careful tightening of the simulated housing with the pins in place provided the final alignment. The centerbody was then fit into place and secured. The data for these configurations are given in tables I to III.

Concentric Position

Flow Rate Data

Although problems of accuracy and reproducibility were encountered with the pressure transducers at very low flow rates, the same transducers were used over the entire range of data for these seal tests.

Initial testing with gaseous nitrogen demonstrated that the design concept of the 12-, 11-, and 10-labyrinth-tooth seal in its revised configuration (newly machined seal with reworked housing) had substantially better leakage characteristics than either the straight or three-step cylindrical seals (refs. 1 and 2, respectively). The resulting data for reduced mass flow rate[5] G_R are given as a function of reduced inlet stagnation pressure $P_{R,o}$ in figure 5. Subsequent tests with gaseous hydrogen revealed similar results (fig. 6) while extending the applicability over a wider range of reduced inlet stagnation pressure and temperature. For this configuration mass flux does increase with eccentricity, but it is small.

Since the labyrinth seal design was based on gas dynamics concepts, some questions about its performance at fluid states between gas and liquid had to be resolved. Tests with fluid nitrogen (fig. 7) indicated that the seal pressure drop and flow rate behaved more like flow in a large-L/D tube (ref. 4). Aside from the flow rate being about one-third that for the straight cylindrical seal (ref. 1), the isotherms for fluid nitrogen were similar to those of references 1 to 6 and indicated the applicability of similarity parameters related through the corresponding-states principles. As such, these results can be applied to liquid oxygen and other fluids of simple molecular structure.

With liquid hydrogen[6] as the test fluid the reduced mass flow rates (fig. 8) were quite similar to those with fluid nitrogen. However, an anomalous region appeared along the nominal 0.82 reduced isotherm (fig. 8(a)). A similar anomaly, noted in reference 1 for some pressure profiles, could not be

[3]An important factor in a practical application such as the space shuttle main engine (SSME) turbopumps.

[4]The partially assembled configuration was placed on a lathe faceplate, and an extensometer (indicator) was used at the exit plane to determine seal-passage alignment.

[5]Technically, this is mass flux, but for a constant-area duct mass flow rate and mass flux are the same to within the constant area A (also could be termed leakage rate).

[6]Herein hydrogen is equilibrum hydrogen—99+ percent parahydrogen in the liquid or fluid state (i.e., 75 percent orthohydrogen gas and 25 percent parahydrogen ambient pressurizing gas).

resolved but was believed to be a fault in the recording system. In this case, however, the flow tests were repeated at a later date and, as indicated in figure 8(b), the anomalous region did not appear to be valid. Still some question remains, since the flow rates do tend to ''hump'' above the theory in this region (e.g., refs. 5 and 6).

The use of liquid hydrogen not only satisfies the direct question of seal performance in fluid hydrogen, but also extends the range of application of the results to higher reduced pressures.

Pressure Profiles

As with previous seal studies (refs. 1 to 3) the pressure profiles were very sensitive to variations in eccentricity. For the concentric configuration the profiles become a measure of the accuracy with which the seal was centered, the concentricity of the centerbody and housing, the expected profile deviations, and the systematic errors. With highly sensitive and selectively placed instrumentation it should be possible to map the seal geometry. However, the instrumentation for these tests was not sensitive enough to provide such a map.

Except for the abnormal drops marking the inlets to each of the three steps, typical pressure profiles for gaseous flows of nitrogen and hydrogen (figs. 9 and 10) resembled those for flows in high-*L*/*D* tubes (ref. 4). Choking conditions were quite apparent at the exit, and subsequent changes of backpressure had little effect on the profile, to a point. (See fig. 11.) With gaseous nitrogen the maximum backpressure was attained at about 40 percent of the inlet pressure at the third step. Above that point the profiles were affected throughout the seal (the criterion for unchoking). The profiles were found to be asymmetric from side to side. This indicates that the eccentricity was perhaps not zero as anticipated or that the concentricity of the machined seal was not as expected. This point is discussed further in sections dealing with the eccentric positions. As shown in figure 12, flows with gaseous hydrogen had characteristics similar to flows with gaseous nitrogen. Again unchoking occurred for backpressures near 40 percent of the inlet pressure at the third step.

The fluid nitrogen profiles also appeared similar to those for a high-*L*/*D* tube (ref. 4). However, these tests did not include the control venturi used in reference 4 for determining choking conditions, and a distinctive assessment of choking could not be made. Figures 13 and 14 show that the profiles were nearly linear with both fluid nitrogen and fluid hydrogen, respectively, but that the exit pressure drop was slightly higher with hydrogen. It appeared that two-phase flows could occur in the latter part of the third stage, as was assumed to be the case in reference 4. The application of backpressure significantly altered the pressure profiles and to some extent decreased the flow rate with both fluid nitrogen and fluid hydrogen (figs. 15 and 16, respectively). Although the inlet stagnation temperature increased during the test because of pressurant gas mixing, the response of the pressure profiles to backpressure appeared to be more than a simple temperature effect. Such profile response was also noted for two-phase flow through single orifices, but to a lesser extent. Here the response appeared to be amplified by the multiplicity of the orifices or sharp edges of the labyrinth teeth. (See also refs. 7 and 8.) Although the flow appeared to be choked at low backpressure, orifices do not completely choke. Comparing the pressure profiles in figures 13 to 16 shows a significant backpressure effect due to the liquid state. Such was not the case for either the straight (ref. 1) or the three-step cylindrical seal (ref. 2). Variations in backpressure, if not properly damped, lead to unstable pressure distributions. Increasing backpressure lowers the flow rate slightly. This in turn can decrease the backpressure, which increases flow rate. Thus either the system is locked into a loop or the shock is moved to an extreme location. The total effect depends heavily on the system time constant (i.e., system response to perturbations).

Fully Eccentric Position

Although it is generally agreed that the primary purpose of a seal is to reduce leakage rates, we must always be concerned with dynamics. A seal that excites instability is undesirable; a seal that may leak a little more but promotes stability is obviously more desirable. The previous section indicated that the fluid state may have a significant influence on stability. The following sections show how geometric displacement, or eccentricity, affects flow rates and pressure profiles, which in turn affect stability. As in previous seal tests (refs. 1 to 3) the seal centerbody was set in its fully eccentric (to the point of rub) position to determine seal response to a simulated dynamic condition.

Flow Rate Data

The flow rate data as in previous seal tests (refs. 1 to 3) were only marginally affected by the fully eccentric position. With gaseous nitrogen (fig. 17) the fully eccentric flow rates were at most 5 percent higher than the concentric flows rates. Similar results were noted with gaseous hydrogen (fig. 6). Superposition of the flow rate data for fluid nitrogen (fig. 18) on figure 7 revealed little change in flow rate between the concentric and fully eccentric positions. Similar results were noted with fluid hydrogen (fig. 19) when compared with figure 8. Again the eccentric flow rates were only a little higher.

It could be concluded that the fully eccentric configuration has reasonably low flow rates (leakage) and that these results are applicable to other fluids of simple molecular structure, including liquid oxygen, by using the corresponding-states principles. However, seal response to dynamic conditions remains to be investigated.

Pressure Profiles

In tests of the straight and three-step cylindrical seal configurations (refs. 1 to 3), the magnitude of the pressure profiles on the maximum-clearance side of the seal was lower than that on the minimum-clearance side. This resulted in restoring forces, or positive direct stiffness, a favorable response to system dynamics.[7]

Typical pressure profiles for the labyrinth seal in the fully eccentric position for gaseous nitrogen (fig. 20) indicated a favorable response to dynamics at the entrance of each step, but an unfavorable response at the exit of each step. The net response appeared to be neither favorable nor unfavorable (i.e., the direct stiffness was small and there would be no definitive response to system dynamics). Similar pressure profiles for fluid hydrogen (fig. 21) extended the range of application to higher reduced pressures.[8]

As anticipated, the pressure drops across the inlet of the first labyrinth tooth of each step were dynamically favorable for the fully eccentric shaft position. However, note from figure 3 that the expansion cavity volume between labyrinth teeth was large as compared with the tooth volume (5:1) but only one-half of the total clearance volume. Thus in addition to the axial flow the circumferential pressure drop initiated a circumferential flow. The resultant flow was assumed to spiral through the seal with a period equal to the seal length. The pressure due to circumferential flow at the exit was therefore higher at the side opposite the high-pressure side at the inlet. As a result the restoring forces were essentially zero. This is not a practical seal where dynamics are concerned unless upstream flow preconditioning is considered. Although instrumentation was not sufficient for determining details within the expansion cavities between labyrinth teeth, vortex patterns must have existed. It is known that for a rotating flow field vortices can give way to free-standing wave patterns (ref. 9).[9]

Results for the three-step cylindrical seal (ref. 2) indicated a substantial increase in pressure drop due to flow separation. Although the gaseous tests indicated essentially no restoring forces, if flow jetting occurred in the third stage of the labyrinth, the labyrinth seal could possibly be used for dynamic control as well as for leakage control with minimum torque and rubbing effects.

The gaseous nitrogen data for the fully eccentric position (fig. 20) indicate no such separation. Although there may have been a small favorable direct stiffness value, within the error of these experiments the net restoring forces and hence the direct stiffness were nearly zero. Remember that there was no rotation. In an actual case, rotation effects enter as noted in the **Introduction** and must be considered. Tests with fluid hydrogen revealed the same type of results, namely that the differences in the pressure profiles were essentially balanced and that the direct stiffness was nearly zero (fig. 21).

Backpressure tests did not alter these conclusions. Profiles with significant applied backpressure are discussed in the following section. Again these results apply to other simple fluids such as liquid oxygen via the corresponding-states principles.

[7]Because this configuration is static (nonrotating), only direct stiffness can be inferred. Nothing can be stated about mass, damping, or cross-coupling coefficients.

[8]Combining the merits of each configuration (i.e., using a labyrinth seal with a cylindrical inlet section) could provide leakage and dynamic control.

[9]Vortex shedding from sharp edges is well known. Here it was anticipated that the "doughnut" vortex shed from the sharp leading edge and a second vortex within the cavity were moderated and set into circumferential motion by the pressure differential between the minimum and maximum passage clearances. Since this pressure differential was cyclic, circumferential motion of the vortex was probably reversed, and the second vortex became dominant. Vortex motion is difficult to damp out and can lead to cavity-like formations that affect both flow rate and dynamic stability.

Two-thirds Fully Eccentric Position

On several occasions researchers working with the hardware and theoretical approaches cited the need for data at various eccentricities. Although it is well known (refs. 1 to 3) that the pressure profiles are sensitive to small displacements and that the fully eccentric data represent the limiting case, the question still remains as to the quantitative behavior of the eccentricity and the restoring forces.

By using the alignment pins mentioned in the section **Apparatus** the seal centerbody was set two-thirds fully eccentric. As anticipated, the resulting flow rate was virtually unaffected by the offset, as noted in figure 17 for gaseous nitrogen and in figure 6 for gaseous hydrogen. Flow rate data for fluid hydrogen are given in figures 22 and 23. No fluid nitrogen data were taken for this configuration. The effects of initial inlet stagnation pressure on flow rate, as shown in figure 23, were investigated because some anomalous points had been noted and thought to be connected with the initial inlet pressure.[10] No real trend was found.

Equally undramatic were the effects of two-thirds eccentricity on the pressure profiles for gaseous nitrogen and fluid hydrogen. Circumferential flows are no less significant for the two-thirds fully eccentric case than for the fully eccentric case.

Comparing the pressure profiles for gaseous hydrogen (fig. 24) and fluid hydrogen (fig. 25) with figures 10 and 14 revealed few differences between the concentric and two-thirds fully eccentric profiles. As a comparison, gaseous nitrogen data with the seal centerbody set in the two-thirds fully eccentric, concentric, and fully eccentric positions (fig. 26) showed that the differences due to eccentric positioning were not large.

[10]Test runs were usually begun at some high pressure and sequentially reduced to lower pressures in discrete steps while taking data.

The effects of backpressure, noted in the section **Pressure rofiles**, showed similar trends for the two-thirds fully eccentric osition. Backpressure had little effect on the gaseous hydrogen ressure profiles (fig. 27) until it reached about 40 percent of ıe inlet pressure at the third step, as noted for the other ›ositions (and perhaps should have been anticipated from heoretical considerations). On the other hand, the fluid hydro- ȝen pressure profiles (fig. 28) were affected by small increases n backpressure, again as noted for the other eccentric positions.

One-third Fully Eccentric Position

Data taking was severely hampered by an early, unscheduled phaseout of the data acquisition system. However, operation of the cathode-ray tube was retained for another run. This procedure resulted in manual data reduction and visual averaging. Such results were qualitative, but their quantitative value was questionable (no tabulated results are available). Generally the flow rates were good, since fluctuations were small, but the pressure profile accuracy suffered from both averaging the fluctuations and failure to know the precise absolute level. Only gaseous nitrogen data (figs. 29 and 30) were taken for this configuration. Again the pressure profiles indicated essentially no net restoring forces.

Gaseous Helium

In an effort to extend the corresponding-states techniques to higher reduced temperatures and pressures, flow rate data for gaseous helium were taken (fig. 31). The first set of data, designated as ''cold,'' were taken after a fluid nitrogen run. Although the system was purged, the liquid nitrogen radiation shield could have sufficiently cooled the tank for some liquid nitrogen to be retained in the bottom of the tank. Thus some mixture of helium and nitrogen could have passed through the system. Over the weekend the system warmed completely to ambient conditions, and the data taken, designated as ''warm,'' indicated better linearity and less scatter.

Although the mass flow rate data for helium followed those for gaseous hydrogen when multiplied by $\sqrt{M_{He}/M_{H_2}}$, where M is molecular weight, the corresponding-states principles appeared to be violated. These helium data did not appear to reduce properly as did the data for the simple fluids (e.g., nitrogen, oxygen, argon, methane, and parahydrogen). Further investigation into the theory considering nonlinear fluid dynamic effects is required.

A second approach was to calculate the equivalent flow coefficient

$$\frac{G_{R,\psi_Q}\sqrt{T_{R,o}}}{P_{R,o} - P'_{R,o}} = \frac{C_f}{5} = C$$

where ψ_Q is the quantum correction factor, $P_{R,o} - P'_{R,o}$ is the reduced differential pressure, C_f is the flow coefficient, and C is a constant. Figure 32(a) illustrates the variation of C with reduced pressure $P_{R,o}$. The hydrogen and nitrogen data tend to group, but it is clear that the helium data do not follow the corresponding-states principles. Since the thermodynamic critical pressure for helium is quite low, small changes in choking pressure are significant. Figure 32(b) illustrates the variation of flow coefficient with reduced differential pressure, where $P'_{R,o}$ is the minimum choking pressure. For helium $P'_{R,o} = 2$; for hydrogen, 0.25; and for nitrogen, 0.1. The dependency on pressure is strong. Although the calculated flow rates showed the same trend as the experimental data, their magnitude appeared to be low by 15 percent, and this difference was mostly pressure dependent. Carryover and jetting, which tend to increase with flow rate, could account for the remaining difference, but verification is not possible at this time. If one further normalizes the pressure as $(P_{R,o} - P'_{R,o})/10$ for gaseous helium only, all of these results collapse to a single locus with some scatter for the eccentric cases as contrasted with concentric flows (table IV). I have no explanation of why this works and call it an empirical relation accounting for nonlinear effects of expansion perhaps related to quantum fluid at room temperature.

Flow Coefficient

For fluid nitrogen data the flow coefficient $C_f = G_R/G_{R,v}$, where $G_{R,v}$ is the calculated flow through a venturi for inlet conditions $P_{R,o}$ and $T_{R,o}$, can be related to reduced inlet stagnation temperature $T_{R,o}$ but not to $P_{R,o}$ since it varied more than anticipated. The magnitude of C_f was less than one-half that of a Borda inlet tube with a length-to-diameter ratio L/D of 53, but temperature trends for the two tubes were similar (fig. 33). For a large range of reduced inlet stagnation temperatures above $T_{R,o} = 1.3$, C_f was constant. In the near-critical region ($T_{R,o} \sim 1$), calculated flows were less than measured flows, and C_f increased. In this region variations in the thermophysical properties became significant. For lower temperatures C_f decreased, and measured flows were actually less than calculated flows for a venturi at comparable $P_{R,o}$ and $T_{R,o}$. Although there is really no way to complete a locus joining these data bars, a form similar to the 53-L/D curve could be assumed. Equally valid could be two straight lines.

Although the magnitude of C_f for the straight cylindrical seal (ref. 1) more closely approximates that for the 53-L/D Borda inlet, one is not comparing C_f magnitude but trends with inlet stagnation temperature (and pressure). Further, in the absence of information, a form similar to the locus could be assumed.

Circumferential Pressure Drop

In an effort to gain some understanding of the pressure profiles within the three-step labyrinth seal, the circumferential pressure drop in the expansion cavity of the first tooth of each tep ($\Delta P = P_{0^\circ} - P_{180^\circ}$) was investigated as a function of nlet stagnation pressure P_o for gaseous nitrogen.

Concentric Position

The circumferential pressure drops ΔP across the inlets of he first teeth of the first and second steps were nearly the same fig. 34). (The position of the three data points at high pressure for the second step has not been explained.) However, the pressure drop at the third step was significantly larger and nearly equal to the sum of the first and second drops. At this time it is difficult to understand why this should be the case when the number of teeth per step changed from 12 to 11 to 10. However the profile representing the average reservoir pressure for choked flow of gases through N equally spaced orifices is known to be parabolic. For $N = 33$, where $N_1 = 12$, $N_2 = 11$, and $N_3 = 10$ equally spaced orifices, the implication is that the pressure drops across the first two steps could be nearly the same. These results also follow from one-dimensional choked-flow theory.

It was also difficult to accurately position the centerbody within the housing, and at low to zero eccentricities the error could be significant. Any pressure differential indicates some misalignment or other source of instability that could not be measured with this system.

Fully Eccentric Position

In the fully eccentric position the circumferential pressure drops at the first and second steps were again nearly the same (fig. 35), but the drop at the reservoir of the third step was about 85 percent of the sum across the first two steps. Also the pressure drops at the first and second steps were better distributed.

Two-thirds Fully Eccentric Position

In the two-thirds fully eccentric position the circumferential pressure drop at the third step appeared to be nearly the sum of those across the first and second steps, and a slight crossover in the first two steps was noted (fig. 36).

One-third Fully Eccentric Position

In the one-third fully eccentric position the pressure drop at the third step was about four-thirds of the sum across the first and second steps (fig. 37). Further, these pressure drops were less than in the concentric position. This may have been due to misalignment of the seal configuration (i.e., positioning error), where the one-third fully eccentric position was geometrically closer to being concentric than the concentric position, but was more probably due to the errors associated with manual/automatic data acquisition.

The circumferential pressure drops at each step are summarized in figure 38. Plotting the slope of these lines $\Delta P/P_o$ provided a variation with eccentricity, as shown in figure 39, and revealed that the profiles probably were not uniform. For installation purposes the seal had to be reversed in its housing. Generally no significant difference could be attributed to rotating the seal centerbody 180°. If one assumes a 0.02-mm (0.0008-in.) positioning error at small eccentricities, which was possible, reversing the test results of the concentric and one-third fully eccentric positions could give a reasonable figure. At this point all that can be stated is that, as the eccentricity increased, the circumferential pressure drop at the first tooth of each step tended to increase. Further, the magnitude appeared to increase linearly with inlet stagnation pressure.

Summary of Results

Test data for a nonrotating three-step labyrinth seal with 12, 11, and 10 labyrinth teeth per step, respectively, at nominal diameters of 8.077, 7.976, and 7.874 cm (3.180, 3.140, and 3.100 in.) have been presented. These data included mass flux rate and pressure profiles over a wide range of fluid conditions at concentric, partially eccentric, and fully eccentric positions.

The mass fluxes for the nonrotating seal at various eccentric positions differed by at most 5 percent and for all practical purposes can be treated as unaltered by eccentric positioning. This was also found to be true for nonrotating straight and three-step cylindrical seals in similar configurations.

The pressure profiles of the three-step labyrinth seal differed significantly from those of the cylindrical seals. Although the circumferential pressure drop showed positive stiffness at the first tooth of each step, it decreased and showed negative stiffness at the last tooth and in the reservoir between steps. Such crossovers in the axial pressure distribution can provide little if any positive direct stiffness, which is required for stability in seal configurations. Circumferential pressure drop in the expansion cavity of the first tooth of each step generally increased with eccentricity and inlet stagnation pressure, although magnitudes at eccentricities of one-third and less were difficult to measure because of the small differences, the limits of the instrumentation, and difficulties with geometric alignment.

The method of corresponding states showed that the helium mass flux data had a pressure dependency, part of which can be attributed to the simplicity of the normalized flow relation and expansion of a quantum gas at ambient temperature. Data for helium followed the parahydrogen and nitrogen results provided that the normalized pressure dependency was divided by an empirical constant of 10.

The leakage-rate characteristics for the labyrinth seal are quite good, but seal response to dynamic conditions for stabilizing a turbomachine would be quite poor.

National Aeronautics and Space Administration
Lewis Research Center
Cleveland, Ohio 44135, October 16, 1986

Appendix—Used and Newly Machined Three-Step Labyrinth Seals for Space Shuttle Main Engines

Although both the used and newly machined labyrinth seals are discussed here, *only data for the newly machined seal and housing are presented.* Both seals were Inconel; the seals of references 1 and 3 were aluminum.

Measurement of the *used*-shuttle-seal configuration (fig. 4) and the associated housing revealed several geometric malformations:

(1) The average clearance heights were large as compared with the average clearance of 0.0127 cm (0.0050 in.) for the straight and three-step cylindrical seals (refs. 1 and 2):

(a) Step 1, 0.508 cm (0.0200 in.)
(b) Step 2, 0.442 cm (0.0174 in.)
(c) Step 3, 0.340 cm (0.0134 in.)

(2) Steps 2 and 3 were tapered in the flow direction:

(a) Step 1, no appreciable taper
(b) Step 2, 0.023-cm (0.009-in.) taper
(c) Step 3, 0.018-cm (0.007-in.) taper

A closer examination showed that the labyrinth flow-path teeth had been worn down. This indicates several things:

(1) Such wear must have created large amounts of heat (perhaps sparks).

(2) The effectiveness of the labyrinth path would be greatly reduced because the flow coefficient of these geometries is quite sensitive to edge sharpness.

(3) The shaft stiffness must have been considerably less than that required to maintain a stable configuration.

(4) Although it was not indicated directly, measurements implied that an axial shaft-to-housing motion could "valve off" the flow (see fig. 3) and result in a loss of stiffness.

As a result the *used* three-step labyrinth seal revealed several characteristics of which a seal designer should be aware. With an average flow area three times larger than that of the straight or three-step cylindrical seals, it would have flow rates well beyond the capability of the facility.

Although the *newly* machined seal looked much like the used seal (fig. 4), there were several important differences:

(1) The steps were not tapered.

(2) The labyrinth flow-path teeth were not worn.

(3) The average flow area was twice that of the straight or three-step cylindrical seal.

The clearance heights decreased as the step diameter decreased, as shown in figure 3.

(1) Step 1 clearance, 0.0368 cm (0.0145 in.)
(2) Step 2 clearance, 0.0292 cm (0.0115 in.)
(3) Step 3 clearance, 0.0216 cm (0.0085 in.)

Again the average clearance of the straight and three-step cylindrical seals was 0.0127 cm (0.0050 in.). Tests were completed for the used and newly machined labyrinth seals in the original housing, but no data of substance were recorded. Subsequently the housing was reconfigured to provide a nominal 0.0127-cm (0.0050-in.) clearance, and the data herein are based on the reconfigured newly machined seal.

References

1. Hendricks, R.C.: Straight Cylindrical Seal for High-Performance Turbomachines. NASA TP-1850, 1987.
2. Hendricks, R.C.: Three-Step Cylindrical Seal for High-Performance Turbomachines. NASA TP-1849, 1987.
3. Hendricks, R.C.: Some Flow Characteristics of Conventional and Tapered High Pressure Drop Simulated Seals. ASLE Preprint 79-LC-3B-2, Oct. 1979.
4. Hendricks, R.C.; and Simoneau, R.J.: Two-Phase Choke Flow in Tubes with Very Large L/D. NASA TM-73726, 1977.
5. Hendricks, R.C.; and Sengers, J.V.: Application of the Principle of Similarity to Fluid Mechanics. Water and Steam: Their Properties and Current Industrial Applications, J. Straub and K. Scheffler, eds., Pergamon, 1980, pp. 322-335. (Unabridged version as NASA TM-79258, 1979.)
6. Simoneau, R.J.; and Hendricks, R.C.: Two-Phase Choked Flow of Cryogenic Fluids in Converging-Diverging Nozzles. NASA TP-1484, 1979.
7. Hendricks, R.C.; and Stetz, T.T.: Some Flow Phenomena Associated with Aligned, Sequential Apertures with Borda-Type Inlets. NASA TP-1792, 1980.
8. Hendricks, R.C.; and Stetz, T.T.: Flow Through Aligned Sequential Orifice Type Inlets. NASA TP-1967, 1980.
9. Iwatsubo, T.: Evaluation of Instability Forces of Labyrinth Seals in Turbines or Compressors. Rotordynamic Instability Problems in High Performance Turbomachinery, NASA CP-2133, 1980.

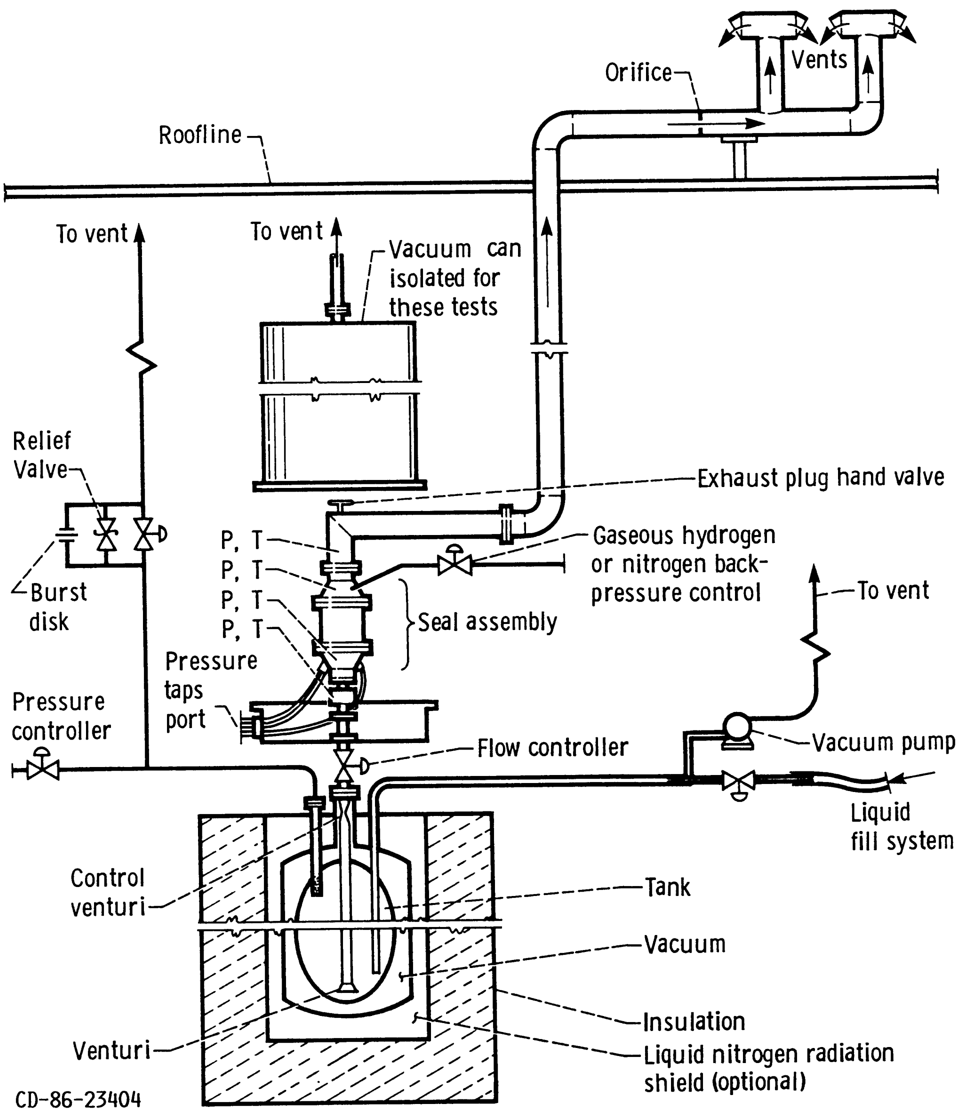

Figure 1.—Schematic of seal test installation.

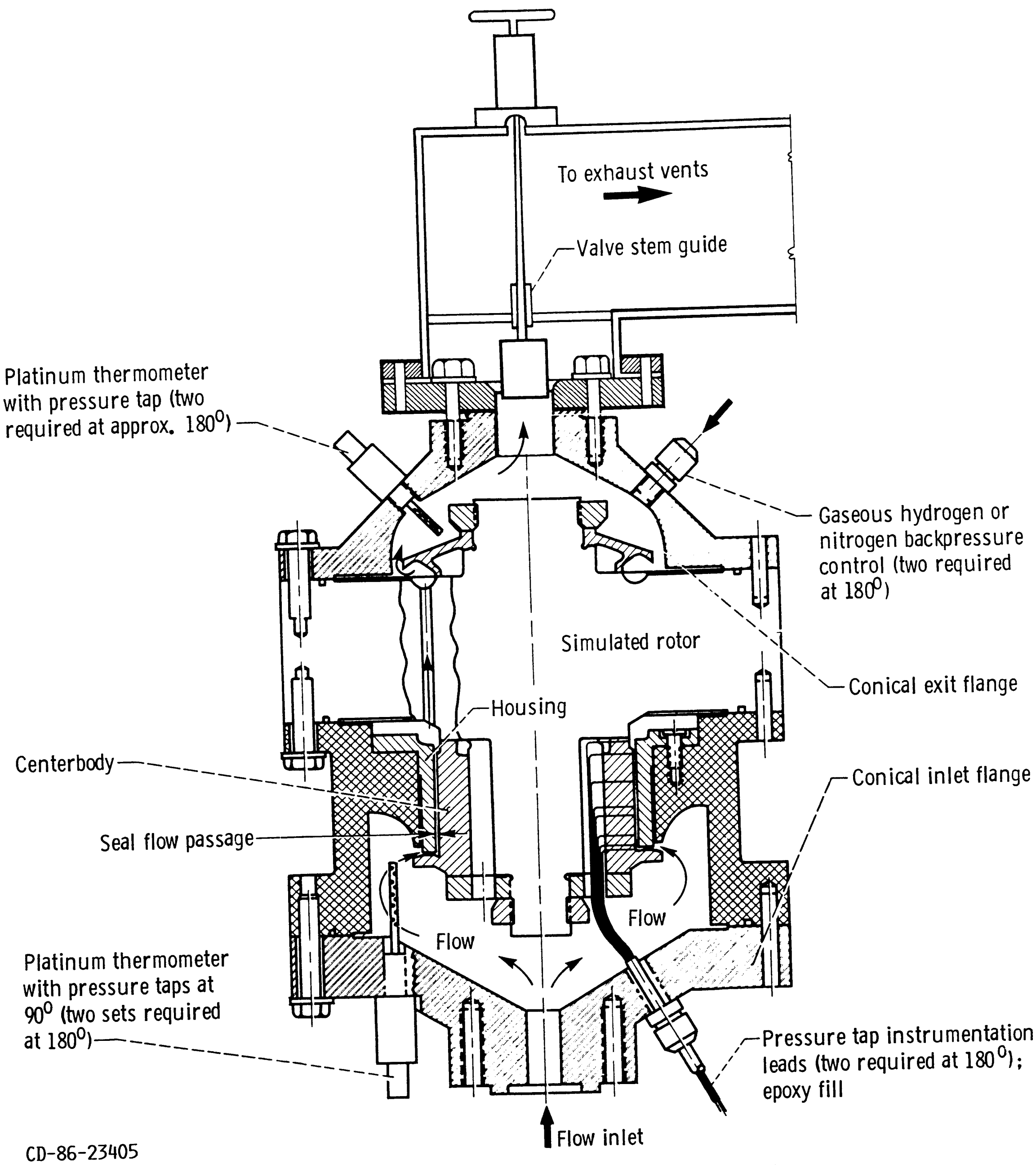

Figure 2.—Cross-sectional view of simulated seal configuration.

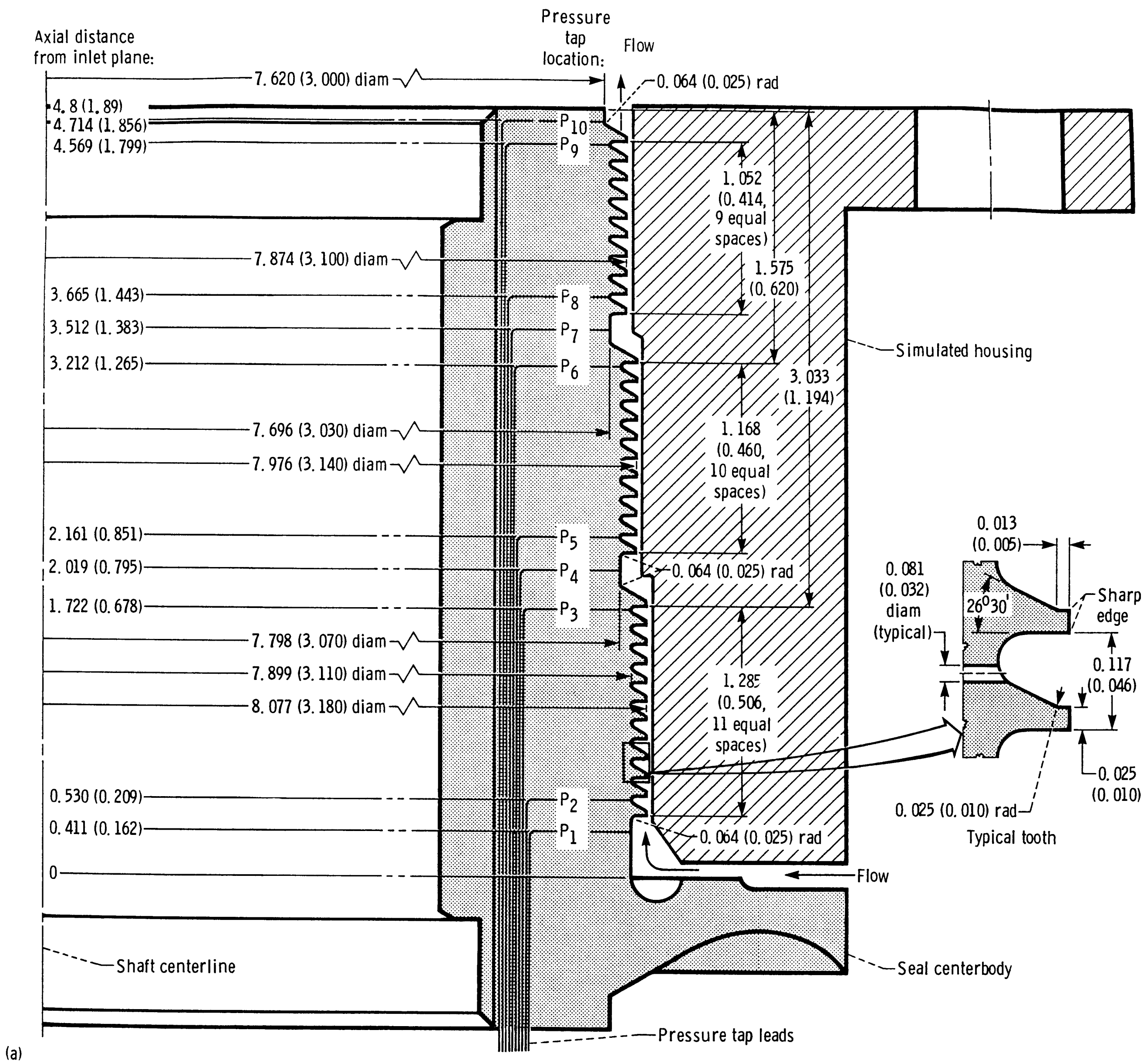

(a) Pressure taps.

Figure 3.—Overview of pressure taps and geometry for three-step labyrinth seal. (Linear dimensions are in centimeters (inches), and surface finish on all machined surfaces is 32.)

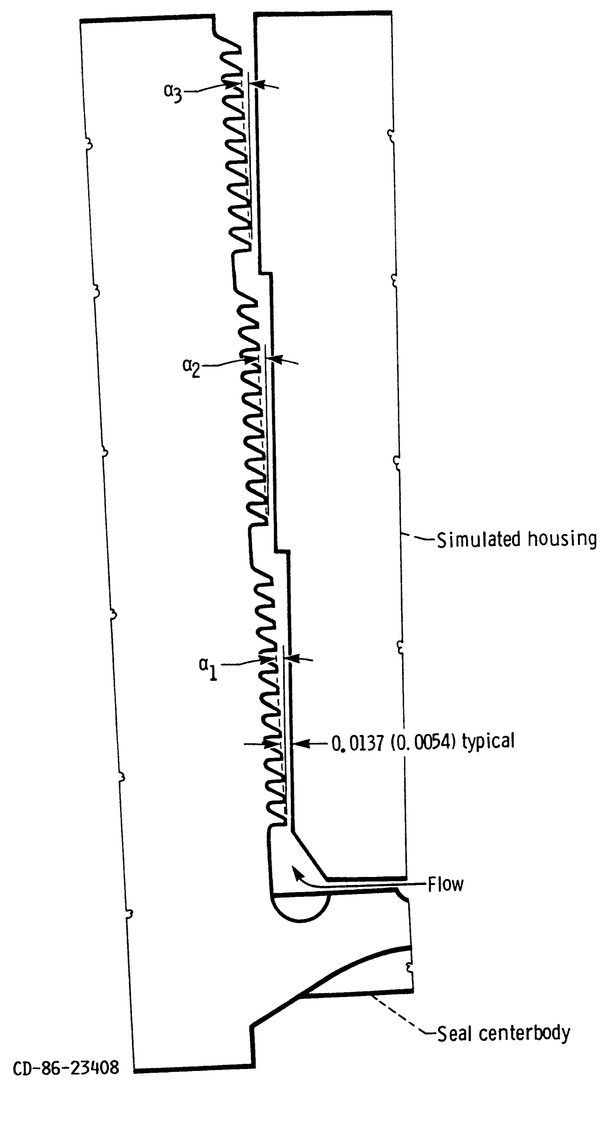

(b) Step geometry.

Figure 3.—Concluded.

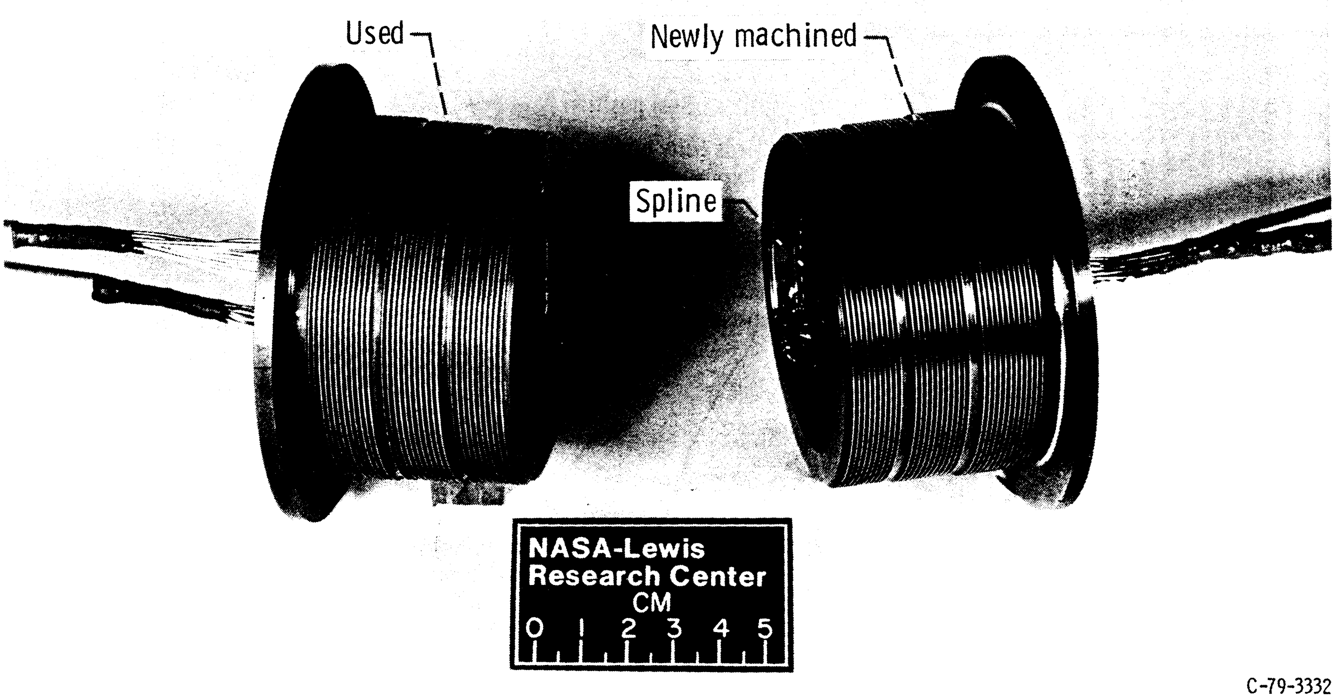

Figure 4.—Newly machined and used three-step labyrinth seals.

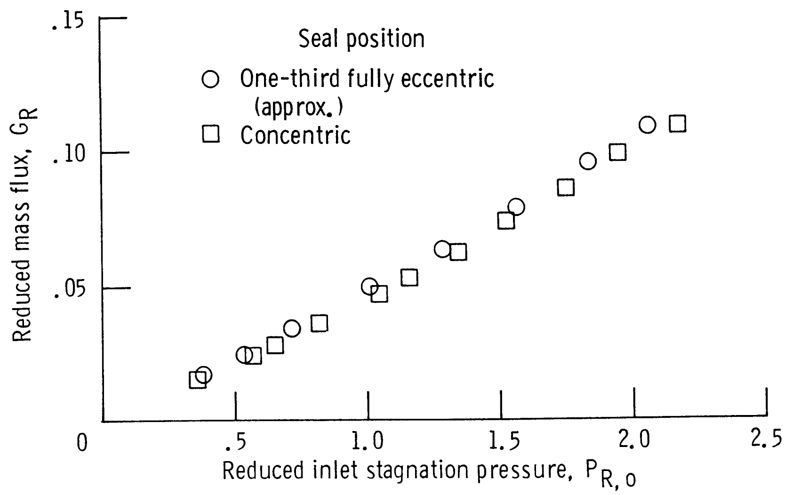

Figure 5.—Reduced mass flux of gaseous nitrogen through three-step labyrinth seal in concentric and one-third fully eccentric positions, as function of reduced inlet stagnation pressure. Area A, 0.3228 cm^2 (0.050 $in.^2$); normalized flow G^*A, 373.8 g/s (0.822 lbm/s).

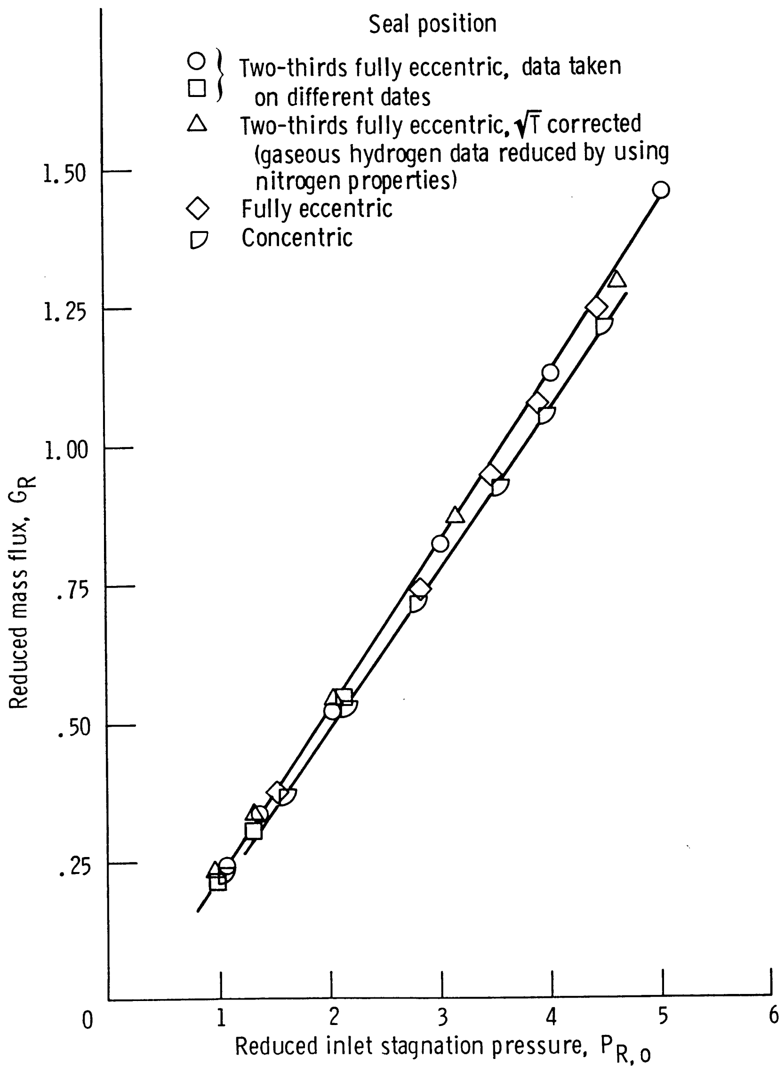

Figure 6.—Reduced mass flux of gaseous hydrogen through three-step labyrinth seal in concentric and two-thirds fully eccentric positions, as function of reduced inlet stagnation pressure. Area A, 0.3228 cm^2 (0.050 $in.^2$); normalized flow G^*A, 373.8 g/s (0.822 lbm/s).

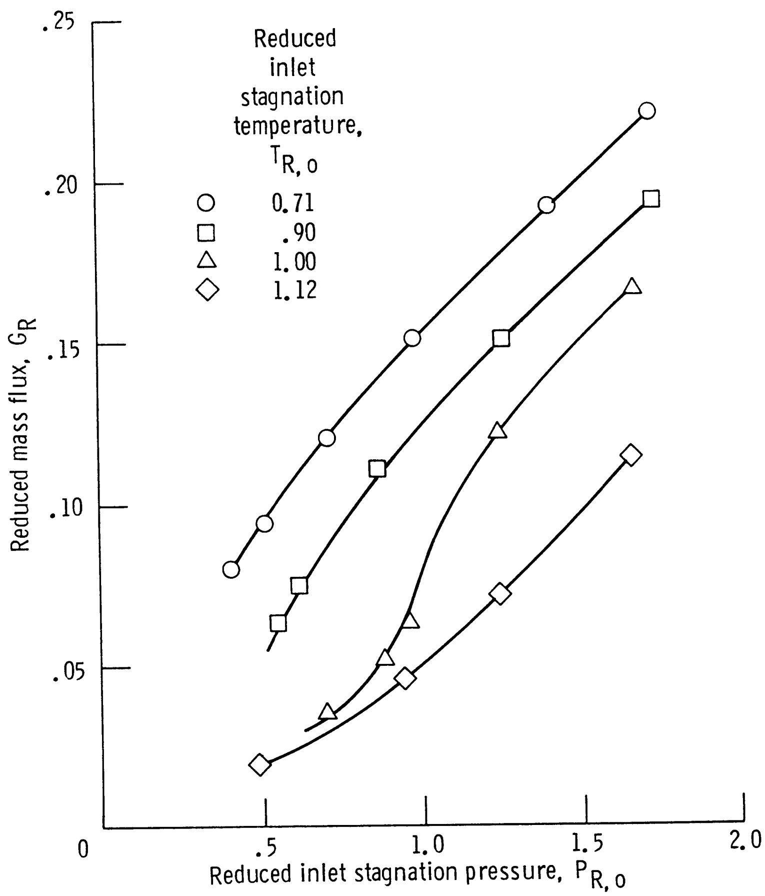

Figure 7.—Reduced mass flux of fluid nitrogen through three-step labyrinth seal in concentric position, as function of reduced inlet stagnation pressure.

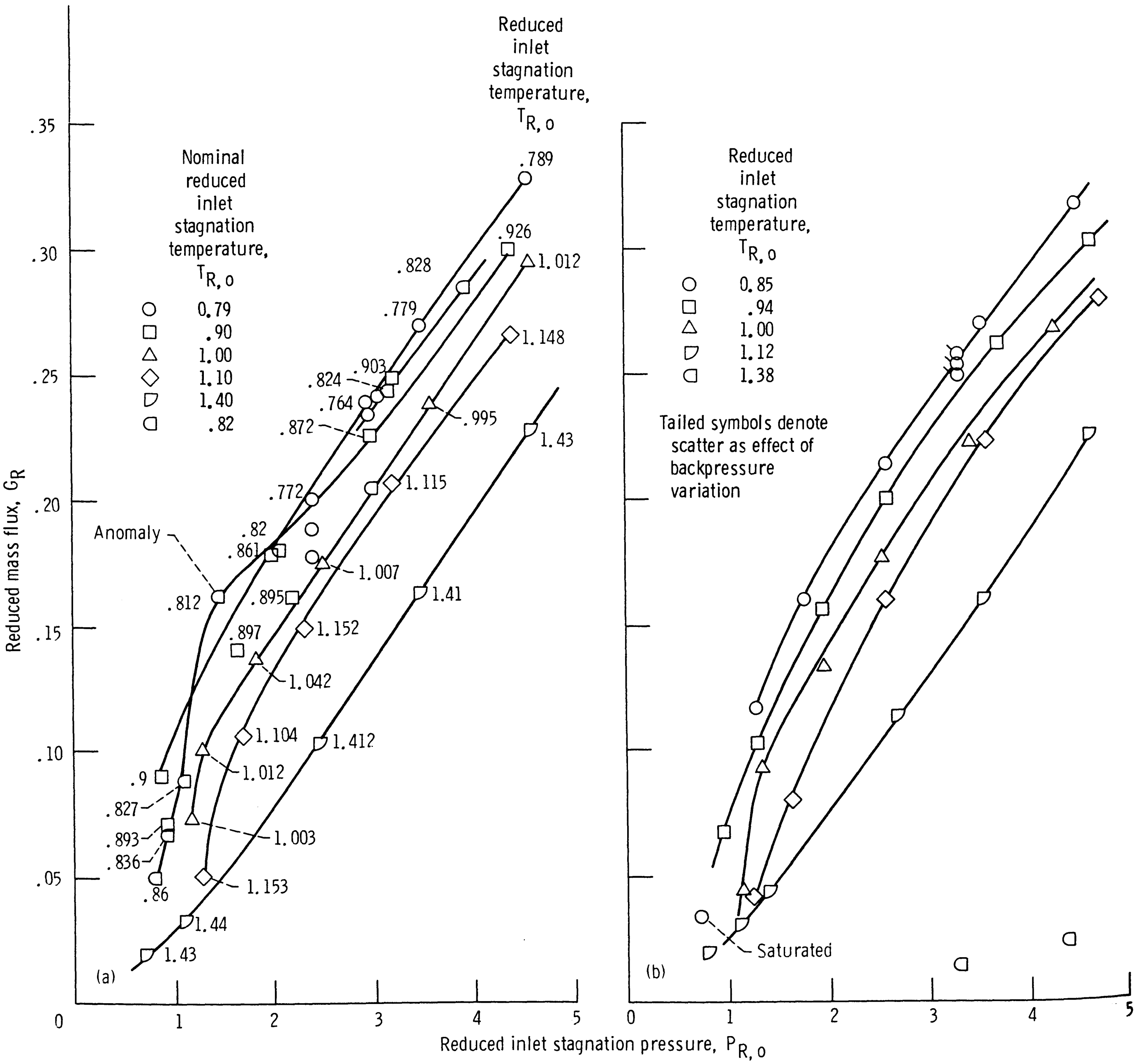

(a) Fluid hydrogen with an anomaly.
(b) Fluid hydrogen with backpressure control.

Figure 8.—Reduced mass flux of fluid hydrogen through three-step labyrinth seal in concentric position, as function of reduced inlet stagnation pressure.

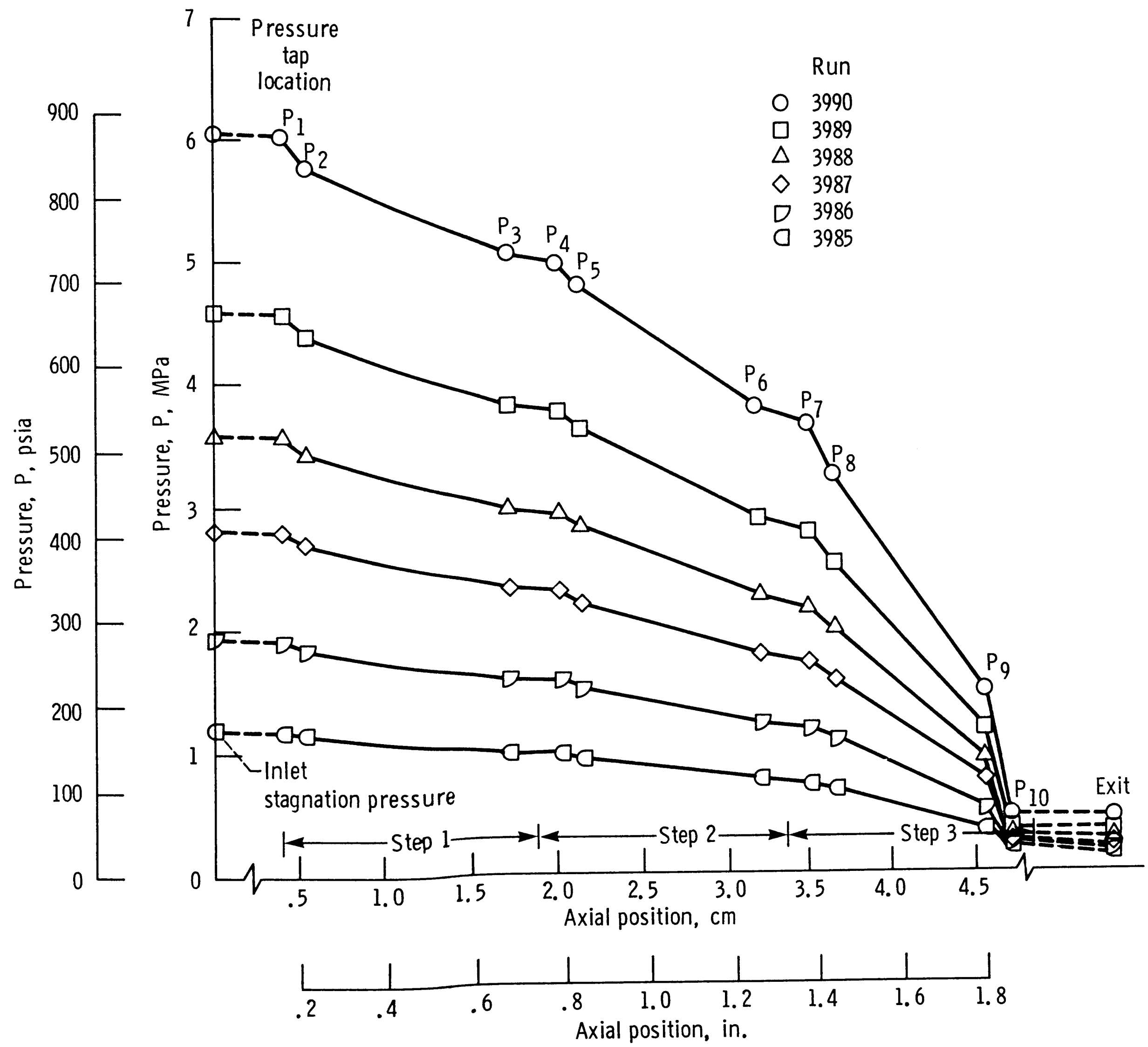

Figure 9.—Axial pressure distribution for gaseous nitrogen flow through three-step labyrinth seal in concentric position. Nominal reduced inlet stagnation temperature $T_{R,o} \approx 2.1$.

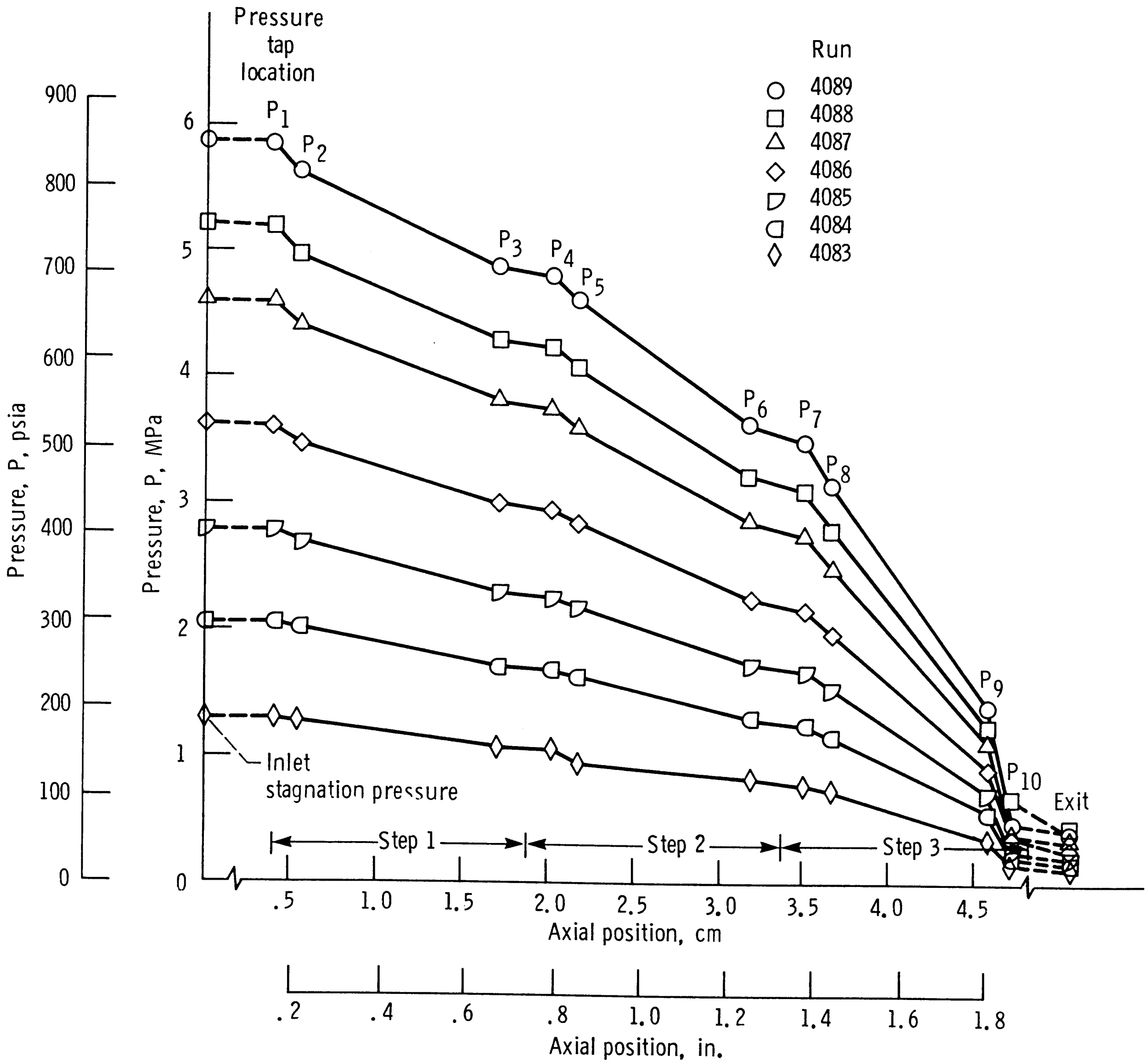

Figure 10.—Axial pressure distribution for gaseous hydrogen flow through three-step labyrinth seal in concentric position. Nominal reduced inlet stagnation temperature $T_{R,o} \approx 9$.

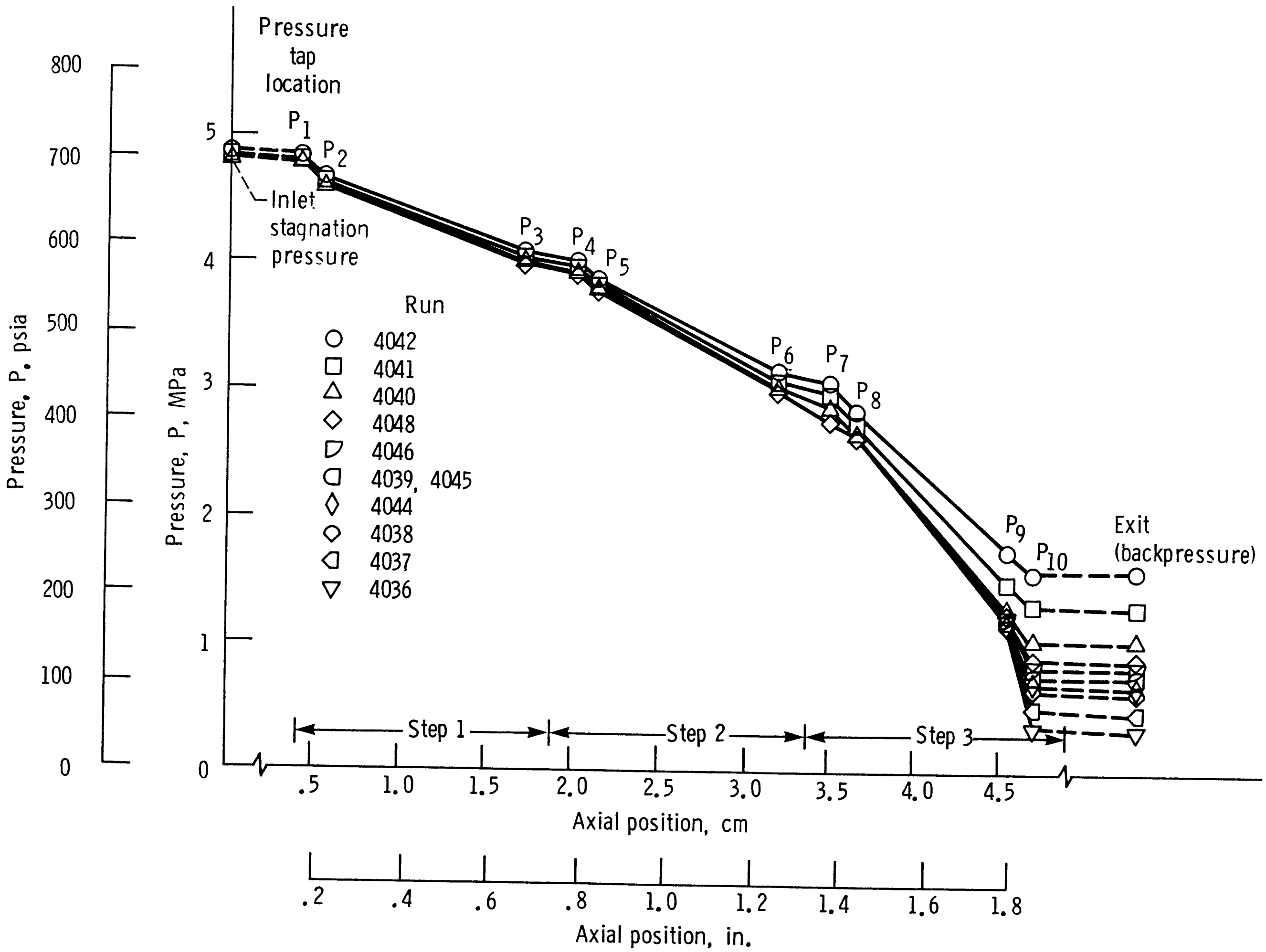

Figure 11.—Axial pressure distribution for gaseous nitrogen flow through three-step labyrinth seal in concentric position, with backpressure control. Nominal reduced inlet stagnation temperature $T_{R,o} \approx 2.2$.

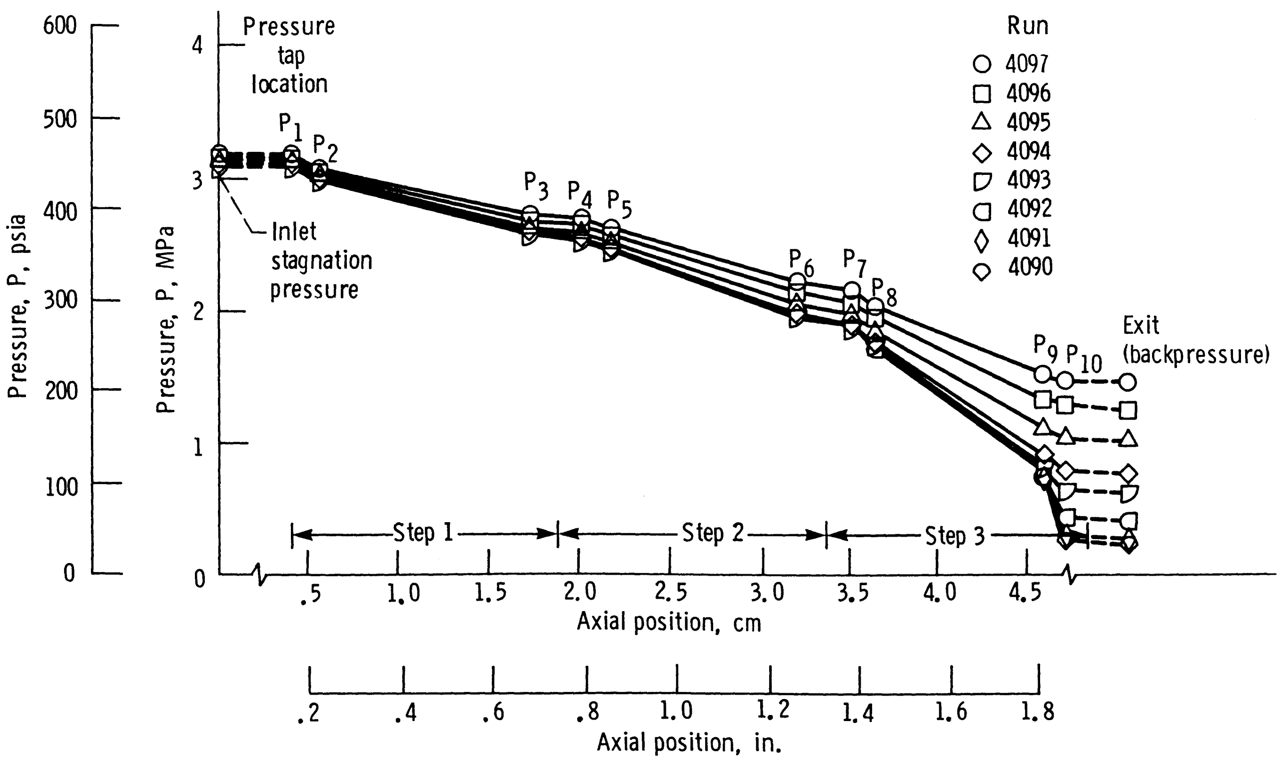

Figure 12.—Axial pressure distribution for gaseous hydrogen flow through three-step labyrinth seal in concentric position, with backpressure control. Nominal reduced inlet stagnation temperature $T_{R,o} \approx 9$.

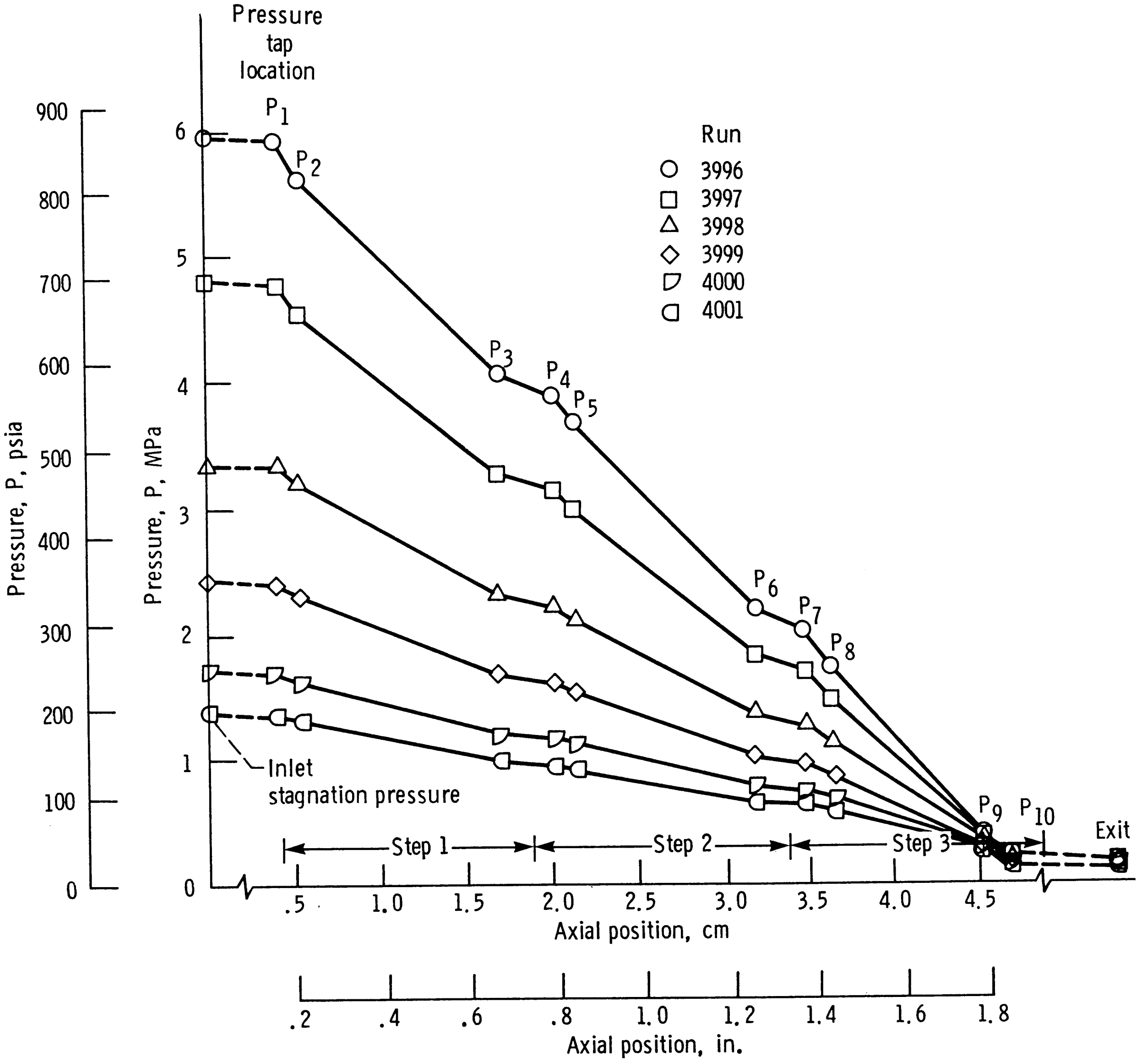

Figure 13.—Axial pressure distribution for fluid nitrogen flow through three-step labyrinth seal in concentric position. Nominal reduced inlet stagnation temperature $T_{R,o} \approx 0.71$.

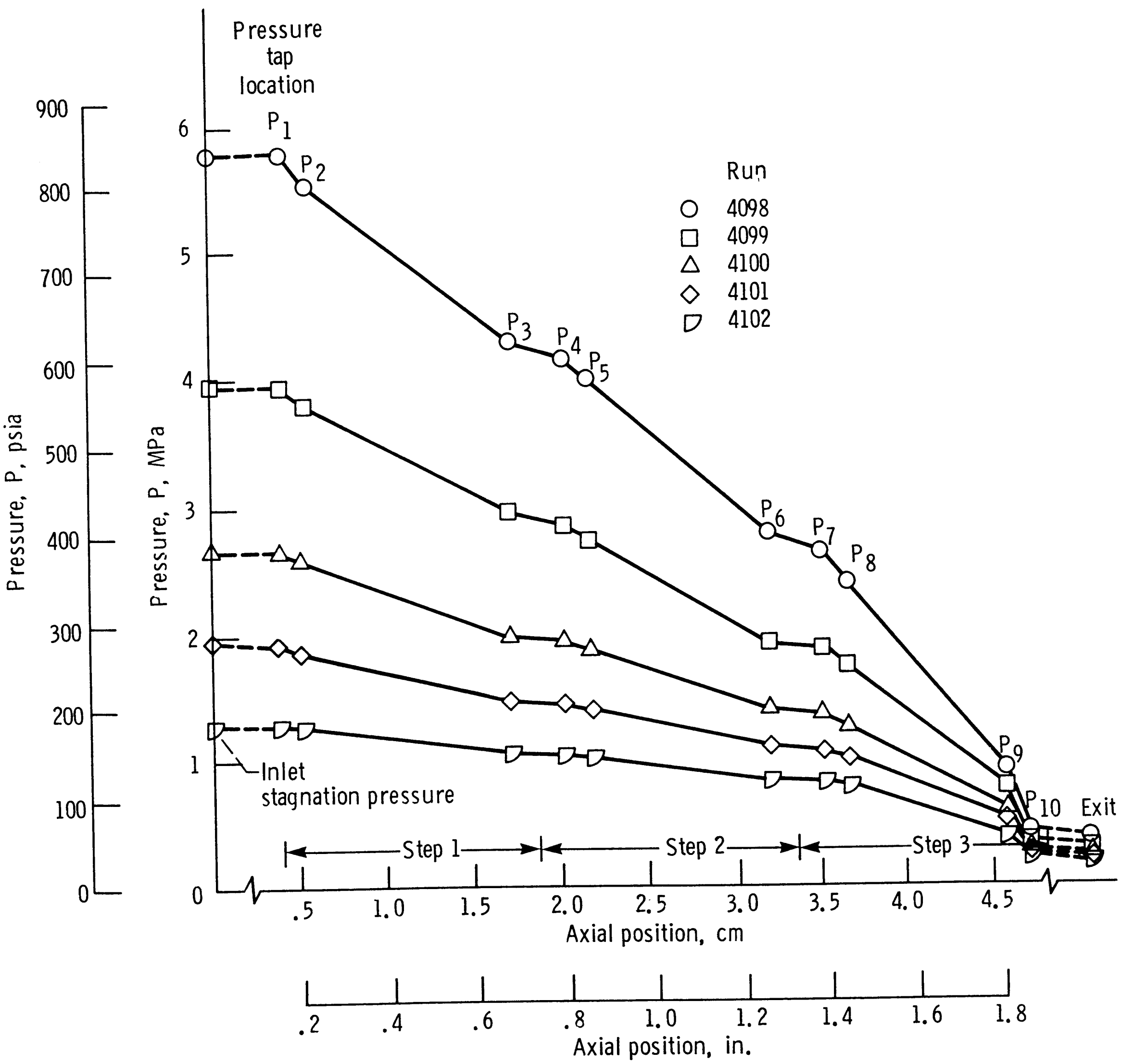

Figure 14.—Axial pressure distribution for fluid hydrogen flow through three-step labyrinth seal in concentric position. Nominal reduced inlet stagnation temperature $T_{R,o} \approx 0.86$.

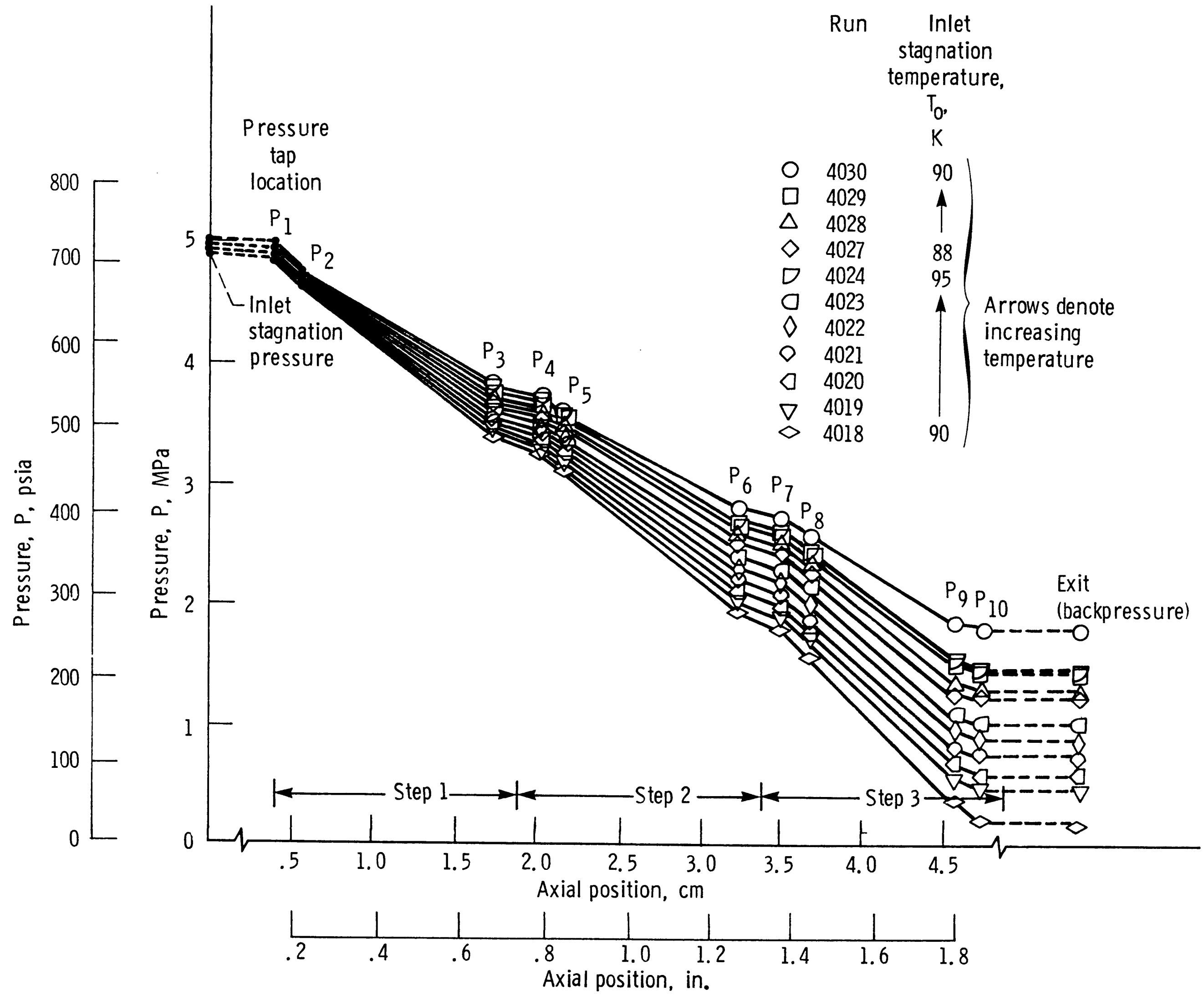

Figure 15.—Axial pressure distribution for fluid nitrogen flow through three-step labyrinth seal in concentric position, with backpressure control. Nominal reduced inlet stagnation temperature $T_{R,o} \approx 0.72$.

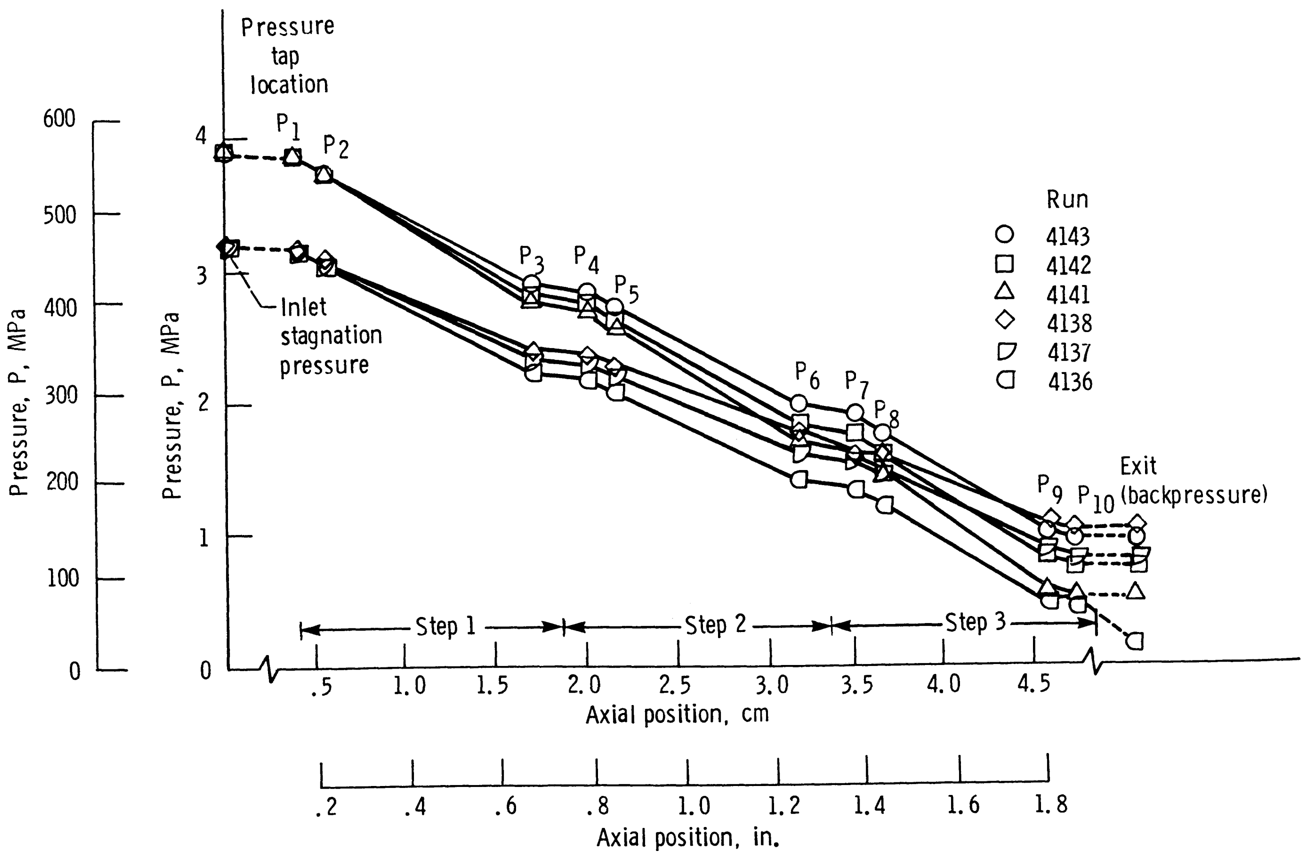

Figure 16.—Axial pressure distribution for fluid hydrogen flow through three-step labyrinth seal in concentric position, with backpressure control. Nominal reduced inlet stagnation temperature $T_{R,o} \approx 0.8$.

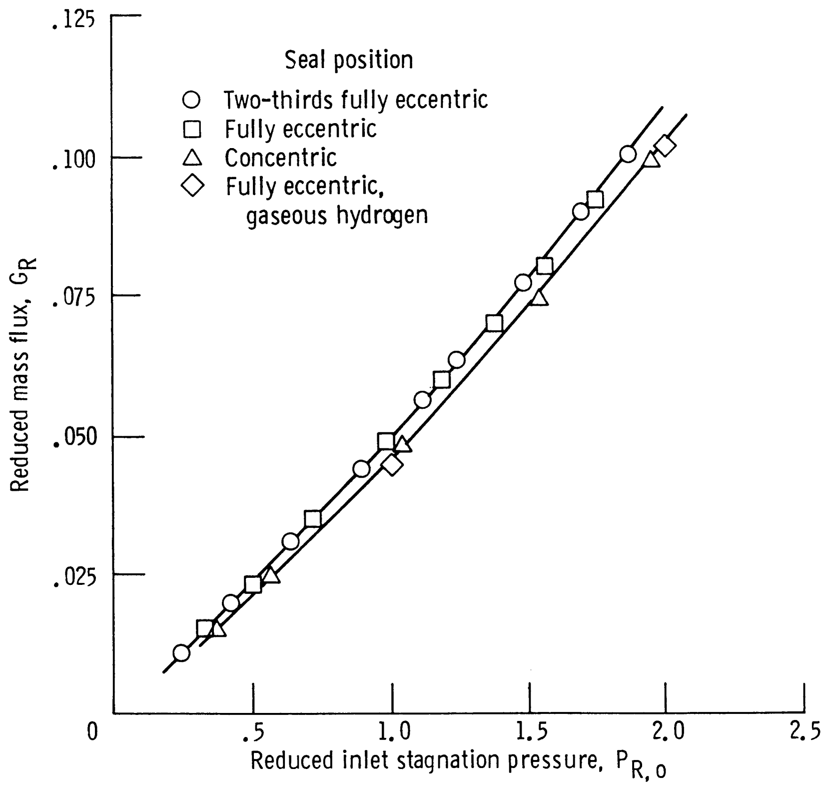

Figure 17.—Reduced mass flux of gaseous nitrogen through three-step labyrinth seal in fully eccentric, two-thirds fully eccentric, and concentric positions, as function of reduced inlet stagnation pressure. Area A, 0.3228 cm^2 (0.050 $in.^2$); normalized flow G^*A, 1940 g/s (4.27 lbm/s).

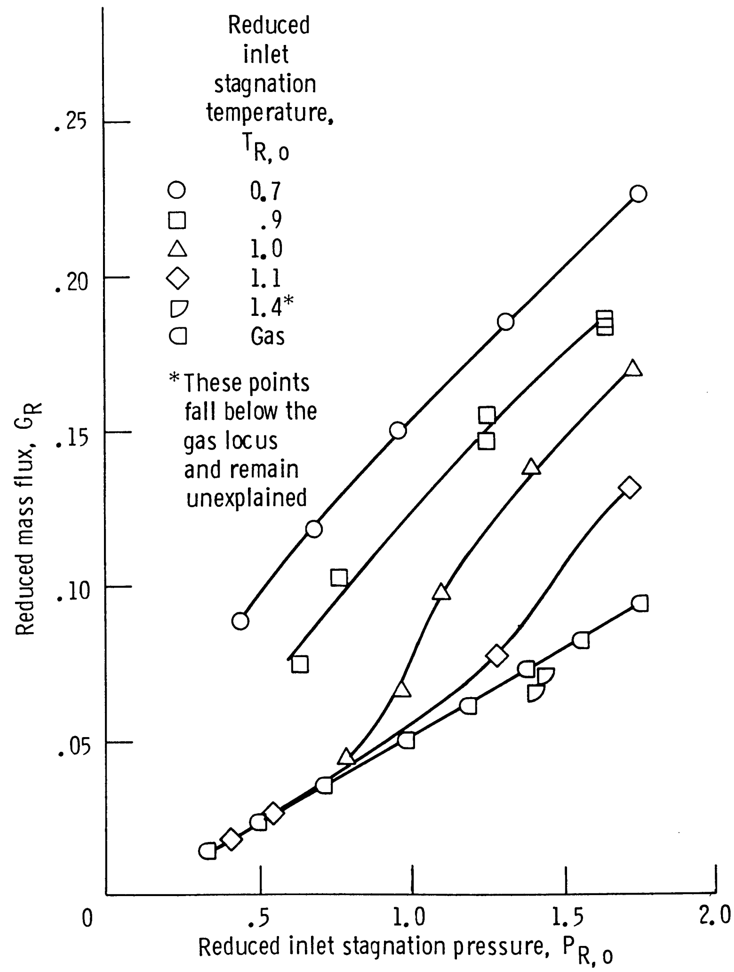

Figure 18.—Reduced mass flux of fluid nitrogen through three-step labyrinth seal in fully eccentric position, with backpressure control, as function of reduced inlet stagnation pressure.

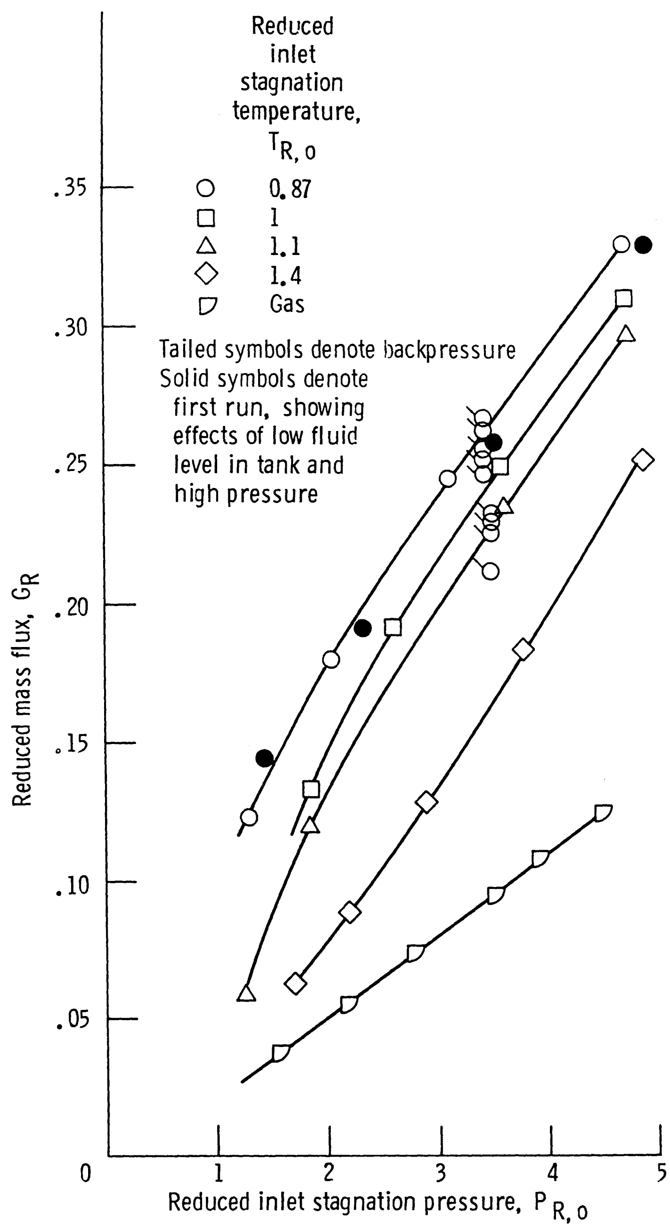

Figure 19.—Reduced mass flux of fluid hydrogen through three-step labyrinth seal in fully eccentric position, with backpressure control, as function of reduced inlet stagnation pressure.

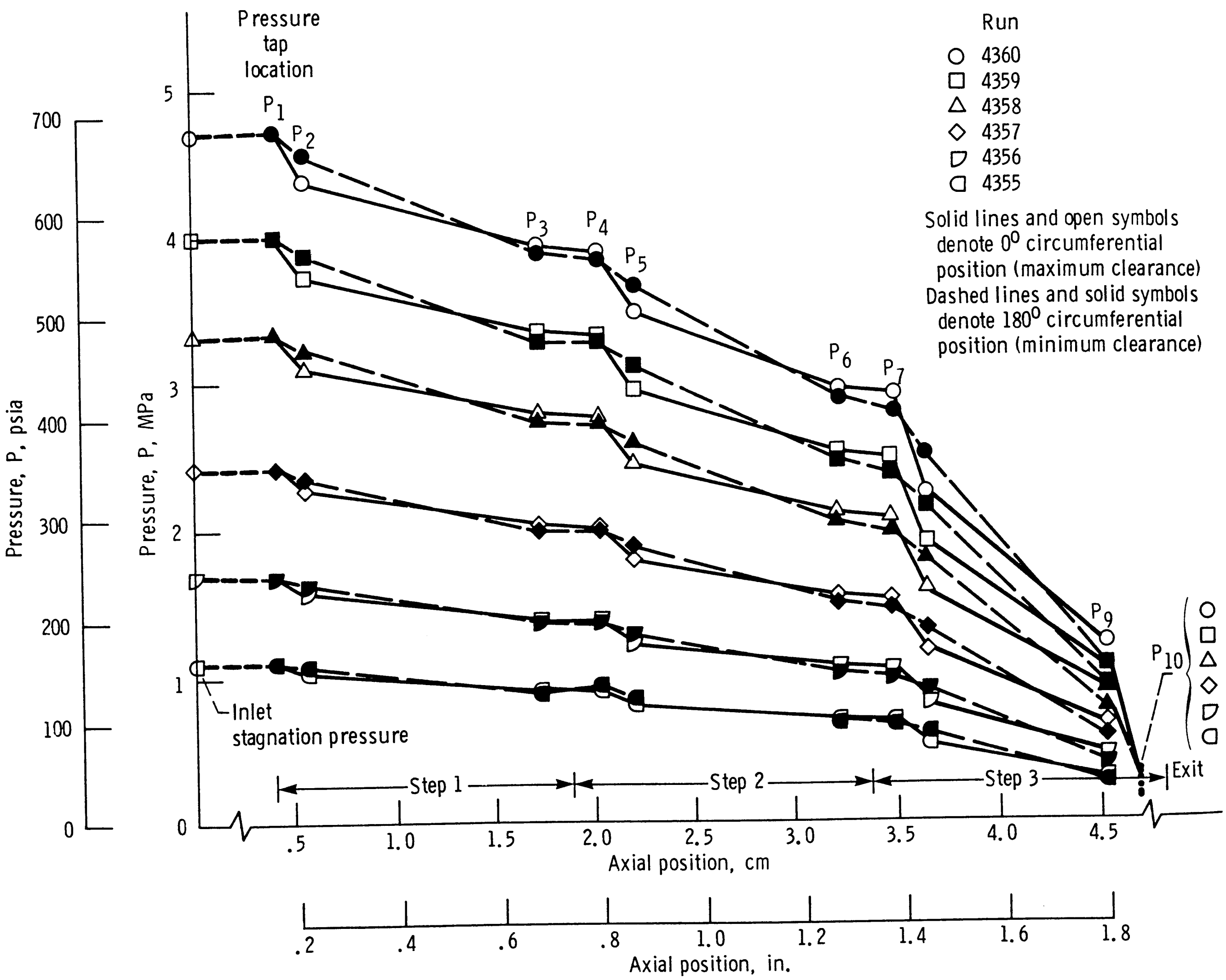

Figure 20.—Axial pressure distribution for gaseous nitrogen flow through three-step labyrinth seal in fully eccentric position. Nominal reduced inlet stagnation temperature $T_{R,o} \approx 2.3$.

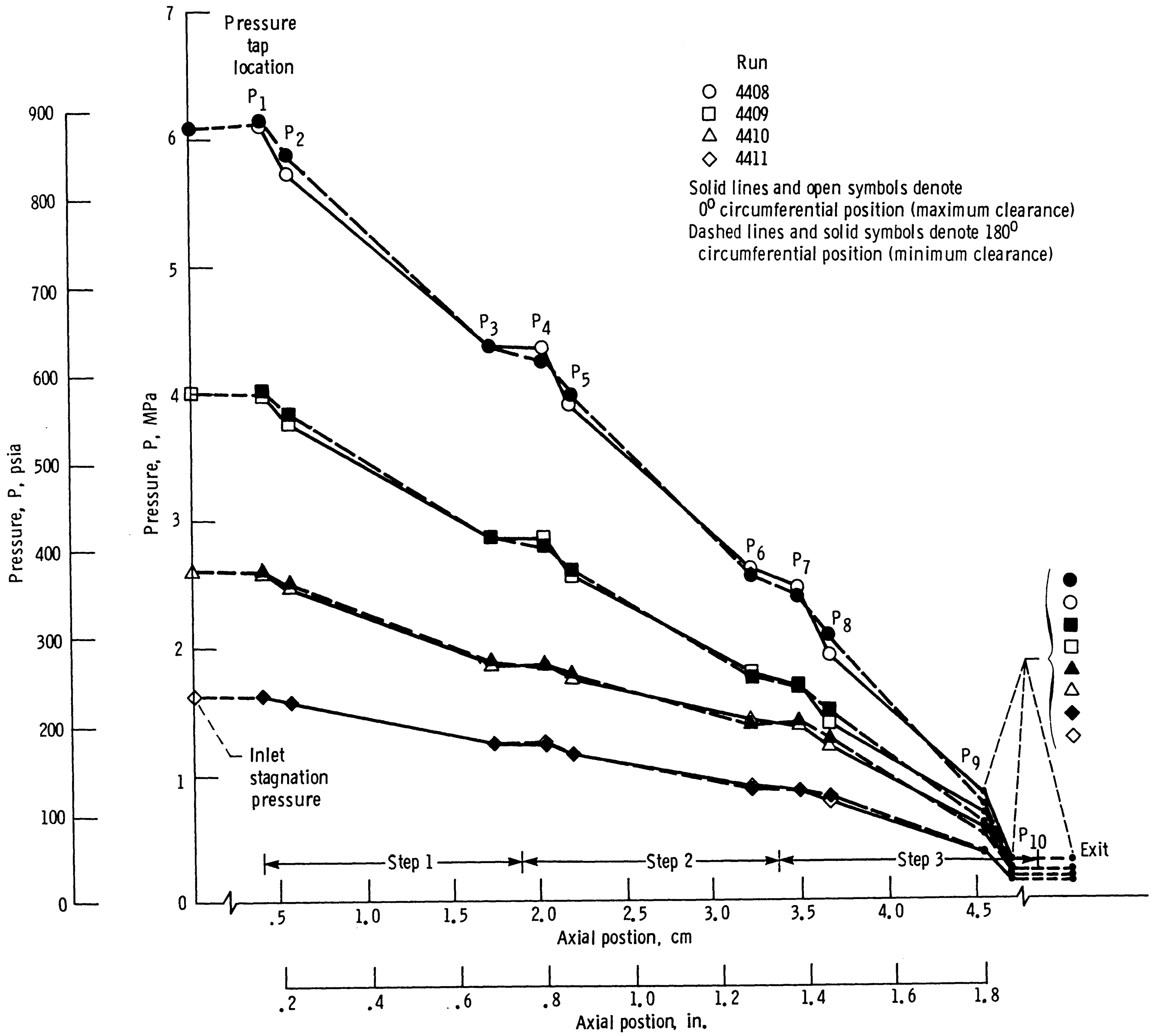

Figure 21.—Axial pressure distribution for fluid hydrogen flow through three-step labyrinth seal in fully eccentric position.

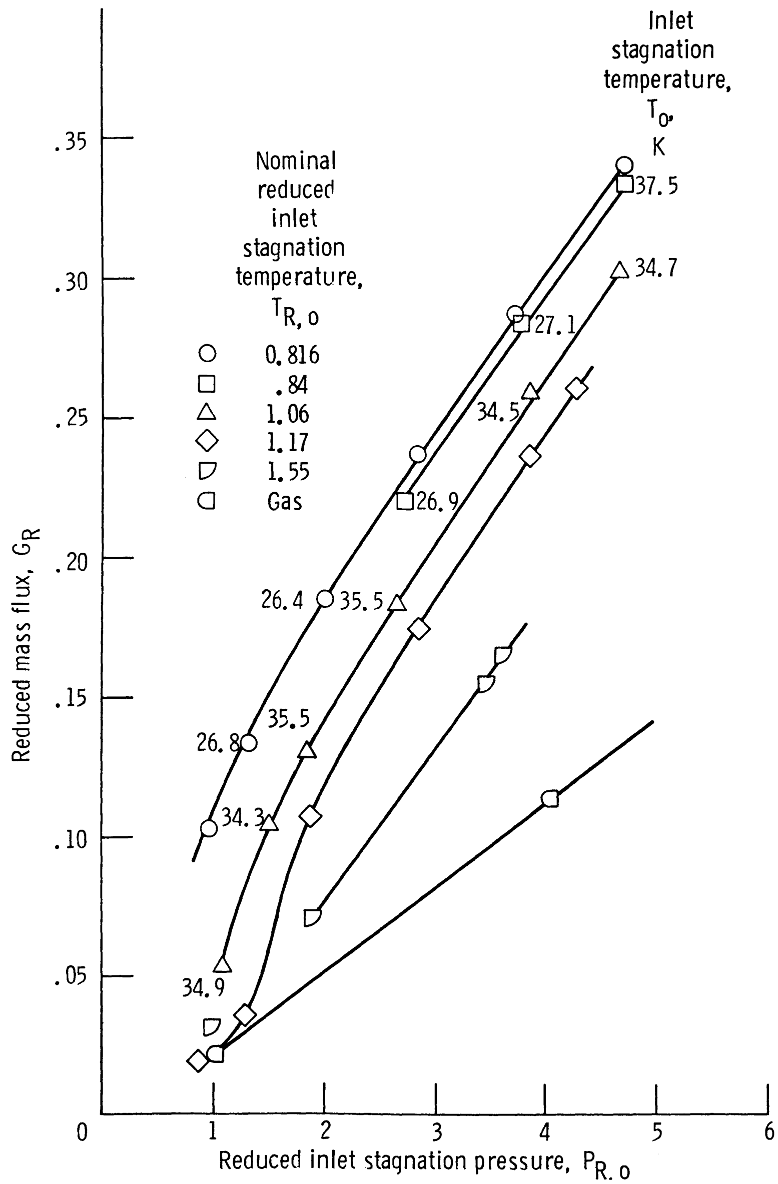

Figure 22.—Reduced mass flux of fluid hydrogen through three-step labyrinth seal in two-thirds fully eccentric position, as function of reduced inlet stagnation pressure.

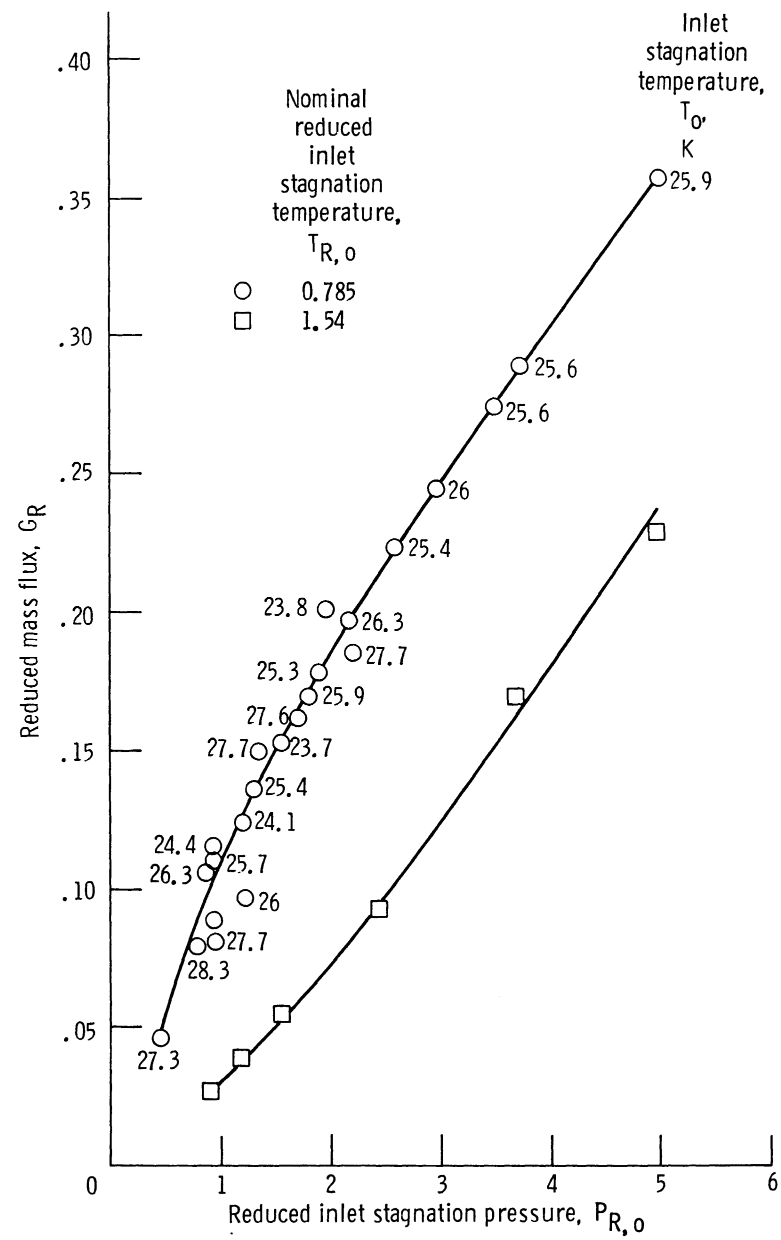

Figure 23.—Reduced mass flux of fluid hydrogen through three-step labyrinth seal in two-thirds fully eccentric position, as function of reduced inlet stagnation pressure.

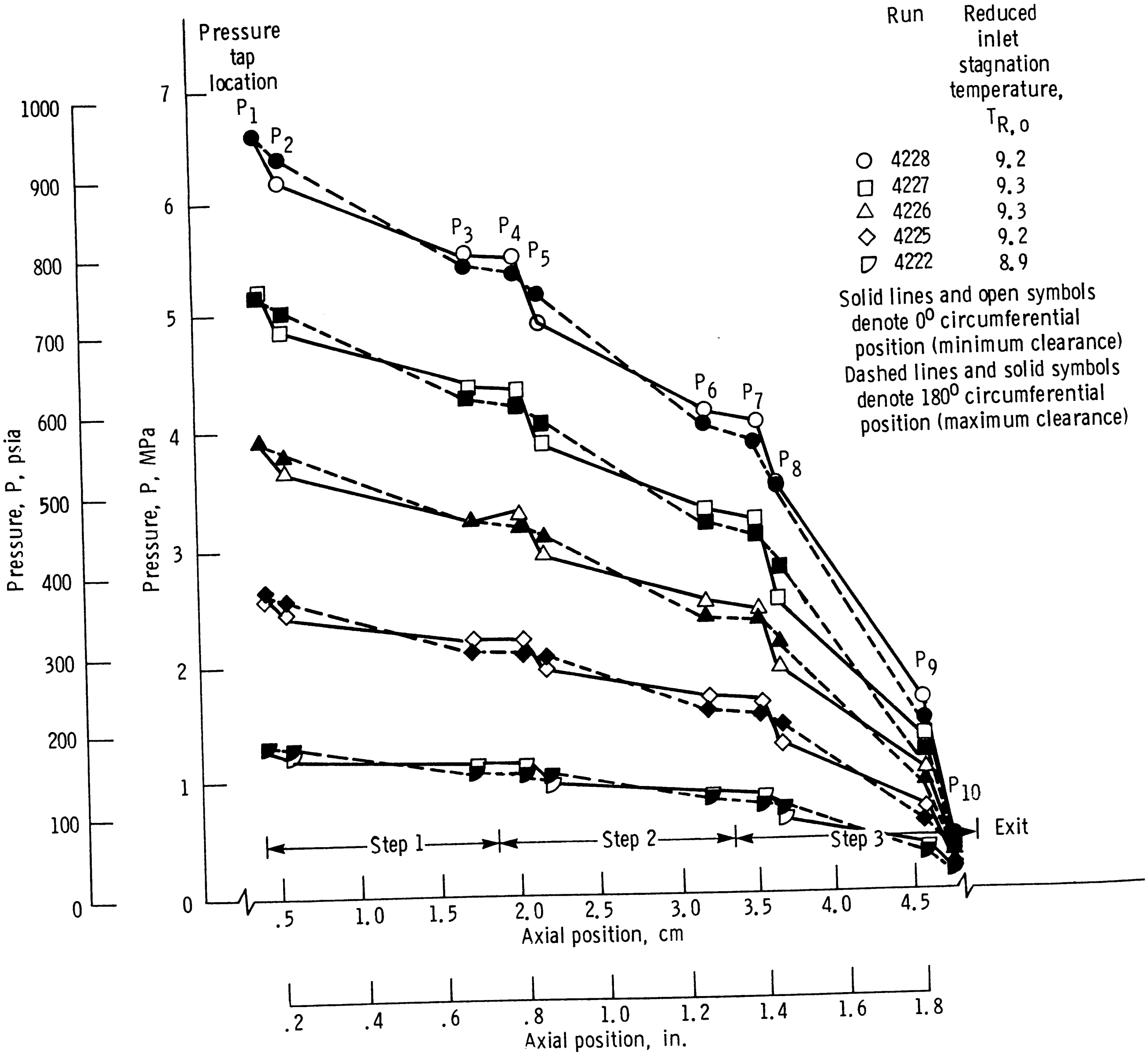

Figure 24.—Axial pressure distribution for gaseous hydrogen flow through three-step labyrinth seal in two-thirds fully eccentric position.

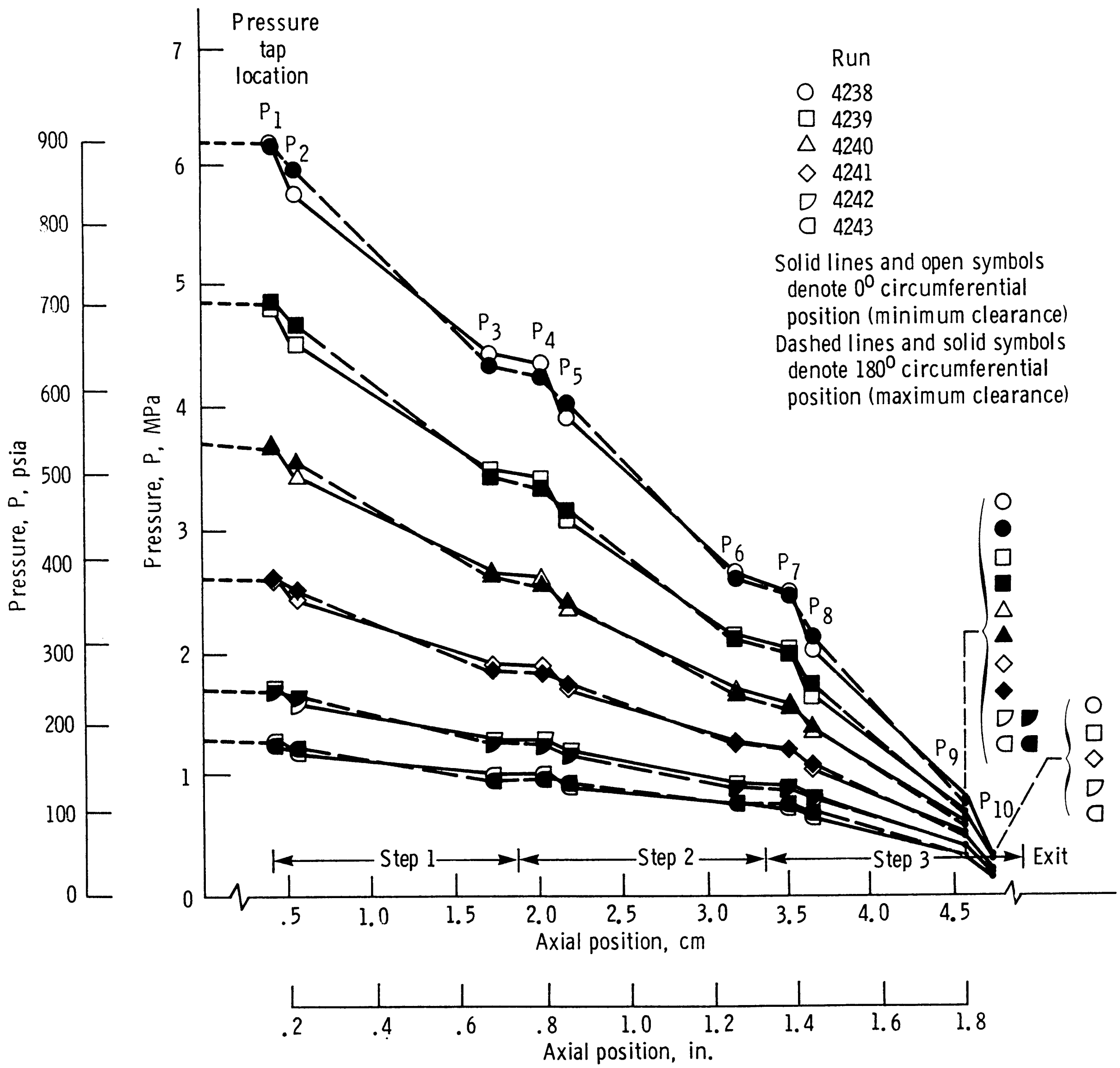

Figure 25.—Axial pressure distribution for fluid hydrogen flow through three-step labyrinth seal in two-thirds fully eccentric position.

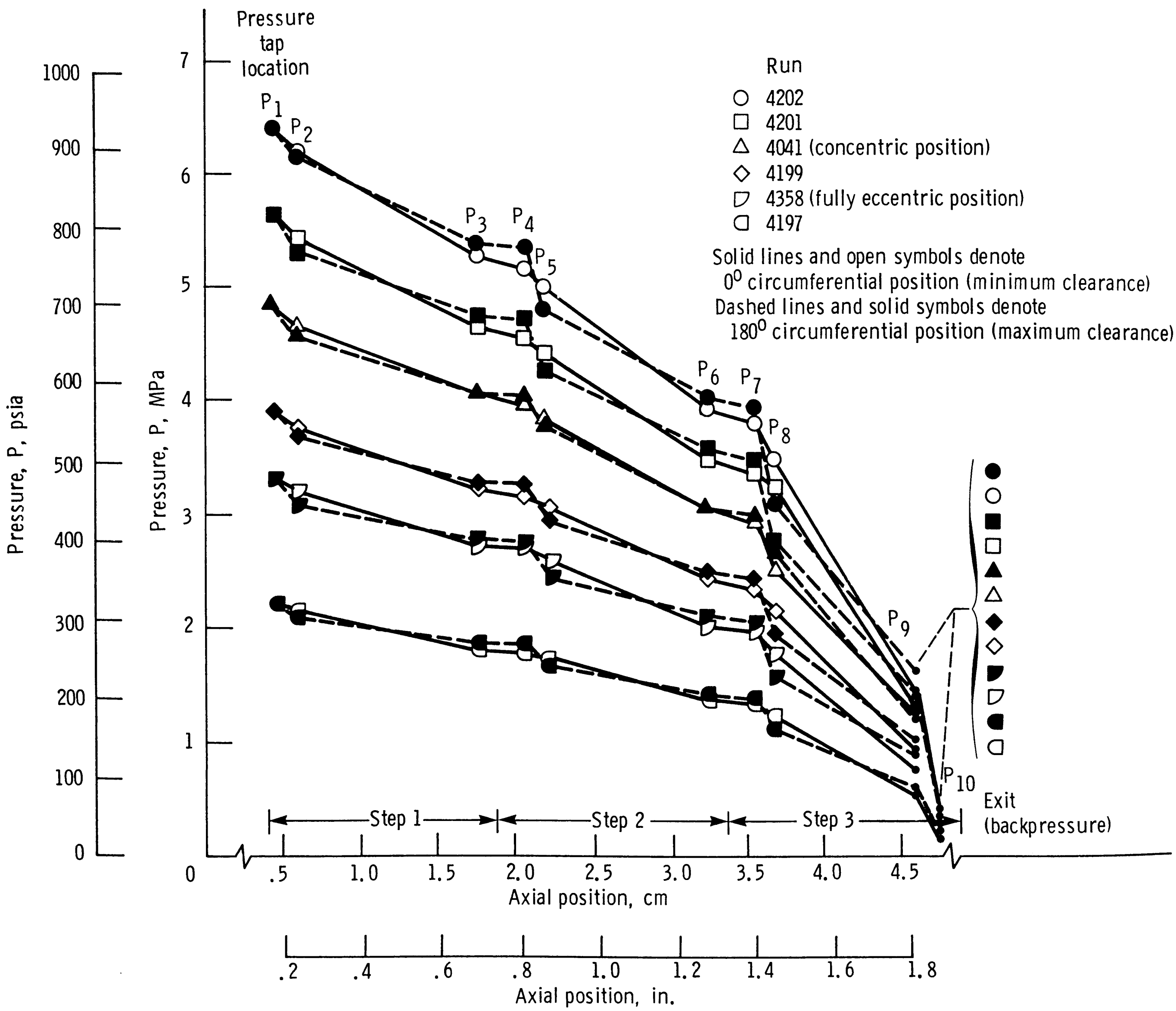

Figure 26.—Axial pressure distribution for gaseous nitrogen flow through three-step labyrinth seal in two-thirds fully eccentric, fully eccentric, and concentric positions.

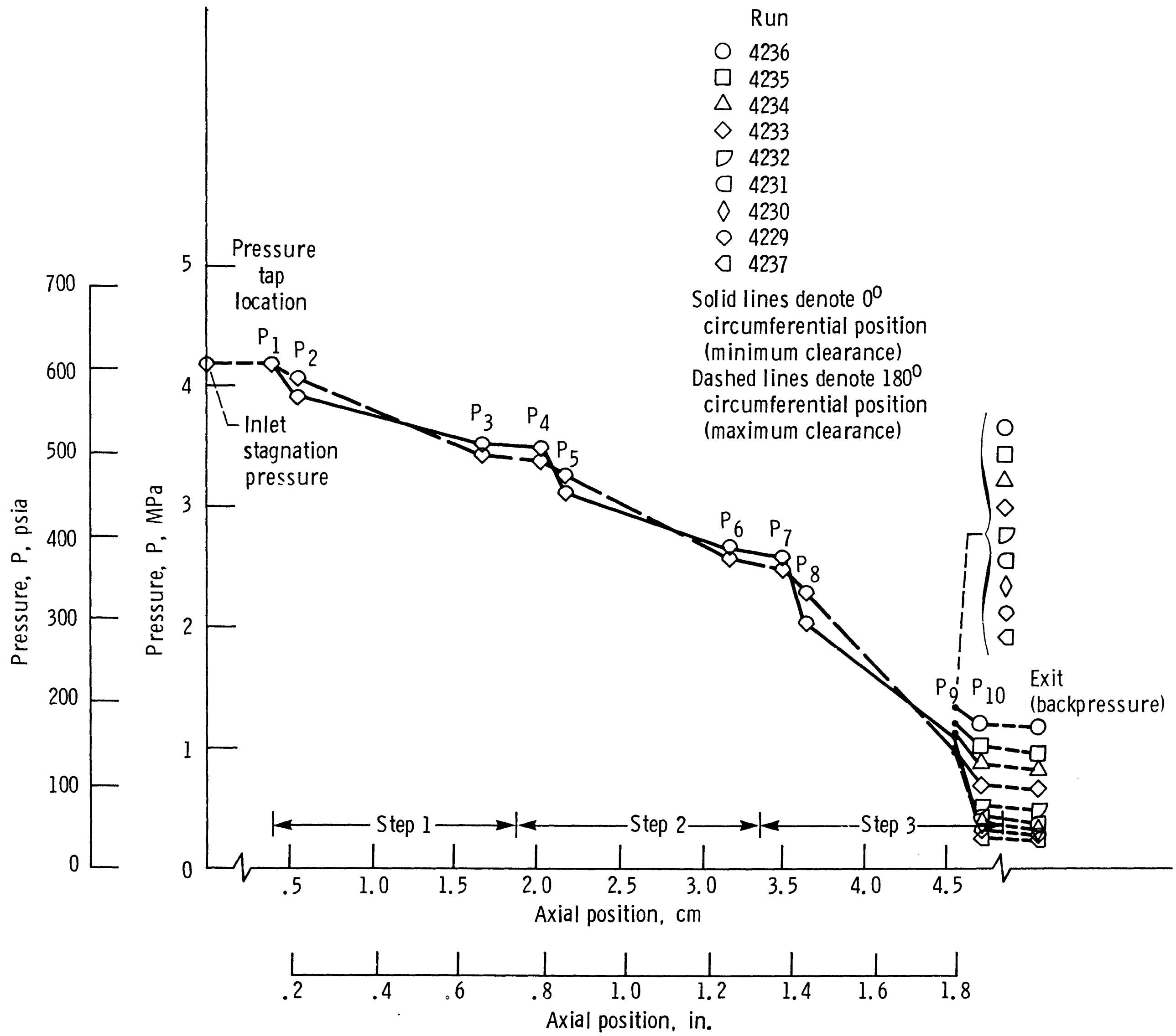

Figure 27.—Axial pressure distribution for gaseous hydrogen flow through three-step labyrinth seal in two-thirds fully eccentric position, with backpressure control. Nominal reduced inlet stagnation temperature $T_{R,o} \approx 9$.

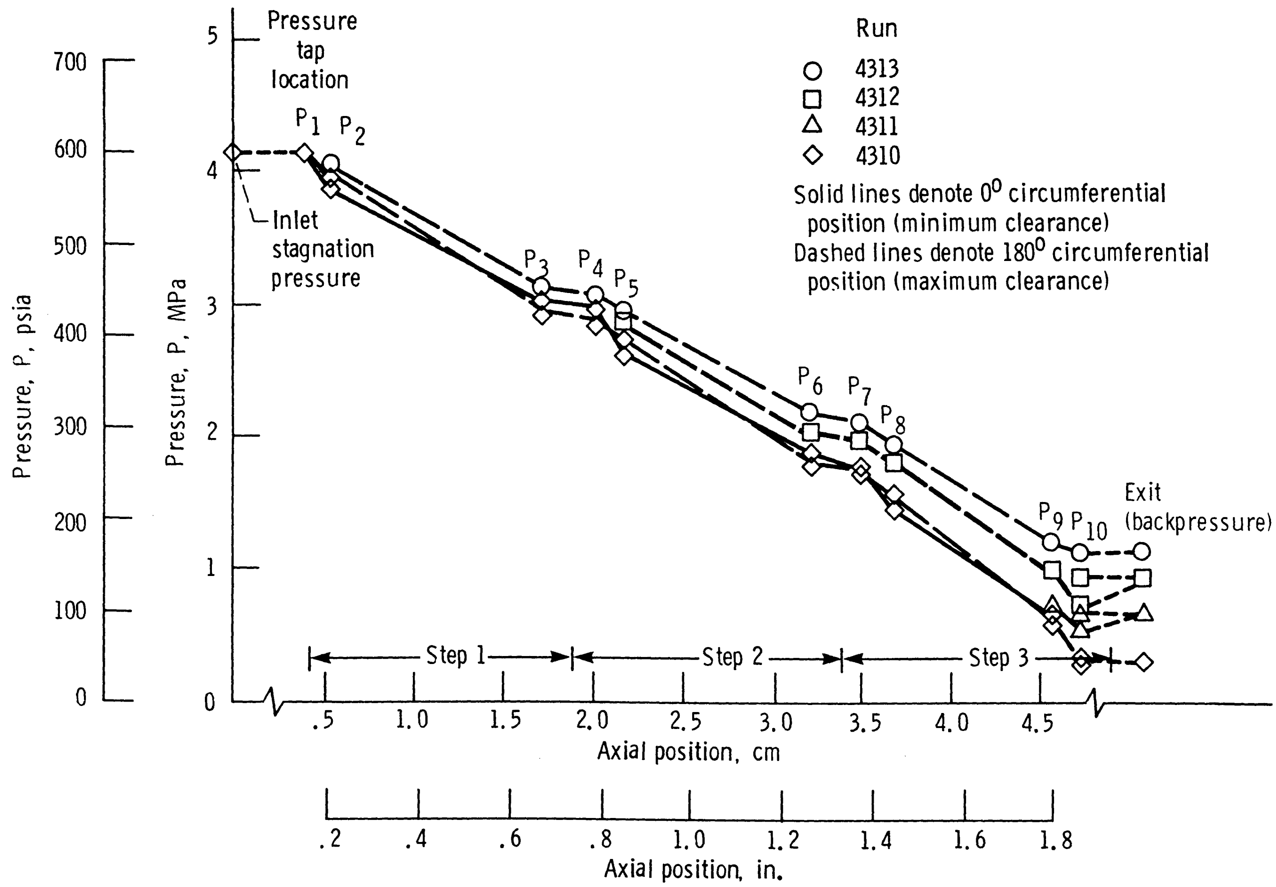

Figure 28.—Axial pressure distribution for fluid hydrogen flow through three-step labyrinth seal in two-thirds fully eccentric position, with backpressure control. Nominal reduced inlet stagnation temperature $T_{R,o} \approx 0.8$.

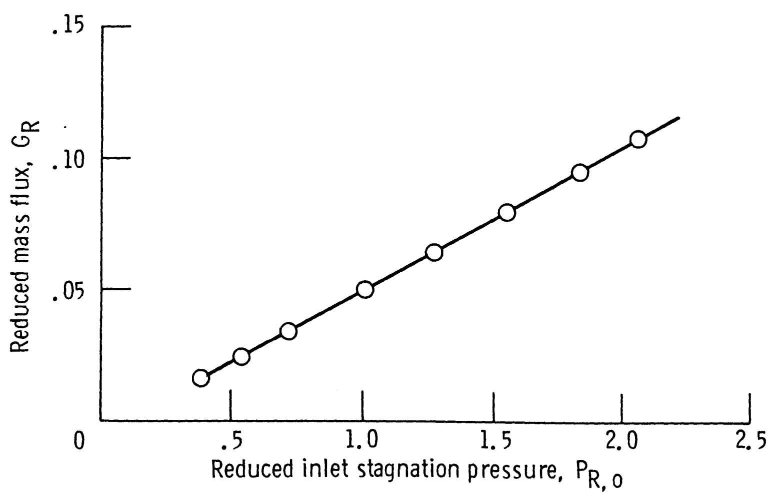

Figure 29.—Reduced mass flux of gaseous nitrogen through three-step labyrinth seal in one-third fully eccentric position, as function of reduced inlet stagnation pressure.

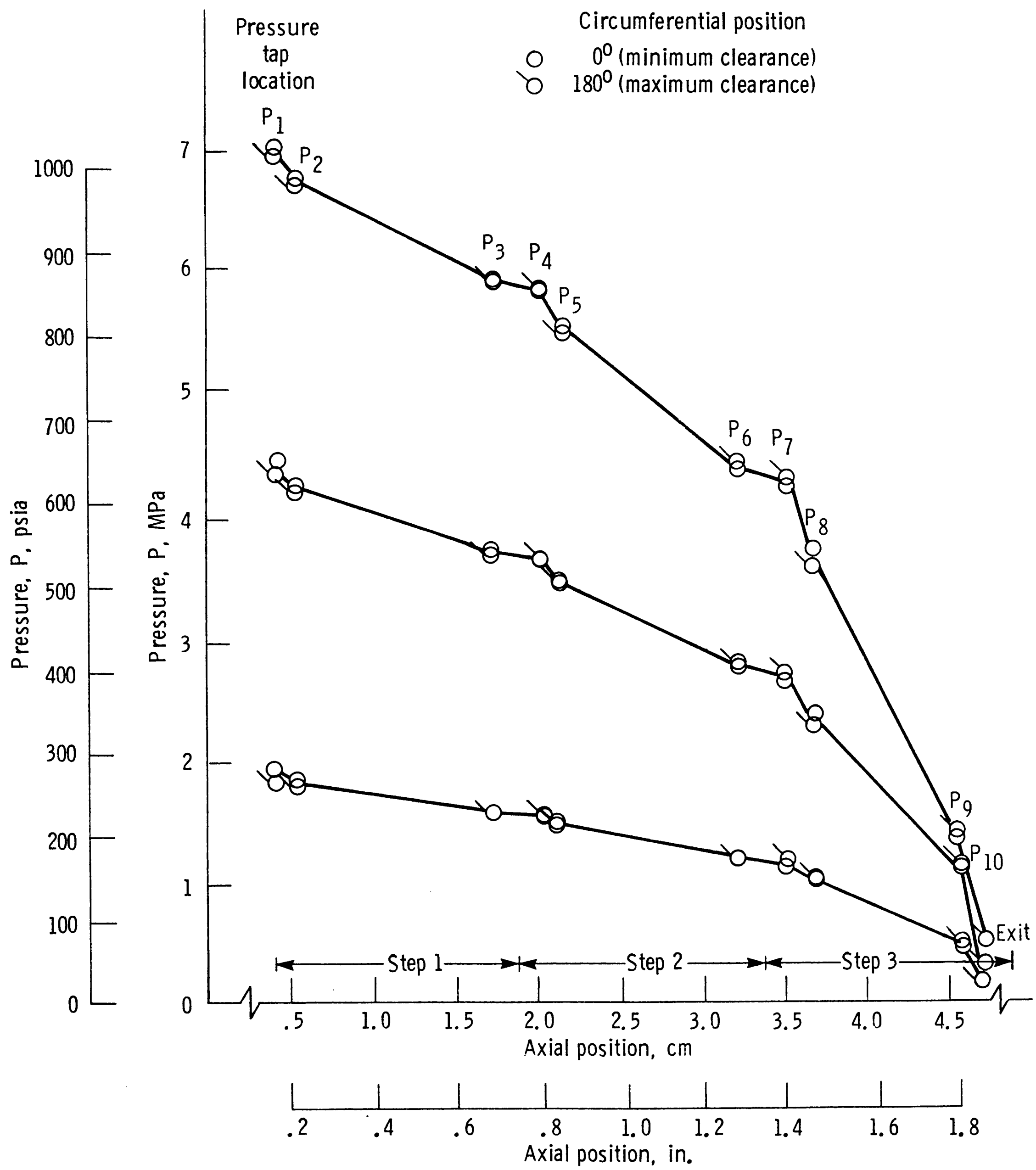

Figure 30.—Axial pressure distribution for gaseous nitrogen flow through three-step labyrinth seal in one-third fully eccentric position. (No tabulated data availiable.)

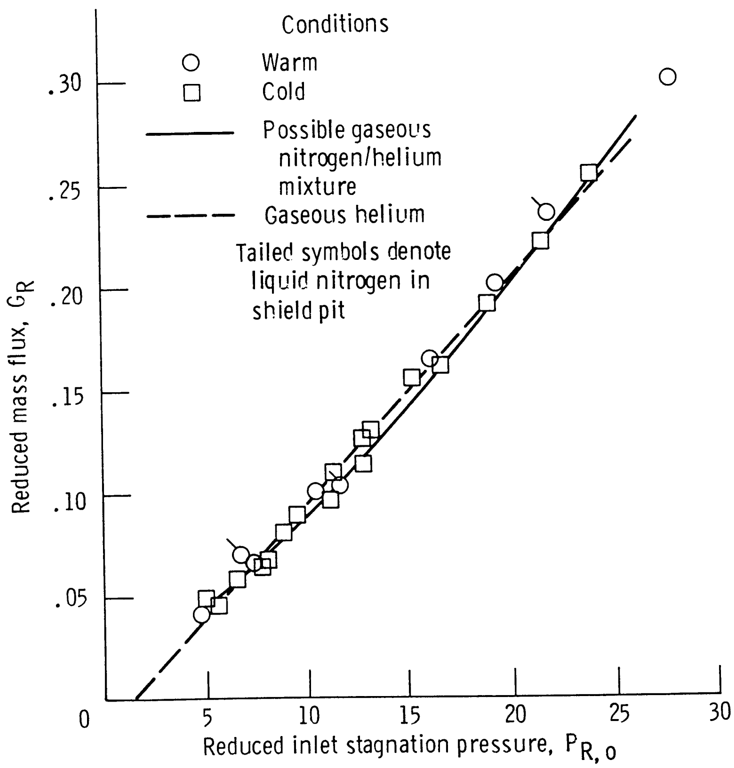

Figure 31.—Reduced mass flux of gaseous helium through three-step labyrinth seal in two-thirds fully eccentric position, as function of reduced inlet stagnation pressure. Area A, 0.3228 cm^2 (0.050 in.^{2}); normalized flow G^*A, 232.8 g/s (0.512 lbm/s).

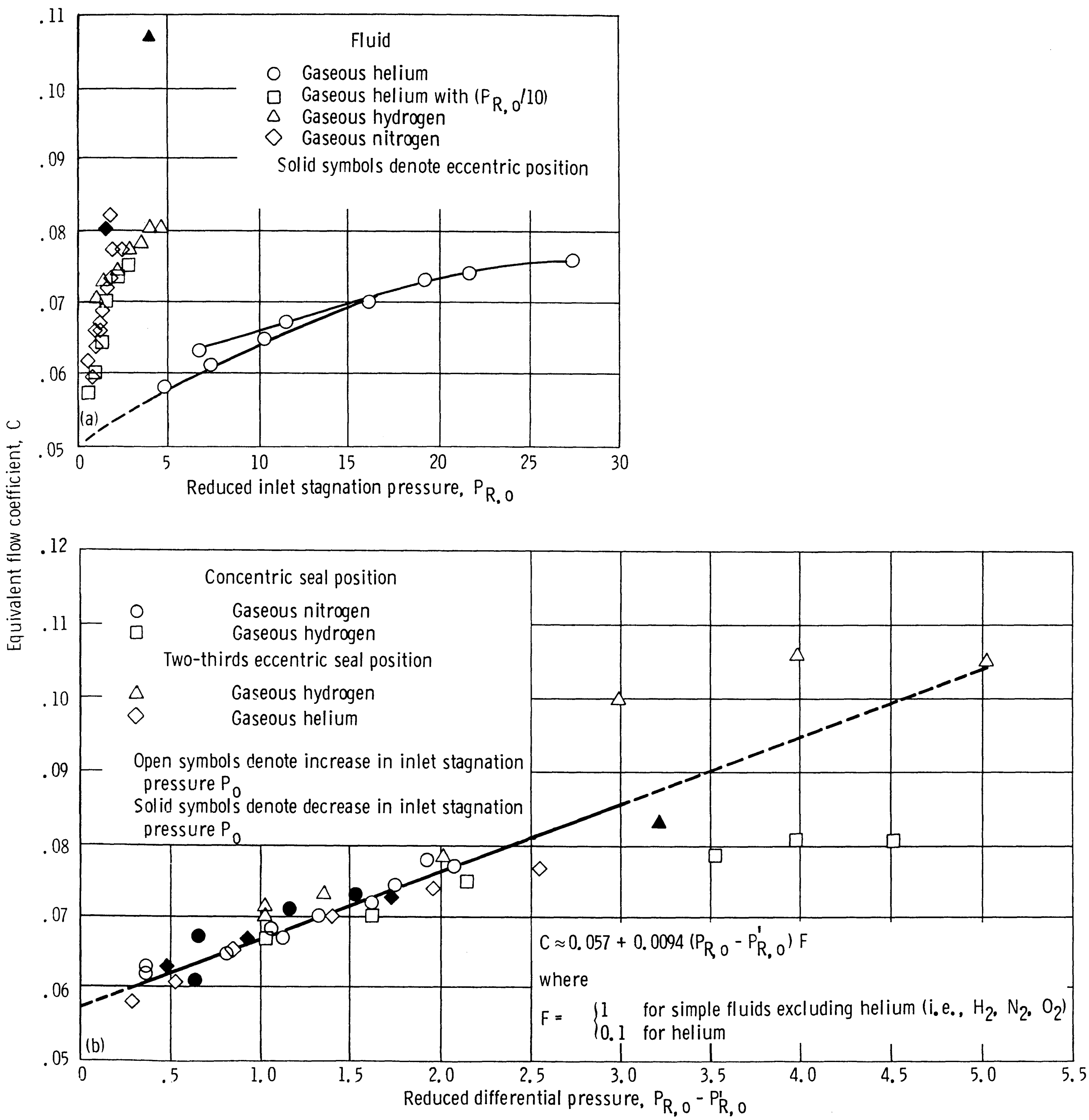

(a) Normalized with respect to inlet stagnation pressure.
(b) Normalized with respect to pressure differential $P_{R,o} - P'_{R,o}$, where $P_{R,o} - P'_{R,o}$ is $(P_{R,o} - P'_{R,o})/10$ for helium.

Figure 32.—Equivalent flow coefficient for gaseous nitrogen, hydrogen, and helium.

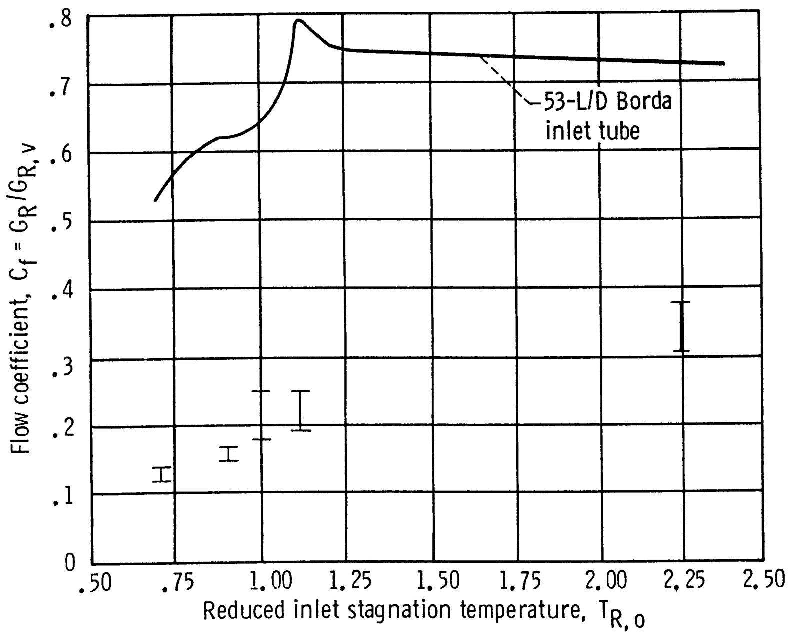

Figure 33.—Variation of flow coefficient with reduced inlet stagnation temperature for fluid nitrogen, with curve for Borda inlet tube with length-to-diameter ratio of 53.

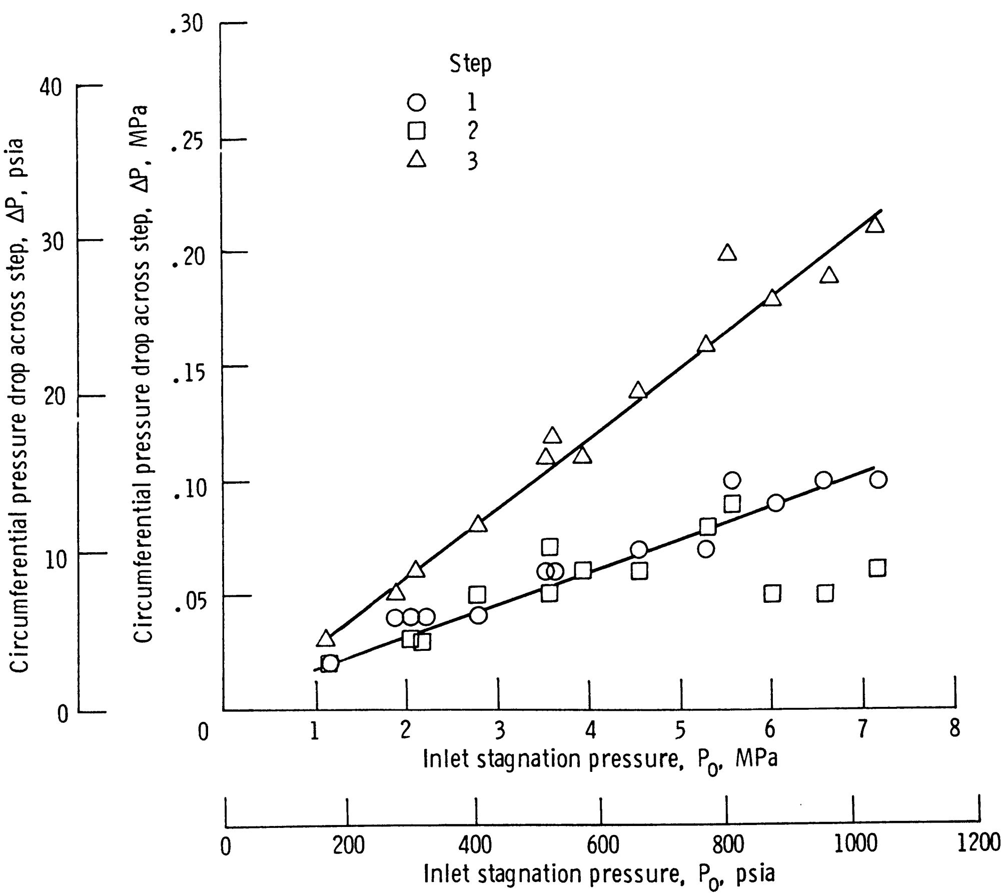

Figure 34.—Circumferential pressure drop in expansion cavity of first tooth of each step of three-step labyrinth seal in concentric position, for gaseous nitrogen, as function of reduced inlet stagnation pressure.

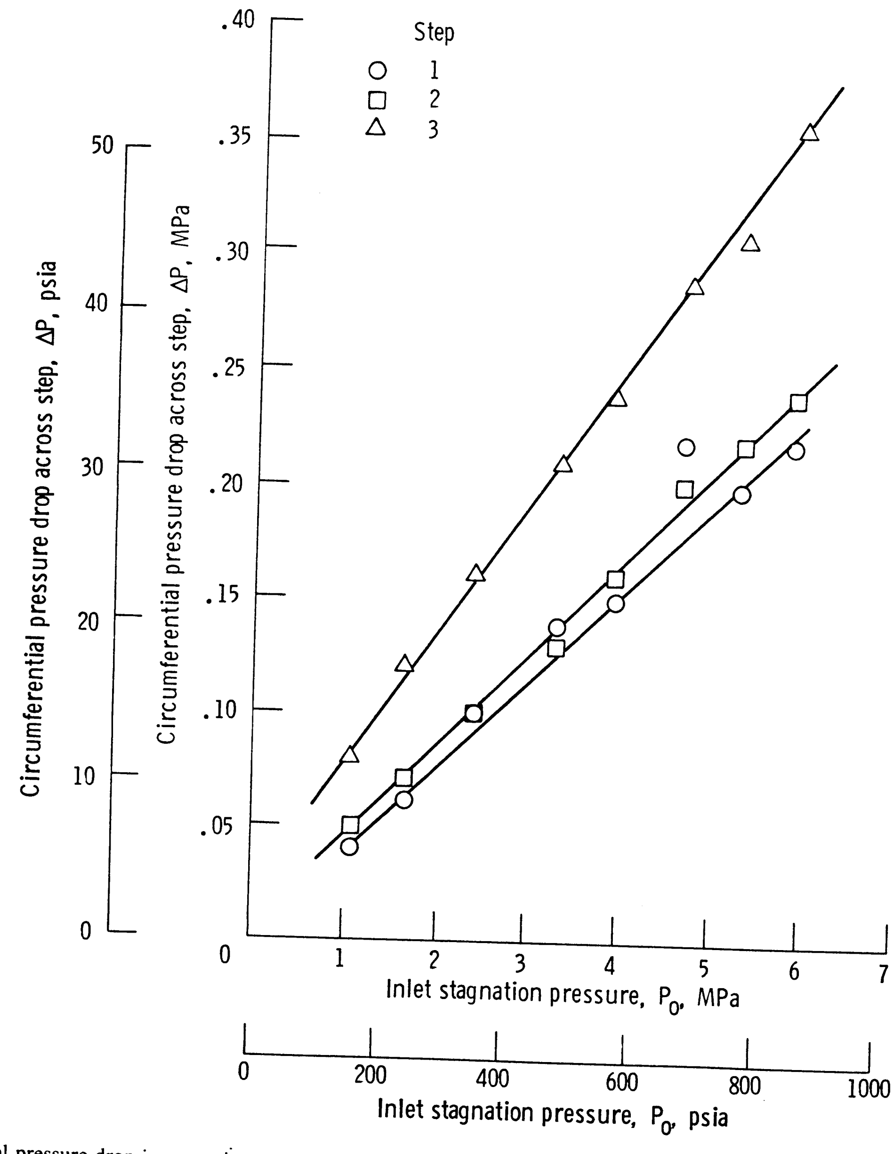

Figure 35.—Circumferential pressure drop in expansion cavity of first tooth of each step of three-step labyrinth seal in fully eccentric position, for gaseous nitrogen, as function of reduced inlet stagnation pressure.

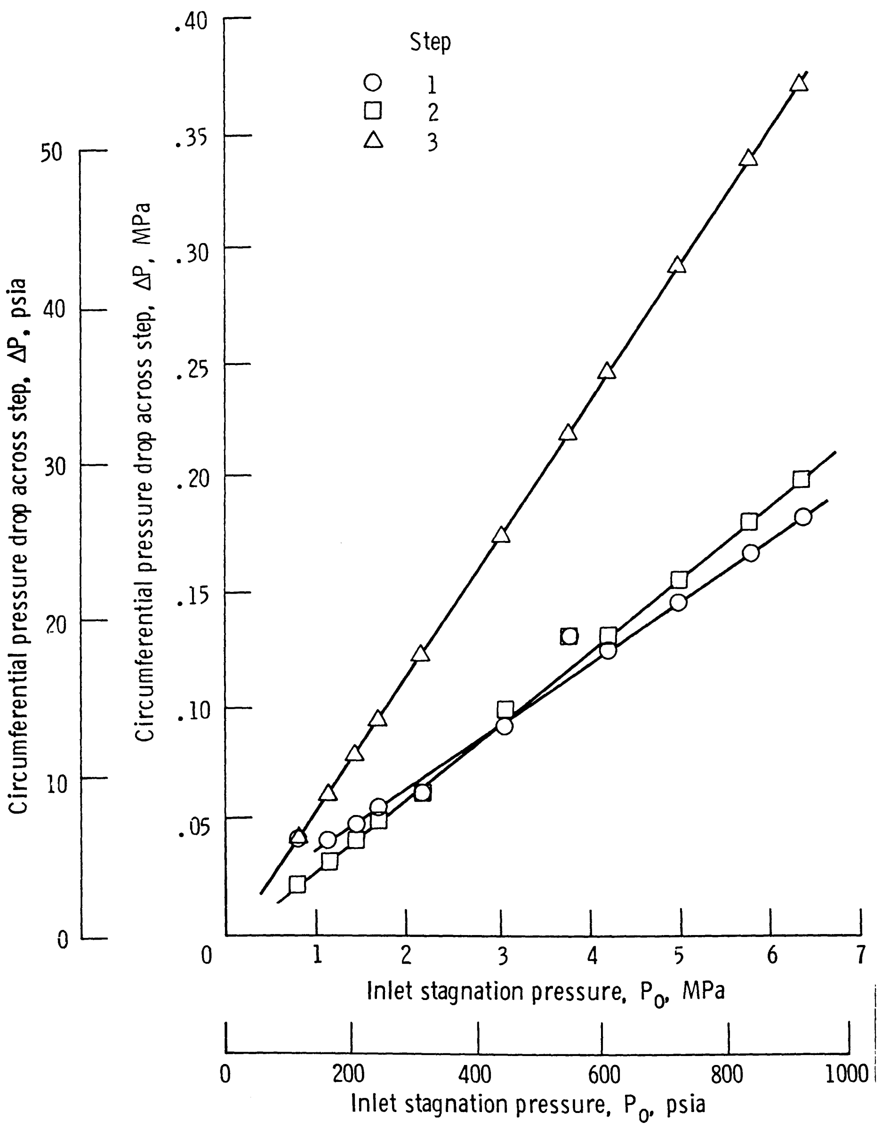

Figure 36.—Circumferential pressure drop in expansion cavity of first tooth of each step of three-step labyrinth seal in two-thirds fully eccentric position, for gaseous nitrogen, as function of reduced inlet stagnation pressure.

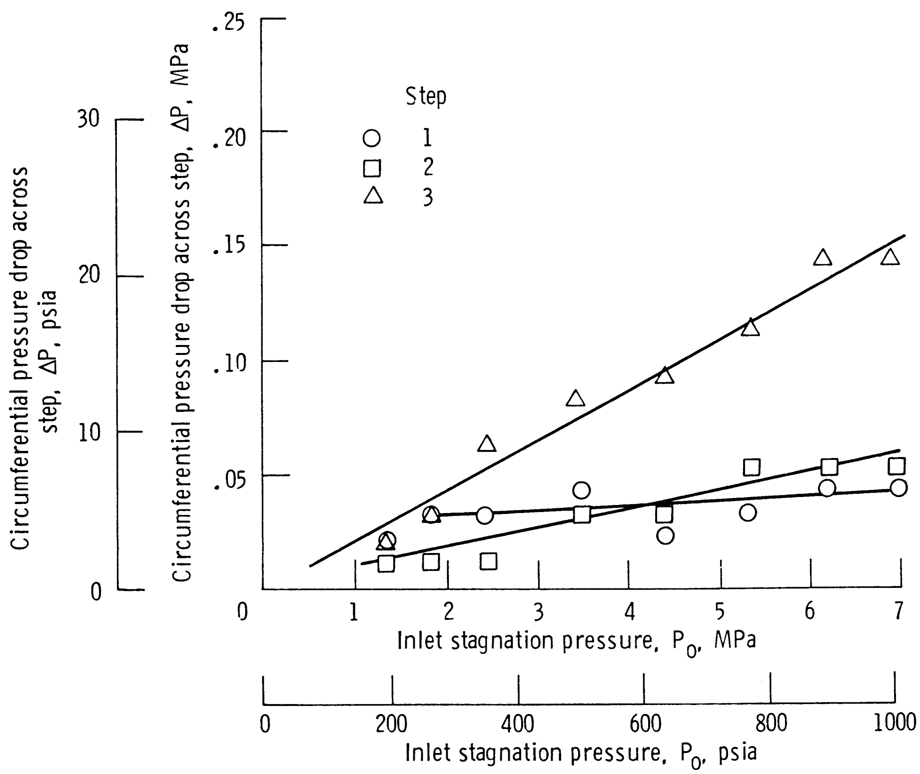

Figure 37.—Circumferential pressure drop in expansion cavity of first tooth of each step of three-step labyrinth seal in one-third fully eccentric position, for gaseous nitrogen, as function of reduced inlet stagnation pressure.

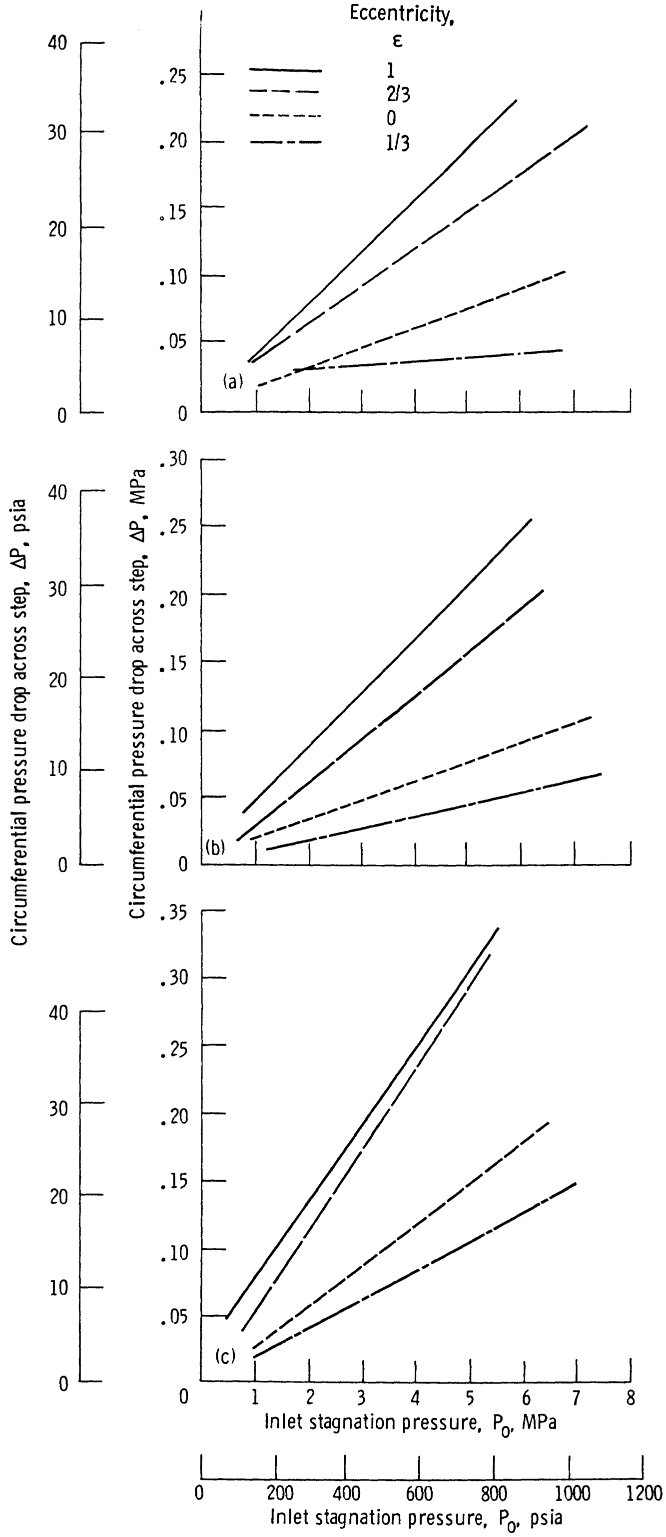

(a) Step 1.
(b) Step 2.
(c) Step 3.

Figure 38.—Circumferential pressure drop at each step of three-step labyrinth seal in concentric, one-third fully eccentric, two-thirds fully eccentric, and fully eccentric positions, for gaseous nitrogen, as function of reduced inlet stagnation pressure.

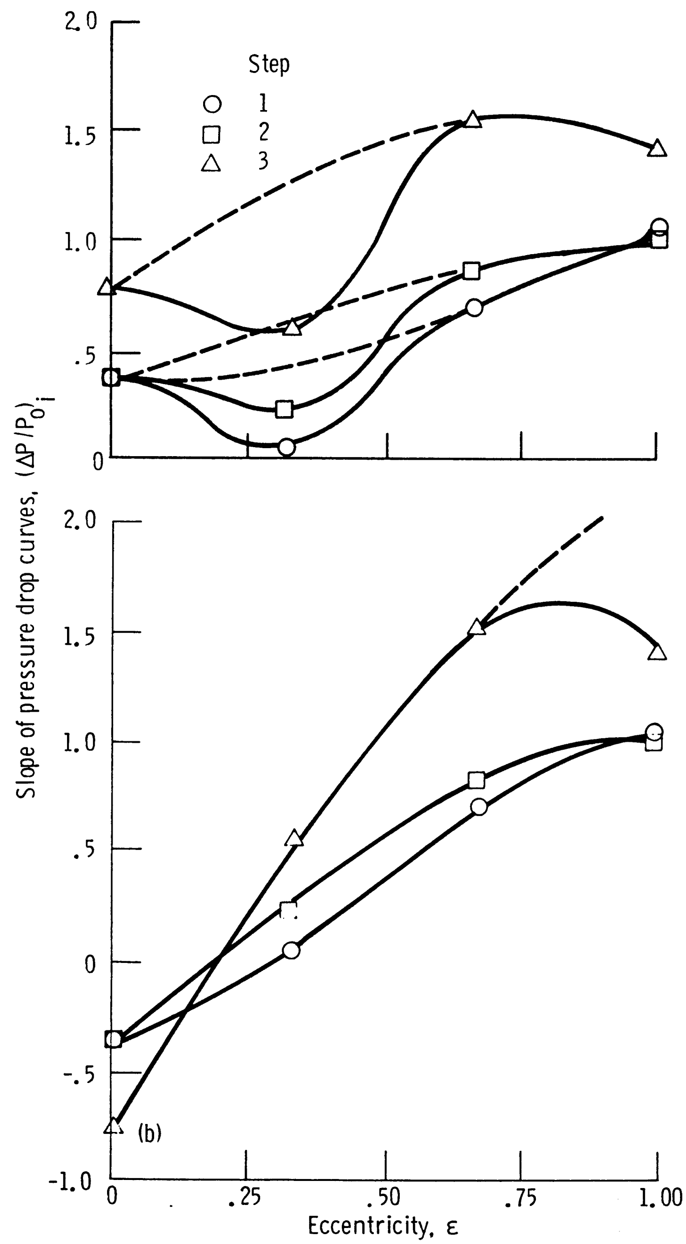

(a) True position.
(b) Positioning error, 0.002 cm (0.0008 in.).

Figure 39.—Slope of pressure difference, $\Delta P = P_{0^\circ} - P_{180^\circ}$, to inlet stagnation pressure P_o, at entrance of each step of three-step labyrinth seal, as function of eccentricity.

TABLE I.—FLOW RATE AND PRESSURE DROP DATA FOR THREE-STEP LAYBRINTH SEAL, CONCENTRIC POSITION

[Where two values are given, the top value is for the 0° circumferential position, and the bottom value is for the 180° circumferential position.]

(a) Nitrogen

Run	$\dot{w}$, g/s	T_o, K	P_o, MPa	$P_{R,o}$	G_R	$T_{R,o}$	P_B, MPa	Pressure at pressure tap locations 1 to 10, MPa										P_e, MPa
								P_1	P_2	P_3	P_4	P_5	P_6	P_7	P_8	P_9	P_{10}	
3985	28.17	268.3	1.19 1.19	0.349	0.015	2.124	0.115	1.16 1.16	1.14 1.11	0.97 0.97	0.96 1.00	0.92 0.90	0.73 0.73	0.71 0.72	0.65 0.63	0.32 0.32	0.22 0.10	0.12
3986	46.86	268.7	1.92 1.92	0.562	0.024	2.127	0.143	1.90 1.90	1.84 1.80	1.58 1.59	1.55 1.59	1.50 1.46	1.20 1.19	1.15 1.18	1.05 1.00	0.50 0.51	0.19 0.10	0.14
3987	70.51	272.0	2.79 2.81	0.817	0.036	2.154	0.192	2.78 2.79	2.69 2.64	2.32 2.34	2.28 2.33	2.19 2.15	1.75 1.76	1.69 1.72	1.54 1.46	0.72 0.74	0.23 0.10	0.19
3988	92.19	274.1	3.55 3.58	1.039	0.048	2.170	0.239	3.55 3.55	3.42 3.37	2.95 2.98	2.91 2.97	2.80 2.74	2.23 2.24	2.15 2.19	1.96 1.85	0.90 0.93	0.27 0.10	0.24
3989	122.09	277.9	4.54 4.59	1.329	0.063	2.200	0.308	4.56 4.56	4.38 4.32	3.80 3.83	3.74 3.79	3.60 3.53	2.86 2.87	2.76 2.80	2.50 2.36	1.13 1.17	0.34 0.10	0.31
3990	168.84	282.3	5.99 6.05	1.753	0.087	2.235	0.420	6.02 6.02	5.75 5.70	5.02 5.06	4.94 5.02	4.76 4.67	3.76 3.78	3.63 3.68	3.27 3.09	1.46 1.52	0.44 0.00	0.42
3991	145.21	281.2	5.24 5.30	1.534	0.075	2.226	0.361	5.26 5.26	5.05 4.98	4.39 4.42	4.32 4.38	4.16 4.08	3.30 3.31	3.18 3.23	2.88 2.72	1.30 1.34	0.39 0.00	0.36
3992	208.66	285.8	7.13 0.31	2.087	0.108	2.263	0.517	7.18 7.17	6.85 6.79	5.99 6.03	5.89 5.97	5.67 5.57	4.47 4.50	4.31 4.37	3.87 3.66	1.71 1.78	0.53 0.00	0.52
3993	106.17	281.0	3.93 3.97	1.150	0.055	2.225	0.270	3.92 3.93	3.78 3.72	3.28 3.30	3.22 3.28	3.11 3.05	2.48 2.49	2.39 2.44	2.16 2.07	0.99 1.03	0.30 0.00	0.27
3994	56.29	280.4	2.21 2.22	0.646	0.029	2.220	0.162	2.18 2.19	2.12 2.08	1.82 1.84	1.79 1.85	1.73 1.70	1.38 1.38	1.33 1.36	1.21 1.17	0.57 0.59	0.20 0.10	0.16
3995	193.11	288.8	6.63 6.71	1.942	0.100	2.287	0.484	6.67 6.67	6.37 6.32	5.57 5.60	5.47 5.56	5.27 5.17	4.16 4.18	4.01 4.06	3.59 3.40	1.61 1.66	0.50 0.00	0.48
3996	428.51	89.5	5.89 5.97	1.725	0.221	0.709	0.197	5.94 5.94	5.64 5.60	4.08 4.11	3.92 4.00	3.70 3.66	2.21 2.20	2.04 2.06	1.75 1.69	0.41 0.44	0.25 0.10	0.20
3997	372.08	89.8	4.77 4.83	1.397	0.192	0.711	0.191	4.80 4.80	4.56 4.52	3.29 3.32	3.16 3.23	3.00 2.96	1.84 1.83	1.71 1.73	1.48 1.44	0.38 0.41	0.24 0.00	0.19
3998	291.98	90.5	3.34 3.37	0.977	0.151	0.717	0.175	3.36 3.35	3.21 3.15	2.32 2.34	2.24 2.29	2.13 2.09	1.38 1.36	1.29 1.30	1.14 1.11	0.37 0.39	0.22 0.00	0.18
3999	234.86	89.7	2.42 2.44	0.708	0.121	0.710	0.159	2.41 2.41	2.31 2.27	1.68 1.70	1.63 1.68	1.55 1.53	1.04 1.02	0.98 0.99	0.88 0.86	0.33 0.35	0.21 0.10	0.16
4000	182.94	90.0	1.73 1.74	0.507	0.094	0.713	0.147	1.71 1.71	1.66 1.62	1.23 1.23	1.18 1.23	1.14 1.12	0.80 0.78	0.76 0.77	0.69 0.69	0.31 0.33	0.20 0.10	0.15

TABLE I.—Continued.

(a) Continued.

Run	$\dot{w}$, g/s	T_o, K	P_o, MPa	$P_{R,o}$	G_R	$T_{R,o}$	P_B, MPa	Pressure at pressure tap locations 1 to 10, MPa										P_e, MPa
								P_1	P_2	P_3	P_4	P_5	P_6	P_7	P_8	P_9	P_{10}	
4001	154.99	90.7	1.40 1.40	0.409	0.080	0.718	0.142	1.37 1.37	1.33 1.30	1.00 1.01	0.97 1.02	0.93 0.93	0.68 0 67	0.65 0.66	0.60 0.60	0.31 0.32	0.19 0.10	0.14
4002	376.31	116.2	5.89 5.96	1.725	0.194	0.920	0.373	5.94 5.94	5.67 5.63	4.45 4.49	4.33 4.40	4.16 4.11	3.00 2.98	2.86 2.88	2.62 2.55	1.29 1.35	0.43 0.10	0.37
4003	291.30	115.2	4.25 4.30	1.244	0.150	0.912	0.267	4.27 4.27	4.11 4.06	3.29 3.31	3.21 3.26	3.10 3.07	2.37 2.36	2.29 2.30	2.13 2.09	1.11 1.14	0.31 0.10	0.27
4004	214.27	114.0	2.93 2.96	0.858	0.110	0.903	0.208	2.93 2.93	2.84 2.81	2.35 2.36	2.31 2.35	2.24 2.22	1.83 1.82	1.78 1.79	1.69 1.67	0.87 0.89	0.25 0.00	0.21
4005	144.89	115.2	2.07 2.08	0.606	0.075	0.912	0.166	2.06 2.06	2.02 2.00	1./7 1.77	1.74 1.78	1.71 1.69	1.42 1.40	1.37 1.38	1.28 1.26	0.64 0.66	0.22 0.00	0.17
4006	121.51	115.1	1.90 1.91	0.556	0.063	0.911	0.155	1.88 1.89	1.86 1.84	1.62 1.63	1.59 1.63	1.56 1.53	1.27 1.25	1.23 1.24	1.14 1.12	0.57 0.59	0.21 0.10	0.16
4007	322.40	127.4	5.69 5.76	1.664	0.166	1.009	0.339	5.74 5.73	5.51 5.46	4.54 4.57	4.44 4.51	4.30 4.26	3.37 3.36	3.27 3.28	3.06 2.99	1.44 1.50	0.38 0.00	0.34
4008	234.77	127.4	4.23 4.28	1.238	0.121	1.009	0.268	4.25 4.25	4.13 4.08	3.51 3.53	3.45 3.50	3.37 3.34	2.80 2.79	2.72 2.73	2.55 2.49	1.17 1.21	0.31 0.10	0.27
4009	121.56	126.2	3.28 3.32	0.959	0.063	0.999	0.212	3.29 3.30	3.22 3.19	2.78 2.79	2.73 2.78	2.66 2.62	2.17 2.16	2.11 2.11	1.95 1.88	0.90 0.94	0.26 0.10	0.21
4010	102.37	127.1	3.03 3.07	0.888	0.053	1.006	0.170	3.04 3.04	2.97 2.93	2.54 2.56	2.50 2.54	2.44 2.41	1.99 1.98	1.93 1.94	1.81 1.75	0.82 0.86	0.22 0.00	0.17
4011	68.78	126.5	2.38 2.41	0.698	0.035	1.002	0.138	2.38 2.38	2.32 2.29	1.96 1.98	1.93 1.98	1.88 1.87	1.52 1.51	1.47 1.49	1.39 1.36	0.62 0.66	0.19 0.00	0.14
4012	33.86	127.7	1.45 1.46	0.426	0.017	1.011	0.108	1.43 1.43	1.41 1.38	1.17 1.18	1.15 1.20	1.12 1.11	0.90 0.89	0.87 0.89	0.82 0.81	0.37 0.39	0.16 0.10	0.11
4013	222.26	143.6	5.69 5.77	1.666	0.115	1.137	0.401	5.74 5.74	5.55 5.51	4.74 4.77	4.65 4.70	4.53 4.49	3.63 3.63	3.52 3.54	3.30 3.21	1.48 1.56	0.44 0.00	0.40
4014	140.67	140.5	4.23 4.29	1.239	0.073	1.112	0.231	4.27 4.27	4.16 4.10	3.54 3.56	3.47 3.52	3.39 3.34	2.73 2.71	2.64 2.65	2.47 2.40	1.12 1.17	0.27 0.00	0.23
4015	89.96	141.2	3.21 3.24	0.939	0.046	1.118	0.171	3.21 3.22	3.13 3.09	2.66 2.68	2.61 2.65	2.55 2.53	2.05 2.04	1.99 2.00	1.85 1.81	0.83 0.87	0.22 0.10	0.17
4016	37.22	142.0	1.64 1.65	0.479	0.019	1.124	0.112	1.62 1.62	1.58 1.56	1.33 1.34	1.31 1.35	1.27 1.26	1.03 1.01	0.99 1.01	0.92 0.92	0.42 0.44	0.16 0.10	0.11
4017	370.28	89.6	4.85 4.91	1.420	0.191	0.709	0.298	4.88 4.88	4.65 4.60	3.40 3.43	3.28 3.34	3.12 3.08	1.97 1.95	1.83 1.85	1.60 1.56	0.44 0.47	0.35 0.00	0.30

TABLE I.—Continued.

(a) Concluded.

Run	$\dot{w}$, g/s	T_o, K	P_o, MPa	$P_{R,o}$	G_R	$T_{R,o}$	P_B, MPa	Pressure at pressure tap locations 1 to 10, MPa										P_e, MPa
								P_1	P_2	P_3	P_4	P_5	P_6	P_7	P_8	P_9	P_{10}	
4032	52.44	247.3	2.10 2.10	0.615	0.027	1.958	0.154	2.07 2.08	2.01 1.98	1.72 1.74	1.70 1.74	1.64 1.60	1.30 1.30	1.25 1.28	1.16 1.10	0.53 0.55	0.20 0.10	0.15
4033	52.48	248.7	2.12 2.12	0.619	0.027	1.969	0.152	2.09 2.09	2.04 1.98	1.73 1.75	1.71 1.77	1.65 1.61	1.31 1.31	1.27 1.30	1.17 1.11	0.53 0.56	0.19 0.09	0.15
4034	94.41	259.7	3.59 3.62	1.052	0.049	2.056	0.241	3.58 3.59	3.46 3.40	2.98 3.01	2.94 3.01	2.84 2.77	2.25 2.26	2.18 2.22	2.00 1.88	0.89 0.94	0.28 0.09	0.24
4035	155.72	268.7	5.53 5.59	1.619	0.080	2.127	0.380	5.55 5.55	5.34 5.25	4.63 4.67	4.55 4.62	4.40 4.30	3.48 3.50	3.35 3.41	3.06 2.86	1.34 1.42	0.41 0.10	0.38

(b) Nitrogen with backpressure control

Run	$\dot{w}$, g/s	T_o, K	P_o, MPa	$P_{R,o}$	G_R	$T_{R,o}$	P_B, MPa	Pressure at pressure tap locations 1 to 10, MPa										P_e, MPa
								P_1	P_2	P_3	P_4	P_5	P_6	P_7	P_8	P_9	P_{10}	
4018	370.91	89.8	4.85 4.91	1.418	0.191	0.711	0.192	4.88 4.87	4.64 4.59	3.40 3.42	3.27 3.35	3.11 3.07	1.95 1.94	1.82 1.83	1.58 1.54	0.40 0.44	0.24 0.00	0.19
4019	363.66	90.4	4.85 4.91	1.420	0.187	0.716	0.479	4.89 4.88	4.65 4.60	3.44 3.46	3.32 3.38	3.16 3.12	2.05 2.03	1.92 1.94	1.70 1.65	0.58 0.59	0.51 0.10	0.48
4020	357.56	91.6	4.86 4.92	1.421	0.184	0.725	0.614	4.89 4.89	4.66 4.61	3.48 3.50	3.36 3.43	3.21 3.17	2.13 2.12	2.01 2.02	1.79 1.75	0.71 0.72	0.64 0.10	0.61
4021	351.66	92.4	4.86 4.93	1.424	0.181	0.732	0.756	4.90 4.89	4.67 4.63	3.53 3.55	3.41 3.47	3.26 3.23	2.22 2.21	2.10 2.12	1.89 1.85	0.85 0.85	0.79 0.10	0.76
4022	345.66	93.0	4.87 4.93	1.426	0.178	0.736	0.899	4.90 4.90	4.68 4.64	3.57 3.60	3.46 3.53	3.32 3.28	2.31 2.30	2.20 2.22	2.00 1.95	0.99 0.99	0.92 0.10	0.90
4023	338.78	93.9	4.88 4.94	1.428	0.175	0.743	1.036	4.91 4.91	4.70 4.65	3.62 3.64	3.51 3.58	3.38 3.34	2.40 2.39	2.30 2.31	2.10 2.06	1.13 1.13	1.06 0.00	1.04
4024	316.96	95.0	4.90 4.97	1.435	0.163	0.752	1.525	4.94 4.94	4.74 4.70	3.78 3.80	3.68 3.74	3.56 3.53	2.71 2.69	2.62 2.63	2.44 2.41	1.59 1.59	1.53 0.10	1.52
4025	346.02	87.9	4.86 4.91	1.421	0.178	0.696	0.923	4.89 4.89	4.67 4.61	3.51 3.53	3.39 3.47	3.25 3.21	2.24 2.22	2.12 2.14	1.92 1.88	1.00 1.01	0.95 0.10	0.92
4026	340.80	88.4	4.85 4.92	1.421	0.176	0.700	1.023	4.89 4.89	4.67 4.62	3.54 3.57	3.43 3.49	3.29 3.25	2.30 2.29	2.20 2.21	2.00 1.96	1.10 1.10	1.04 0.00	1.02
4027	332.59	88.9	4.87 4.93	1.425	0.171	0.704	1.194	4.90 4.90	4.69 4.64	3.60 3.62	3.49 3.56	3.35 3.32	2.41 2.40	2.31 2.33	2.13 2.09	1.26 1.27	1.21 0.10	1.19

TABLE I.—Continued.

(b) Continued.

Run	$\dot{w}$, g/s	T_o, K	P_o, MPa	$P_{R,o}$	G_R	$T_{R,o}$	P_B, MPa	Pressure at pressure tap locations 1 to 10, MPa										P_e, MPa
								P_1	P_2	P_3	P_4	P_5	P_6	P_7	P_8	P_9	P_{10}	
4028	327.94	89.5	4.87 4.94	1.425	0.169	0.709	1.288	4.91 4.91	4.70 4.65	3.63 3.65	3.53 3.59	3.39 3.36	2.48 2.46	2.38 2.39	2.20 2.16	1.36 1.36	1.30 0.00	1.29
4029	318.96	90.1	4.88 4.95	1.428	0.164	0.713	1.476	4.92 4.92	4.72 4.67	3.70 3.72	3.60 3.66	3.47 3.44	2.60 2.59	2.51 2.52	2.34 2.30	1.54 1.54	1.49 0.00	1.48
4030	301.81	90.7	4.90 4.97	1.435	0.156	0.718	1.818	4.94 4.94	4.75 4.71	3.82 3.84	3.73 3.79	3.62 3.59	2.83 2.82	2.75 2.76	2.60 2.56	1.87 1.87	6.98 0.00	1.82
4031	367.45	90.3	4.82 4.88	1.411	0.189	0.715	0.214	4.85 4.86	4.61 4.55	3.32 3.35	3.19 3.26	3.03 2.99	1.87 1.85	1.73 1.76	1.51 1.46	0.40 0.43	0.71 0.10	0.21
4036	132.33	280.0	4.75 4.79	1.391	0.068	2.217	0.336	4.76 4.76	4.57 4.50	3.96 4.00	3.90 3.98	3.76 3.67	2.98 3.00	2.88 2.93	2.62 2.45	1.17 1.23	0.37 0.10	0.34
4037	132.75	277.9	4.77 4.81	1.395	0.068	2.200	0.474	4.77 4.77	4.59 4.51	3.98 4.01	3.91 3.98	3.77 3.68	2.99 3.01	2.89 2.94	2.63 2.46	1.17 1.24	0.50 0.00	0.47
4038	132.40	278.1	4.77 4.81	1.396	0.068	2.202	0.615	4.78 4.78	4.59 4.52	3.98 4.02	3.92 3.99	3.78 3.69	3.00 3.01	2.89 2.95	2.64 2.47	1.18 1.24	0.63 0.10	0.62
4039	131.88	278.3	4.78 4.82	1.398	0.068	2.203	0.746	4.78 4.78	4.60 4.52	3.99 4.02	3.92 4.00	3.78 3.69	3.00 3.02	2.90 2.95	2.64 2.47	1.18 1.25	0.76 0.10	0.75
4040	130.72	278.5	4.79 4.83	1.401	0.067	2.205	1.020	4.80 4.80	4.61 4.54	4.00 4.04	3.94 4.00	3.80 3.71	3.03 3.04	2.92 2.98	2.67 2.50	1.29 1.31	1.03 0.10	1.02
4041	129.22	278.7	4.80 4.85	1.406	0.067	2.207	1.302	4.81 4.81	4.63 4.56	4.03 4.07	3.97 4.03	3.83 3.75	3.08 3.09	2.98 3.03	2.74 2.57	1.49 1.48	1.31 0.10	1.30
4042	126.93	279.0	4.82 4.87	1.411	0.065	2.209	1.581	4.84 4.83	4.66 4.58	4.07 4.11	4.01 4.07	3.88 3.79	3.16 3.17	3.06 3.11	2.83 2.67	1.73 1.71	1.59 0.10	1.58
4043	133.47	279.1	4.77 4.82	1.397	0.069	2.210	0.339	4.78 4.78	4.61 4.52	3.99 4.02	3.92 3.99	3.79 3.70	3.00 3.02	2.90 2.95	2.64 2.47	1.18 1.24	0.37 0.10	0.34
4044	133.20	281.0	4.80 4.85	1.406	0.069	2.225	0.675	4.81 4.81	4.63 4.55	4.01 4.05	3.95 4.02	3.81 3.72	3.03 3.04	2.92 2.98	2.66 2.49	1.19 1.26	0.69 0.10	0.68
4045	132.90	281.1	4.81 4.85	1.407	0.069	2.226	0.747	4.81 4.81	4.63 4.55	4.02 4.05	3.95 4.03	3.81 3.72	3.03 3.04	2.92 2.98	2.66 2.49	1.20 1.26	0.76 0.10	0.75
4046	132.91	281.2	4.81 4.86	1.408	0.069	2.226	0.819	4.82 4.82	4.63 4.55	4.02 4.06	3.95 4.03	3.82 3.72	3.03 3.05	2.93 2.98	2.67 2.50	1.21 1.27	0.83 0.10	0.82
4048	133.29	282.1	4.83 4.88	1.413	0.069	2.234	0.890	4.84 4.84	4.65 4.57	4.04 4.07	3.97 4.05	3.83 3.74	3.05 3.06	2.94 3.00	2.68 2.51	1.23 1.28	0.89 0.10	0.89
4049	306.39	119.4	4.95 5.01	1.450	0.158	0.945	0.494	4.98 4.98	4.81 4.77	4.01 4.04	3.93 3.98	3.82 3.78	3.06 3.04	2.97 2.97	2.80 2.75	1.40 1.43	0.54 0.00	0.49

TABLE I.—Continued.

(b) Continued.

Run	$\dot{w}$, g/s	T_o, K	P_o, MPa	$P_{R,o}$	G_R	$T_{R,o}$	P_B, MPa	Pressure at pressure tap locations 1 to 10, MPa										P_e, MPa
								P_1	P_2	P_3	P_4	P_5	P_6	P_7	P_8	P_9	P_{10}	
4050	312.66	118.5	4.94 5.00	1.446	0.161	0.938	0.525	4.97 4.97	4.80 4.74	3.94 3.96	3.85 3.90	3.73 3.70	2.93 2.91	2.83 2.84	2.65 2.60	1.36 1.39	0.56 0.00	0.52
4051	311.98	118.5	4.94 5.00	1.446	0.161	0.938	0.683	4.97 4.96	4.79 4.74	3.92 3.95	3.84 3.90	3.72 3.69	2.91 2.89	2.81 2.82	2.63 2.58	1.37 1.39	0.71 0.10	0.68
4052	310.26	118.6	4.94 5.00	1.446	0.160	0.939	0.843	4.97 4.97	4.79 4.74	3.92 3.95	3.84 3.89	3.72 3.68	2.91 2.89	2.82 2.82	2.64 2.58	1.38 1.41	0.86 0.00	0.84
4053	307.96	118.8	4.94 5.00	1.446	0.159	0.941	0.975	4.97 4.97	4.79 4.74	3.93 3.95	3.84 3.90	3.72 3.69	2.92 2.90	2.82 2.83	2.65 2.60	1.42 1.43	0.99 0.10	0.98
4054	305.16	119.0	4.95 5.01	1.447	0.157	0.942	1.112	4.97 4.97	4.80 4.75	3.93 3.96	3.85 3.90	3.73 3.70	2.93 2.91	2.84 2.85	2.67 2.61	1.47 1.48	1.13 0.10	1.11
4055	301.81	119.3	4.95 5.01	1.449	0.156	0.945	1.254	4.98 4.98	4.80 4.76	3.95 3.97	3.86 3.91	3.75 3.71	2.95 2.94	2.86 2.87	2.69 2.64	1.54 1.55	1.26 0.10	1.25
4056	297.61	119.7	4.96 5.02	1.451	0.153	0.948	1.383	4.98 4.98	4.81 4.77	3.97 3.99	3.88 3.94	3.77 3.74	2.99 2.97	2.90 2.91	2.73 2.68	1.62 1.63	1.40 0.10	1.38
4057	311.05	119.8	4.94 5.00	1.445	0.160	0.949	0.403	4.96 4.96	4.79 4.74	3.94 3.97	3.86 3.92	3.74 3.71	2.93 2.92	2.84 2.85	2.67 2.61	1.36 1.39	0.44 0.10	0.40
4058	269.52	128.2	4.87 4.93	1.425	0.139	1.015	0.392	4.90 4.90	4.74 4.69	4.00 4.02	3.93 4.01	3.83 3.79	3.13 3.12	3.06 3.06	2.89 2.83	1.31 1.36	0.44 0.00	0.39
4059	269.14	128.3	4.87 4.93	1.425	0.139	1.016	0.473	4.90 4.90	4.74 4.69	4.00 4.02	3.93 4.01	3.82 3.79	3.13 3.12	3.06 3.07	2.89 2.83	1.32 1.37	0.51 0.10	0.47
4060	268.13	128.4	4.87 4.93	1.424	0.138	1.017	0.625	4.90 4.89	4.74 4.69	4.00 4.02	3.93 4.00	3.83 3.79	3.14 3.12	3.06 3.07	2.89 2.84	1.33 1.38	0.65 0.00	0.62
4061	266.86	128.6	4.87 4.93	1.424	0.138	1.018	0.770	4.89 4.90	4.74 4.69	4.00 4.03	3.93 3.99	3.83 3.79	3.14 3.13	3.06 3.08	2.90 2.84	1.35 1.39	0.79 0.00	0.77
4062	265.08	128.7	4.87 4.93	1.425	0.137	1.019	0.897	4.90 4.90	4.74 4.69	4.00 4.03	3.93 3.99	3.83 3.80	3.15 3.13	3.07 3.08	2.91 2.85	1.37 1.41	0.92 0.10	0.90
4063	263.08	128.9	4.87 4.93	1.426	0.136	1.021	1.039	4.90 4.90	4.74 4.70	4.01 4.03	3.94 3.99	3.84 3.81	3.16 3.14	3.08 3.09	2.92 2.87	1.42 1.44	1.06 0.00	1.04
4064	260.45	129.0	4.88 4.94	1.427	0.134	1.021	1.174	4.91 4.90	4.75 4.70	4.02 4.04	3.95 3.99	3.85 3.82	3.17 3.16	3.10 3.11	2.93 2.88	1.48 1.50	1.19 0.00	1.17
4065	257.82	129.2	4.88 4.94	1.428	0.133	1.023	1.322	4.91 4.91	4.76 4.71	4.03 4.05	3.96 4.02	3.86 3.83	3.19 3.18	3.12 3.13	2.96 2.91	1.58 1.58	1.33 0.00	1.32
4066	254.50	129.3	4.89 4.95	1.430	0.131	1.024	1.454	4.91 4.91	4.76 4.72	4.04 4.07	3.97 4.02	3.88 3.85	3.22 3.20	3.14 3.15	2.98 2.94	1.67 1.67	1.46 0.10	1.45

TABLE I.—Continued.

(b) Concluded.

Run	$\dot{w}$, g/s	T_o, K	P_o, MPa	$P_{R,o}$	G_R	$T_{R,o}$	P_B, MPa	Pressure at pressure tap locations 1 to 10, MPa										P_e, MPa
								P_1	P_2	P_3	P_4	P_5	P_6	P_7	P_8	P_9	P_{10}	
4067	264.14	129.4	4.87 4.94	1.426	0.136	1.025	0.417	4.90 4.90	4.75 4.70	4.02 4.04	3.95 4.00	3.85 3.82	3.16 3.15	3.09 3.10	2.91 2.86	1.32 1.37	0.45 0.00	0.42
4068	188.40	140.1	4.93 4.99	1.442	0.097	1.109	0.352	4.96 4.96	4.81 4.77	4.12 4.15	4.05 4.11	3.95 3.91	3.20 3.19	3.10 3.12	2.91 2.83	1.30 1.37	0.39 0.00	0.35
4069	185.71	140.6	4.92 4.98	1.441	0.096	1.113	0.514	4.96 4.95	4.81 4.76	4.12 4.15	4.05 4.10	3.95 3.91	3.20 3.19	3.11 3.12	2.92 2.83	1.31 1.38	0.54 0.00	0.51
4070	183.72	140.8	4.92 4.98	1.441	0.095	1.115	0.622	4.95 4.96	4.81 4.76	4.12 4.15	4.04 4.10	3.94 3.91	3.20 3.18	3.10 3.11	2.91 2.33	1.31 1.38	0.64 0.10	0.62
4071	181.61	141.1	4.92 4.98	1.441	0.094	1.117	0.757	4.95 4.95	4.81 4.77	4.11 4.14	4.04 4.10	3.94 3.90	3.19 3.17	3.09 3.10	2.90 2.82	1.33 1.39	0.77 0.10	0.76
4072	180.25	141.4	4.92 4.99	1.441	0.093	1.120	0.899	4.96 4.95	4.81 4.77	4.11 4.13	4.04 4.08	3.93 3.90	3.18 3.16	3.09 3.09	2.89 2.82	1.35 1.39	0.91 0.10	0.90
4073	179.00	141.7	4.92 4.99	1.441	0.092	1.122	1.033	4.96 4.96	4.81 4.77	4.11 4.13	4.03 4.10	3.93 3.89	3.17 3.16	3.08 3.09	2.89 2.81	1.38 1.42	1.05 0.10	1.03
4074	177.13	142.0	4.92 4.99	1.441	0.091	1.124	1.170	4.96 4.96	4.81 4.77	4.10 4.13	4.03 4.08	3.93 3.89	3.17 3.16	3.08 3.09	2.89 2.81	1.45 1.47	1.18 0.10	1.17
4075	174.82	142.4	4.93 4.99	1.442	0.090	1.127	1.307	4.96 4.96	4.81 4.77	4.11 4.13	4.04 4.09	3.93 3.90	3.19 3.18	3.09 3.11	2.91 2.83	1.54 1.55	1.31 0.00	1.31
4076	169.75	143.2	4.93 4.99	1.442	0.087	1.134	1.444	4.96 4.96	4.81 4.78	4.12 4.14	4.05 4.09	3.94 3.92	3.21 3.19	3.12 3.13	2.94 2.86	1.64 1.64	1.45 0.10	1.44
4077	171.07	144.7	4.90 4.97	1.435	0.088	1.146	0.357	4.94 4.93	4.79 4.75	4.08 4.10	4.00 4.06	3.89 3.86	3.12 3.10	3.01 3.02	2.82 2.74	1.28 1.34	0.38 0.00	0.36

TABLE I.—Continued.

(c) Hydrogen

Run	$\dot{w}$, g/s	T_o, K	P_o, MPa	$P_{R,o}$	G_R	$T_{R,o}$	P_B, MPa	Pressure at pressure tap locations 1 to 10, MPa										P_e, MPa
								P_1	P_2	P_3	P_4	P_5	P_6	P_7	P_8	P_9	P_{10}	
4083	8.63	293.9	1.33 1.33	1.027	0.023	8.906	0.116	1.30 1.30	1.28 1.24	1.07 1.09	1.06 1.09	1.02 1.00	0.82 0.82	0.79 0.81	0.73 0.69	0.34 0.36	0.17 0.00	0.12
4084	14.37	296.0	2.10 2.10	1.619	0.038	8.970	0.158	2.08 2.08	2.02 1.97	1.71 1.74	1.70 1.74	1.63 1.60	1.30 1.31	1.25 1.28	1.15 1.08	0.54 0.56	0.20 0.00	0.16
4085	20.00	297.1	2.79 2.81	2.157	0.054	9.003	0.208	2.78 2.78	2.69 2.64	2.30 2.33	2.27 2.32	2.19 2.14	1.74 1.76	1.67 1.71	1.53 1.44	0.71 0.74	0.24 0.00	0.21
4086	26.80	297.8	3.61 3.63	2.784	0.072	9.024	0.267	3.60 3.60	3.48 3.41	2.99 3.02	2.95 3.01	2.83 2.77	2.25 2.28	2.16 2.21	1.97 1.85	0.90 0.94	0.35 0.10	0.27
4087	34.86	298.2	4.58 4.62	3.533	0.093	9.036	0.341	4.59 4.59	4.41 4.34	3.81 3.85	3.75 3.83	3.61 3.53	2.86 2.90	2.75 2.80	2.49 2.33	1.12 1.18	0.36 0.00	0.34
4088	39.83	297.6	5.17 5.21	3.987	0.107	9.018	0.394	5.18 5.18	4.97 4.90	4.30 4.35	4.24 4.31	4.08 3.99	3.23 3.27	3.10 3.16	2.80 2.62	1.25 1.32	0.70 0.10	0.39
4089	45.58	296.9	5.83 5.89	4.501	0.122	8.997	0.440	5.86 5.85	5.62 5.54	4.87 4.92	4.80 4.88	4.61 4.51	3.64 3.69	3.50 3.56	3.15 2.95	1.40 1.47	0.46 0.10	0.44
4098	111.74	29.2	5.69 5.77	4.392	0.299	0.885	0.340	5.74 5.74	5.53 5.47	4.25 4.30	4.14 4.19	3.97 3.92	2.75 2.76	2.61 2.61	2.35 2.28	0.89 0.95	0.39 0.10	0.34
4099	84.32	28.8	3.88 3.93	2.997	0.226	0.873	0.254	3.90 3.90	3.76 3.72	2.88 2.92	2.82 2.86	2.71 2.67	1.94 1.94	1.85 1.86	1.69 1.64	0.72 0.76	0.30 0.10	0.25
4100	67.20	28.1	2.62 2.64	2.021	0.180	0.852	0.208	2.62 2.62	2.54 2.49	1.94 1.97	1.91 1.96	1.84 1.81	1.37 1.36	1.31 1.32	1.22 1.19	0.57 0.59	0.25 0.10	0.21
4101	54.42	28.4	1.89 1.90	1.461	0.146	0.861	0.174	1.88 1.88	1.83 1.80	1.43 1.46	1.41 1.45	1.37 1.35	1.06 1.06	1.03 1.04	0.97 0.96	0.46 0.47	0.23 0.10	0.17
4102	39.18	28.7	1.28 1.28	0.985	0.105	0.870	0.143	1.25 1.26	1.24 1.21	1.01 1.03	1.01 1.05	0.98 0.97	0.81 0.80	0.79 0.79	0.75 0.73	0.36 0.35	0.20 0.10	0.14
4103	106.51	27.3	5.08 5.14	3.918	0.285	0.827	0.290	5.11 5.12	4.91 4.83	3.63 3.68	3.52 3.58	3.36 3.31	2.21 2.23	2.09 2.10	1.86 1.80	0.68 0.74	0.34 0.10	0.29
4104	90.15	27.2	4.00 4.05	3.086	0.241	0.824	0.239	4.02 4.02	3.87 3.79	2.85 2.89	2.77 2.83	2.65 2.61	1.79 1.80	1.70 1.71	1.52 1.48	0.60 0.66	0.29 0.00	0.24
4105	67.30	27.0	2.72 2.75	2.100	0.180	0.818	0.199	2.72 2.72	2.63 2.58	1.96 1.99	1.91 1.96	1.84 1.81	1.31 1.30	1.24 1.26	1.14 1.11	0.52 0.54	0.24 0.10	0.20
4106	61.09	26.8	1.92 1.93	1.478	0.163	0.812	0.173	1.90 1.90	1.85 1.81	1.40 1.43	1.39 1.42	1.34 1.32	1.00 1.00	0.97 0.97	0.90 0.88	0.43 0.44	0.22 0.00	0.17
4107	32.43	27.3	1.46 1.47	1.128	0.087	0.827	0.152	1.44 1.44	1.41 1.38	1.10 1.12	1.10 1.14	1.06 1.05	0.85 0.83	0.82 0.83	0.78 0.77	0.36 0.38	0.20 0.10	0.15

TABLE I.—Continued.

(c) Continued.

Run	$\dot{w}$, g/s	T_o, K	P_o, MPa	$P_{R,o}$	G_R	$T_{R,o}$	P_B, MPa	Pressure at pressure tap locations 1 to 10, MPa										P_e, MPa
								P_1	P_2	P_3	P_4	P_5	P_6	P_7	P_8	P_9	P_{10}	
4108	25.86	27.6	1.22 1.23	0.943	0.069	0.836	0.144	1.20 1.20	1.18 1.15	0.95 0.97	0.95 0.98	0.92 0.91	0.76 0.75	0.74 0.74	0.70 0.69	0.33 0.33	0.19 0.00	0.14
4109	18.59	28.4	1.04 1.04	0.800	0.050	0.861	0.129	1.01 1.01	1.01 0.98	0.83 0.85	0.84 0.86	0.81 0.80	0.66 0.64	0.63 0.64	0.60 0.58	0.29 0.29	0.18 0.10	0.13
4110	112.71	30.6	5.71 5.78	4.406	0.302	0.927	0.304	5.76 5.76	5.54 5.45	4.15 4.20	4.03 4.10	3.85 3.80	2.57 2.60	2.44 2.44	2.18 2.11	0.85 0.92	0.35 0.00	0.30
4111	93.20	29.8	4.16 4.21	3.211	0.249	0.903	0.238	4.18 4.18	4.03 3.96	3.01 3.06	2.94 3.00	2.81 2.77	1.95 1.95	1.85 1.86	1.68 1.63	0.71 0.76	0.29 0.00	0.24
4112	60.54	29.5	2.91 2.93	2.243	0.162	0.894	0.194	2.90 2.91	2.81 2.75	2.13 2.15	2.08 2.13	2.00 1.97	1.45 1.45	1.39 1.40	1.28 1.25	0.59 0.61	0.24 0.10	0.19
4113	53.20	29.4	2.16 2.18	1.671	0.142	0.891	0.170	2.15 2.16	2.10 2.05	1.61 1.64	1.59 1.63	1.53 1.52	1.17 1.16	1.12 1.14	1.05 1.04	0.49 0.51	0.22 0.10	0.17
4115	26.02	29.5	1.16 1.16	0.894	0.070	0.894	0.130	1.13 1.14	1.13 1.10	0.93 0.95	0.93 0.97	0.91 0.90	0.73 0.72	0.71 0.72	0.66 0.65	0.32 0.31	0.18 0.09	0.13
4116	33.58	29.8	1.14 1.14	0.879	0.090	0.903	0.128	1.11 1.12	1.11 1.08	0.92 0.93	0.92 0.95	0.89 0.88	0.72 0.70	0.69 0.70	0.64 0.64	0.32 0.31	0.18 0.10	0.13
4117	110.54	33.4	5.95 6.03	4.592	0.296	1.012	0.305	6.00 6.00	5.78 5.69	4.38 4.43	4.26 4.33	4.08 4.03	2.77 2.80	2.63 2.65	2.37 2.30	0.94 1.02	0.35 0.10	0.30
4118	89.35	32.8	4.46 4.52	3.445	0.239	0.994	0.238	4.49 4.49	4.34 4.26	3.29 3.33	3.21 3.27	3.08 3.04	2.18 2.19	2.08 2.09	1.89 1.85	0.81 0.86	0.29 0.10	0.24
4119	65.60	33.2	3.24 3.27	2.498	0.175	1.006	0.197	3.24 3.24	3.14 3.08	2.42 2.45	2.37 2.42	2.29 2.26	1.70 1.71	1.63 1.65	1.52 1.49	0.68 0.71	0.25 0.10	0.20
4120	51.83	34.4	2.34 2.36	1.806	0.139	1.042	0.162	2.32 2.33	2.27 2.23	1.81 1.84	1.80 1.83	1.74 1.72	1.38 1.38	1.34 1.35	1.27 1.25	0.54 0.57	0.22 0.00	0.16
4121	38.00	33.4	1.67 1.67	1.289	0.102	1.012	0.135	1.64 1.65	1.62 1.59	1.33 1.35	1.33 1.37	1.29 1.28	1.04 1.04	1.01 1.02	0.94 0.92	0.41 0.42	0.19 0.10	0.14
4122	99.72	37.9	5.69 5.76	4.387	0.267	1.148	0.293	5.73 5.73	5.53 5.45	4.27 4.32	4.17 4.24	4.01 3.96	2.83 2.86	2.71 2.72	2.46 2.40	1.01 1.09	0.34 0.10	0.29
4123	77.70	36.8	4.15 4.20	3.204	0.208	1.115	0.242	4.17 4.17	4.04 3.97	3.14 3.18	3.08 3.13	2.97 2.93	2.19 2.20	2.10 2.11	1.94 1.89	0.84 0.89	0.28 0.00	0.24
4124	55.75	38.0	3.01 3.04	2.320	0.149	1.152	0.195	3.01 3.01	2.93 2.88	2.34 2.37	2.31 2.36	2.24 2.21	1.74 1.74	1.68 1.69	1.57 1.54	0.67 0.72	0.24 0.10	0.20
4125	39.26	36.4	2.19 2.20	1.687	0.105	1.103	0.149	2.17 2.17	2.13 2.09	1.73 1.75	1.71 1.77	1.67 1.65	1.32 1.33	1.29 1.30	1.22 1.19	0.53 0.55	0.20 0.10	0.15

TABLE I.—Continued.

(c) Continued.

Run	$\dot{w}$, g/s	T_o, K	P_o, MPa	$P_{R,o}$	G_R	$T_{R,o}$	P_B, MPa	Pressure at pressure tap locations 1 to 10, MPa										P_e, MPa
								P_1	P_2	P_3	P_4	P_5	P_6	P_7	P_8	P_9	P_{10}	
4126	27.82	33.1	1.45 1.46	1.121	0.074	1.003	0.128	1.43 1.43	1.42 1.38	1.17 1.18	1.16 1.20	1.13 1.12	0.91 0.90	0.88 0.89	0.83 0.81	0.43 0.41	0.17 0.10	0.13
4127	18.64	38.1	1.65 1.66	1.275	0.050	1.155	0.113	1.63 1.64	1.63 1.59	1.39 1.41	1.39 1.42	1.36 1.35	1.16 1.15	1.13 1.14	1.09 1.07	0.56 0.56	0.17 0.09	0.11
4128	85.43	47.2	5.94 6.02	4.587	0.229	1.430	0.292	6.00 6.00	5.81 5.75	4.67 4.73	4.58 4.64	4.43 4.39	3.27 3.30	3.14 3.15	2.88 2.81	1.33 1.32	0.34 0.10	0.29
4129	61.57	46.6	4.48 4.54	3.455	0.165	1.412	0.224	4.51 4.51	4.39 4.33	3.58 3.62	3.52 3.58	3.42 3.38	2.64 2.66	2.55 2.56	2.38 2.33	1.30 1.24	0.33 0.10	0.22
4130	38.92	46.6	3.22 3.25	2.483	0.104	1.412	0.170	3.23 3.23	3.16 3.11	2.60 2.63	2.57 2.62	2.50 2.47	1.97 1.98	1.91 1.91	1.79 1.75	0.91 0.91	0.22 0.10	0.17
4132	12.39	47.5	1.40 1.40	1.078	0.033	1.439	0.110	1.37 1.37	1.36 1.32	1.11 1.13	1.10 1.14	1.07 1.06	0.85 0.84	0.82 0.83	0.78 0.76	0.32 0.35	0.16 0.00	0.11
4133	7.90	47.3	0.93 0.93	0.720	0.021	1.433	0.105	0.90 0.91	0.91 0.88	0.73 0.74	0.73 0.77	0.71 0.70	0.57 0.55	0.55 0.56	0.52 0.51	0.23 0.24	0.16 0.00	0.10
4134	122.42	26.3	6.04 6.12	4.662	0.328	0.797	0.253	6.09 6.09	5.85 5.75	4.29 4.35	4.15 4.23	3.96 3.90	2.50 2.53	2.35 2.36	2.06 2.00	0.66 0.73	0.30 0.00	0.25
4135	100.40	25.7	4.54 4.59	3.502	0.269	0.779	0.210	4.56 4.56	4.39 4.30	3.20 3.24	3.10 3.18	2.96 2.91	1.93 1.94	1.82 1.84	1.61 1.57	0.57 0.63	0.84 0.10	0.21
4136	75.32	25.5	3.16 3.19	2.438	0.201	0.773	0.177	3.16 3.16	3.05 2.98	2.22 2.26	2.17 2.22	2.08 2.04	1.41 1.41	1.34 1.35	1.21 1.17	0.49 0.53	0.52 0.10	0.18
4137	70.15	26.2	3.16 3.20	2.441	0.188	0.794	0.807	3.16 3.17	3.06 3.01	2.33 2.37	2.29 2.34	2.21 2.18	1.63 1.63	1.57 1.58	1.46 1.43	0.86 0.87	0.83 0.10	0.81
4138	66.14	26.6	3.17 3.21	2.449	0.177	0.806	1.040	3.17 3.18	3.08 3.03	2.40 2.44	2.37 2.42	2.29 2.27	1.77 1.77	1.71 1.73	1.61 1.59	1.06 1.09	1.04 0.10	1.04
4139	58.83	27.7	3.19 3.23	2.462	0.157	0.839	1.399	3.19 3.20	3.11 3.08	2.54 2.57	2.51 2.56	2.45 2.43	2.01 2.02	1.96 1.97	1.88 1.86	1.43 1.44	1.31 0.10	1.40
4140	89.77	25.2	3.88 3.92	2.994	0.240	0.764	0.252	3.89 3.90	3.75 3.67	2.73 2.77	2.66 2.72	2.54 2.50	1.68 1.69	1.60 1.60	1.43 1.38	0.53 0.58	0.30 0.10	0.25
4141	88.62	25.4	3.88 3.93	2.993	0.237	0.770	0.521	3.89 3.90	3.75 3.67	2.75 2.79	2.67 2.74	2.55 2.52	1.72 1.72	1.63 1.64	1.46 1.42	0.60 0.64	0.53 0.10	0.52
4142	85.08	26.0	3.89 3.93	3.002	0.228	0.788	0.750	3.90 3.91	3.76 3.69	2.81 2.85	2.75 2.81	2.63 2.60	1.85 1.86	1.77 1.78	1.61 1.57	0.81 0.83	0.76 0.09	0.75
4143	81.54	26.5	3.90 3.95	3.008	0.218	0.803	0.988	3.91 3.92	3.78 3.71	2.89 2.93	2.83 2.88	2.73 2.70	2.00 2.01	1.92 1.94	1.78 1.74	1.03 1.06	0.99 0.09	0.99

TABLE I.—Continued.

(c) Continued.

Run	$\dot{w}$, g/s	T_o, K	P_o, MPa	$P_{R,o}$	G_R	$T_{R,o}$	P_B, MPa	Pressure at pressure tap locations 1 to 10, MPa										P_e, MPa
								P_1	P_2	P_3	P_4	P_5	P_6	P_7	P_8	P_9	P_{10}	
4144	33.98	59.6	3.93	3.029	0.091	1.806	1.286	3.94	3.85	3.23	3.19	3.11	2.51	2.44	2.31	1.40	1.33	1.29
			3.98					3.95	3.81	3.26	3.23	3.09	2.52	2.45	2.26	1.39	0.10	
4149	0.00	30.1	1.02	0.787	0.000	0.912	0.066	1.01	1.00	0.82	0.82	0.79	0.64	0.61	0.57	0.26	0.17	0.07
			1.01					1.01	0.98	0.83	0.85	0.77	0.64	0.61	0.55	0.26	0.00	
4150	117.17	30.6	6.05	4.666	0.313	0.927	0.067	6.10	5.86	4.37	4.25	4.05	2.69	2.53	2.26	0.87	0.34	0.07
			6.06					6.11	5.80	4.44	4.32	4.01	2.71	2.55	2.21	0.93	0.10	
4151	98.29	31.1	4.82	3.720	0.263	0.942	0.068	4.85	4.67	3.49	3.40	3.25	2.24	2.12	1.91	0.80	0.28	0.07
			4.84					4.86	4.61	3.55	3.47	3.22	2.26	2.14	1.88	0.84	0.10	
4152	75.05	31.0	3.42	2.637	0.201	0.939	0.069	3.43	3.31	2.50	2.45	2.35	1.71	1.63	1.50	0.67	0.24	0.07
			3.42					3.44	3.26	2.55	2.51	2.32	1.72	1.64	1.47	0.69	0.10	
4153	58.24	31.1	2.54	1.958	0.156	0.942	0.069	2.54	2.46	1.90	1.86	1.79	1.37	1.31	1.23	0.56	0.22	0.07
			2.53					2.54	2.42	1.93	1.91	1.77	1.38	1.32	1.21	0.57	0.00	
4154	38.55	30.8	1.66	1.282	0.103	0.933	0.068	1.65	1.61	1.30	1.29	1.25	1.02	0.99	0.93	0.44	0.19	0.07
			1.66					1.65	1.58	1.32	1.32	1.24	1.03	0.99	0.92	0.42	0.10	
4155	25.41	30.8	1.20	0.924	0.068	0.933	0.065	1.18	1.17	0.96	0.96	0.93	0.75	0.73	0.68	0.37	0.18	0.06
			1.19					1.18	1.14	0.98	0.99	0.91	0.75	0.73	0.66	0.33	0.10	
4156	12.89	29.5	0.94	0.723	0.034	0.894	0.068	0.92	0.91	0.75	0.75	0.73	0.60	0.58	0.55	0.36	0.16	0.07
			0.93					0.92	0.89	0.76	0.78	0.71	0.61	0.58	0.54	0.32	0.10	
4157	119.28	27.6	5.84	4.508	0.319	0.836	0.067	5.89	5.65	4.17	4.05	3.85	2.50	2.35	2.08	0.74	0.33	0.07
			5.85					5.90	5.58	4.23	4.13	3.81	2.52	2.36	2.03	0.79	0.10	
4158	100.80	27.3	4.59	3.544	0.270	0.827	0.068	4.62	4.45	3.26	3.17	3.02	2.02	1.90	1.69	0.64	0.27	0.07
			4.61					4.63	4.38	3.31	3.23	2.98	2.03	1.91	1.65	0.68	0.10	
4159	80.08	27.2	3.37	2.600	0.214	0.824	0.068	3.37	3.25	2.39	2.34	2.23	1.55	1.47	1.33	0.57	0.23	0.07
			3.37					3.38	3.19	2.44	2.39	2.20	1.56	1.48	1.30	0.59	0.10	
4160	59.80	27.3	2.32	1.789	0.160	0.827	0.066	2.31	2.24	1.67	1.65	1.58	1.16	1.10	1.02	0.47	0.21	0.07
			2.32					2.32	2.20	1.71	1.69	1.56	1.16	1.11	1.00	0.49	0.00	
4161	43.60	28.1	1.65	1.277	0.117	0.852	0.068	1.64	1.60	1.24	1.23	1.18	0.93	0.89	0.84	0.40	0.19	0.07
			1.65					1.64	1.57	1.26	1.27	1.17	0.93	0.90	0.84	0.40	0.00	
4166	105.52	37.0	6.16	4.752	0.282	1.121	0.063	6.21	6.00	4.71	4.61	4.43	3.17	3.03	2.75	1.17	0.52	0.06
			6.18					6.21	5.92	4.78	4.70	4.39	3.20	3.04	2.69	1.24	0.09	
4167	83.64	36.9	4.66	3.600	0.224	1.118	0.068	4.69	4.55	3.58	3.52	3.39	2.52	2.42	2.22	1.01	0.47	0.07
			4.68					4.70	4.47	3.64	3.58	3.36	2.54	2.43	2.18	1.04	0.09	
4168	59.76	37.5	3.37	2.601	0.160	1.136	0.068	3.38	3.28	2.63	2.60	2.51	1.96	1.89	1.76	0.83	0.43	0.07
			3.38					3.38	3.23	2.68	2.66	2.49	1.97	1.90	1.74	0.85	0.10	

TABLE I.—Continued.

(c) Continued.

Run	$\dot{w}$, g/s	T_o, K	P_o, MPa	$P_{R,o}$	G_R	$T_{R,o}$	P_B, MPa	Pressure at pressure tap locations 1 to 10, MPa										P_e, MPa
								P_1	P_2	P_3	P_4	P_5	P_6	P_7	P_8	P_9	P_{10}	
4169	29.81	37.2	2.14 2.14	1.652	0.080	1.127	0.067	2.13 2.13	2.09 2.06	1.74 1.78	1.74 1.78	1.69 1.68	1.40 1.41	1.36 1.38	1.30 1.29	0.67 0.66	0.44 0.10	0.07
4170	15.60	36.8	1.62 1.62	1.253	0.042	1.115	0.067	1.61 1.61	1.61 1.58	1.46 1.48	1.46 1.49	1.45 1.43	1.34 1.35	1.33 1.33	1.30 1.31	0.60 0.53	0.68 0.09	0.07
4171	100.41	33.4	5.58 5.60	4.308	0.269	1.012	0.066	5.62 5.64	5.44 5.40	4.37 4.43	4.29 4.34	4.14 4.10	3.07 3.08	2.93 2.92	2.69 2.63	1.16 1.20	0.55 0.10	0.07
4172	83.34	33.5	4.41 4.43	3.407	0.223	1.015	0.068	4.44 4.45	4.30 4.26	3.42 3.48	3.37 3.40	3.25 3.22	2.44 2.45	2.34 2.34	2.16 2.12	0.97 1.00	0.48 0.10	0.07
4173	66.29	33.2	3.29 3.30	2.541	0.177	1.006	0.067	3.30 3.31	3.20 3.16	2.54 2.58	2.50 2.55	2.42 2.39	1.85 1.86	1.78 1.79	1.66 1.64	0.79 0.80	0.69 0.10	0.07
4174	49.61	33.7	2.58 2.58	1.988	0.133	1.021	0.067	2.57 2.58	2.50 2.47	2.01 2.05	2.00 2.04	1.93 1.92	1.54 1.55	1.49 1.50	1.40 1.39	0.67 0.67	0.42 0.10	0.07
4175	34.73	33.1	1.78 1.77	1.371	0.093	1.003	0.068	1.76 1.76	1.73 1.70	1.43 1.46	1.42 1.45	1.39 1.37	1.15 1.16	1.11 1.11	1.05 1.03	0.51 0.50	1.22 0.00	0.07
4176	16.16	34.4	1.44 1.43	1.109	0.043	1.042	0.067	1.42 1.42	1.42 1.40	1.29 1.31	1.30 1.33	1.28 1.27	0.92 0.92	0.86 0.87	0.81 0.81	0.45 0.47	0.32 0.10	0.07
4177	85.29	44.7	5.95 5.97	4.595	0.228	1.355	0.067	6.00 6.02	5.83 5.81	4.83 4.89	4.75 4.80	4.61 4.58	3.61 3.61	3.47 3.47	3.24 3.19	1.60 1.60	0.56 0.10	0.07
4178	60.10	46.5	4.56 4.57	3.519	0.161	1.409	0.067	4.58 4.60	4.47 4.43	3.71 3.76	3.66 3.70	3.56 3.54	2.85 2.86	2.76 2.76	2.59 2.56	1.47 1.46	0.47 0.09	0.07
4179	42.66	46.0	3.49 3.50	2.693	0.114	1.394	0.068	3.50 3.51	3.42 3.39	2.87 2.91	2.85 2.89	2.77 2.75	2.28 2.29	2.21 2.22	2.10 2.08	1.27 1.31	0.42 0.10	0.07
4180	16.79	46.4	1.80 1.79	1.390	0.045	1.406	0.067	1.78 1.79	1.75 1.73	1.45 1.47	1.44 1.47	1.40 1.39	1.14 1.14	1.10 1.10	1.04 1.04	0.49 0.49	0.35 0.10	0.07
4181	12.20	46.1	1.42 1.42	1.100	0.033	1 397	0.065	1.40 1.40	1.39 1.36	1.14 1.17	1.15 1.17	1.11 1.10	0.91 0.92	0.88 0.88	0.84 0.84	0.43 0.42	0.34 0.10	0.07
4182	7.48	45.5	1.00 0.99	0.773	0.020	1.379	0.068	0.98 0.98	0.98 0.95	0.81 0.82	0.82 0.85	0.79 0.78	0.66 0.66	0.64 0.64	0.61 0.62	0.37 0.36	0.32 0.00	0.07
4183	95.87	138.5	5.66 5.67	4.369	0.256	4.197	0.066	5.69 5.71	5.53 5.48	4.78 4.84	4.73 4.79	4.58 4.53	3.64 3.67	3.51 3.54	3.25 3.11	1.33 1.38	0.52 0.10	0.07
4184	57.53	146.7	4.24 4.25	3.270	0.154	4.445	0.068	4.25 4.26	4.13 4.09	3.56 3.61	3.53 3.59	3.41 3.36	2.74 2.76	2.64 2.66	2.44 2.33	1.04 1.07	0.44 0.00	0.07
4185	36.81	147.6	2.99 2.99	2.306	0.098	4.473	0.068	2.99 2.99	2.91 2.87	2.49 2.53	2.48 2.53	2.38 2.34	1.92 1.94	1.86 1.87	1.72 1.65	0.76 0.77	0.40 0.10	0.07

TABLE I.—Concluded.

(c) Concluded.

Run	$\dot{w}$, g/s	T_o, K	P_o, MPa	$P_{R,o}$	G_R	$T_{R,o}$	P_B, MPa	Pressure at pressure tap locations 1 to 10, MPa										P_e, MPa
								P_1	P_2	P_3	P_4	P_5	P_6	P_7	P_8	P_9	P_{10}	
4186	32.91	158.8	2.96	2.283	0.088	4.812	0.068	2.95	2.88	2.47	2.45	2.36	1.91	1.84	1.70	0.74	0.21	0.07
			2.96					2.96	2.83	2.51	2.51	2.31	1.93	1.86	1.62	0.76	0.10	
4187	12.69	152.7	1.28	0.987	0.034	4.627	0.067	1.25	1.24	1.03	1.03	0.99	0.80	0.77	0.72	0.32	0.15	0.07
			1.27					1.26	1.20	1.06	1.08	0.97	0.81	0.78	0.69	0.33	0.10	

(d) Hydrogen with backpressure control

Run	$\dot{w}$, g/s	T_o, K	P_o, MPa	$P_{R,o}$	G_R	$T_{R,o}$	P_B, MPa	Pressure at pressure tap locations 1 to 10, MPa										P_e, MPa
								P_1	P_2	P_3	P_4	P_5	P_6	P_7	P_8	P_9	P_{10}	
4090	22.56	298.2	3.10	2.394	0.060	9.036	0.228	3.09	2.99	2.56	2.53	2.44	1.95	1.87	1.71	0.78	0.26	0.23
			3.12					3.09	2.93	2.60	2.59	2.38	1.96	1.91	1.60	0.82	0.10	
4091	22.56	297.3	3.10	2.395	0.060	9.009	0.269	3.10	2.99	2.56	2.53	2.44	1.95	1.87	1.71	0.78	0.30	0.27
			3.12					3.09	2.93	2.60	2.60	2.38	1.96	1.91	1.60	0.83	0.00	
4092	22.50	297.0	3.11	2.400	0.060	9.000	0.406	3.10	3.00	2.57	2.54	2.44	1.95	1.87	1.72	0.79	0.43	0.41
			3.13					3.10	2.94	2.60	2.60	2.39	1.97	1.92	1.61	0.83	0.10	
4093	22.33	296.8	3.12	2.407	0.060	8.994	0.615	3.11	3.01	2.58	2.55	2.45	1.96	1.89	1.73	0.84	0.64	0.62
			3.14					3.11	2.95	2.61	2.61	2.40	1.98	1.93	1.62	0.85	0.10	
4094	22.12	296.7	3.12	2.410	0.059	8.991	0.761	3.12	3.01	2.59	2.56	2.47	1.99	1.91	1.76	0.92	11.38	0.76
			3.15					3.12	2.96	2.63	2.62	2.42	2.00	1.95	1.65	0.92	0.10	
4095	21.66	296.5	3.14	2.425	0.058	8.985	0.991	3.14	3.04	2.63	2.59	2.51	2.04	1.97	1.83	1.10	7.11	0.99
			3.16					3.14	2.98	2.66	2.65	2.46	2.06	2.01	1.73	1.10	0.10	
4096	20.93	296.4	3.17	2.444	0.056	8.982	1.253	3.16	3.06	2.68	2.64	2.56	2.14	2.07	1.94	1.33	1.34	1.25
			3.19					3.16	3.01	2.71	2.70	2.52	2.15	2.10	1.85	1.32	0.10	
4097	20.30	296.4	3.19	2.458	0.054	8.982	1.450	3.19	3.09	2.72	2.69	2.62	2.22	2.16	2.04	1.52	1.46	1.45
			3.21					3.19	3.04	2.76	2.75	2.57	2.23	2.19	1.96	1.50	0.00	
4162	96.85	26.4	4.31	3.323	0.259	0.800	0.066	4.33	4.16	3.04	2.96	2.82	1.88	1.77	1.58	0.60	0.28	0.07
			4.32					4.34	4.10	3.09	3.02	2.78	1.89	1.78	1.54	0.64	0.10	
4163	95.95	26.8	4.31	3.325	0.257	0.812	0.068	4.33	4.16	3.04	2.96	2.82	1.89	1.78	1.59	0.61	0.32	0.07
			4.31					4.34	4.10	3.09	3.02	2.79	1.90	1.79	1.55	0.65	0.10	
4164	94.98	27.0	4.31	3.325	0.254	0.818	0.068	4.33	4.16	3.05	2.97	2.83	1.90	1.79	1.60	0.64	0.39	0.07
			4.32					4.34	4.10	3.10	3.03	2.80	1.92	1.81	1.57	0.67	0.10	
4165	93.29	28.1	4.31	3.329	0.250	0.852	0.068	4.34	4.16	3.07	2.99	2.85	1.94	1.83	1.64	0.68	0.45	0.07
			4.32					4.34	4.11	3.12	3.05	2.82	1.95	1.85	1.61	0.72	0.10	

TABLE II.—FLOW RATE AND PRESSURE DROP DATA FOR THREE-STEP LABYRINTH SEAL, FULLY ECCENTRIC POSITION

[Where two values are given, the top value is for the 0° circumferential position (maximum clearance), and the bottom value is for the 180° circumferential position (minimum clearance).]

(a) Nitrogen

Run	$\dot{w}$, g/s	T_o, K	P_o, MPa	$P_{R,o}$	G_R	$T_{R,o}$	P_B, MPa	Pressure at pressure tap locations 1 to 10, MPa										P_e, MPa
								P_1	P_2	P_3	P_4	P_5	P_6	P_7	P_8	P_9	P_{10}	
4355	29.58	293.2	1.12 1.10	0.327	0.015	2.321	0.136	1.09 1.09	1.02 1.06	0.90 0.89	0.91 0.92	0.80 0.85	0.70 0.68	0.68 0.65	0.53 0.61	0.30 0.27	0.15 0.16	0.14
4356	46.46	294.7	1.69 1.67	0.495	0.024	2.333	0.160	1.67 1.67	1.56 1.62	1.39 1.37	1.38 1.38	1.22 1.29	1.07 1.03	1.04 1.00	0.80 0.92	0.45 0.40	0.16 0.18	0.16
4357	69.93	293.6	2.45 2.42	0.717	0.036	2.325	0.197	2.42 2.43	2.26 2.36	2.03 2.00	2.02 2.00	1.78 1.88	1.55 1.50	1.52 1.45	1.16 1.32	0.65 0.57	0.19 0.22	0.20
4358	97.74	293.5	3.33 3.31	0.976	0.050	2.324	0.247	3.32 3.33	3.09 3.23	2.78 2.74	2.76 2.72	2.45 2.58	2.11 2.05	2.08 1.98	1.58 1.79	0.89 0.77	0.23 0.27	0.25
4359	118.94	290.4	3.99 3.97	1.169	0.061	2.299	0.286	3.98 4.00	3.72 3.87	3.34 3.29	3.31 3.27	2.95 3.11	2.53 2.46	2.49 2.38	1.90 2.14	1.05 0.91	0.26 0.31	0.29
4360	141.45	289.8	4.68 4.66	1.371	0.073	2.295	0.329	4.69 4.70	4.37 4.55	3.93 3.87	3.89 3.84	3.46 3.66	2.97 2.89	2.92 2.79	2.22 2.51	1.23 1.06	0.30 0.35	0.33
4361	161.55	289.7	5.30 5.27	1.552	0.083	2.294	0.368	5.31 5.32	4.95 5.15	4.45 4.38	4.40 4.34	3.92 4.14	3.35 3.26	3.30 3.15	2.51 2.82	1.38 1.18	0.33 0.40	0.37
4362	183.81	290.6	5.94 5.91	1.738	0.095	2.301	0.411	5.95 5.96	5.55 5.77	4.99 4.92	4.94 4.86	4.41 4.65	3.75 3.65	3.69 3.52	2.80 3.16	1.53 1.31	0.37 0.44	0.41
4363	435.15	88.4	5.95 5.95	1.743	0.224	0.700	0.238	5.99 6.00	5.48 5.74	4.12 4.11	4.02 3.98	3.61 3.69	2.23 2.16	2.07 2.02	1.58 1.68	0.46 0.39	0.26 0.27	0.24
4364	358.95	88.8	4.45 4.44	1.302	0.185	0.703	0.204	4.46 4.47	4.09 4.27	3.06 3.05	3.00 2.96	2.69 2.75	1.72 1.67	1.60 1.57	1.25 1.33	0.40 0.35	0.23 0.23	0.20
4365	291.50	89.1	3.23 3.22	0.946	0.150	0.705	0.186	3.22 3.23	2.98 3.09	2.23 2.23	2.20 2.17	1.97 2.01	1.31 1.28	1.23 1.21	0.99 1.05	0.38 0.33	0.21 0.21	0.19
4366	229.81	88.8	2.25 2.24	0.659	0.118	0.703	0.174	2.24 2.24	2.08 2.14	1.56 1.56	1.54 1.54	1.40 1.42	0.96 0.95	0.91 0.90	0.75 0.80	0.33 0.30	0.20 0.20	0.17
4367	169.80	89.6	1.44 1.42	0.422	0.088	0.709	0.165	1.41 1.42	1.34 1.36	1.02 1.02	1.01 1.02	0.93 0.94	0.68 0.67	0.65 0.64	0.56 0.59	0.31 0.28	0.19 0.19	0.16
4368	359.93	118.1	5.58 5.58	1.634	0.186	0.935	0.293	5.62 5.63	5.23 5.42	4.27 4.26	4.24 4.16	3.87 3.95	2.93 2.89	2.83 2.78	2.42 2.52	1.35 1.24	0.32 0.33	0.29
4369	281.99	117.7	4.14 4.14	1.213	0.145	0.932	0.246	4.16 4.17	3.91 4.02	3.25 3.25	3.25 3.19	3.00 3.05	2.41 2.38	2.34 2.31	2.07 2.14	1.13 1.05	0.26 0.27	0.25
4370	419.13	111.6	2.81 2.95	0.822	0.216	0.884	0.369	2.96 2.74	2.81 3.57	2.23 2.23	2.23 2.85	2.07 2.62	1.69 2.52	1.64 1.88	2.34 1.73	0.97 0.96	0.51 0.50	0.37
4371	146.26	117.3	2.13 2.12	0.624	0.075	0.929	0.181	2.12 2.12	2.05 2.08	1.81 1.81	1.80 1.81	1.70 1.72	1.41 1.40	1.37 1.35	1.20 1.25	0.63 0.60	0.19 0.21	0.18

TABLE II.—Continued

TABLE II.—Continued.

(a) Concluded.

Run	$\dot{w}$, g/s	T_o, K	P_o, MPa	$P_{R,o}$	G_R	$T_{R,o}$	P_B, MPa	Pressure at pressure tap locations 1 to 10, MPa										P_e, MPa
								P_1	P_2	P_3	P_4	P_5	P_6	P_7	P_8	P_9	P_{10}	
4372	328.82	129.2	5.87 5.87	1.719	0.169	1.023	0.313	5.92 5.93	5.55 5.72	4.71 4.70	4.69 4.62	4.34 4.42	3.49 3.45	3.40 3.35	3.00 3.09	1.52 1.39	0.32 0.34	0.31
4373	267.35	128.1	4.72 4.72	1.381	0.138	1.014	0.272	4.75 4.75	4.49 4.61	3.86 3.86	3.85 3.80	3.60 3.65	3.00 2.97	2.94 2.90	2.63 2.69	1.29 1.19	0.28 0.30	0.27
4374	189.97	128.1	3.73 3.73	1.092	0.098	1.014	0.233	3.74 3.75	3.58 3.65	3.16 3.17	3.16 3.14	2.98 3.02	2.46 2.44	2.39 2.36	2.06 2.15	1.04 0.97	0.23 0.26	0.23
4375	128.91	126.4	3.31 3.30	0.968	0.066	1.001	0.207	3.31 3.32	3.19 3.23	2.78 2.78	2.77 2.76	2.59 2.64	2.16 2.13	2.09 2.06	1.79 1.88	0.92 0.84	0.20 0.23	0.21
4376	86.27	127.0	2.72 2.72	0.796	0.044	1.006	0.172	2.71 2.72	2.60 2.64	2.23 2.24	2.23 2.22	2.10 2.13	1.73 1.71	1.68 1.66	1.47 1.54	0.75 0.68	0.17 0.19	0.17
4377	374.60	113.7	5.55 5.53	1.623	0.193	0.900	0.372	5.58 5.59	5.18 5.36	4.19 4.18	4.16 4.08	3.80 3.87	2.83 2.79	2.72 2.67	2.32 2.41	1.31 1.20	0.40 0.42	0.37
4378	302.95	113.3	4.23 4.22	1.239	0.156	0.897	0.257	4.24 4.25	3.97 4.09	3.24 3.24	3.24 3.18	2.97 3.03	2.32 2.29	2.24 2.21	1.95 2.02	1.12 1.04	0.28 0.28	0.26
4379	200.71	113.8	2.64 2.63	0.773	0.103	0.901	0.197	2.63 2.64	2.50 2.55	2.13 2.14	2.13 2.13	2.00 2.03	1.70 1.68	1.66 1.64	1.52 1.55	0.80 0.76	0.22 0.22	0.20
4381	335.08	126.8	5.73 5.73	1.678	0.173	1.004	0.305	5.77 5.78	5.40 5.58	4.54 4.54	4.53 4.45	4.18 4.26	3.33 3.29	3.24 3.19	2.85 2.94	1.48 1.35	0.32 0.34	0.30
4382	253.53	126.9	4.36 4.35	1.275	0.131	1.005	0.256	4.37 4.38	4.13 4.25	3.58 3.58	3.58 3.54	3.34 3.40	2.82 2.79	2.75 2.71	2.45 2.51	1.22 1.12	0.27 0.28	0.26
4383	129.49	126.5	3.33 3.32	0.975	0.067	1.002	0.212	3.34 3.34	3.20 3.26	2.81 2.81	2.80 2.77	2.61 2.66	2.16 2.14	2.10 2.08	1.79 1.88	0.92 0.86	0.20 0.24	0.21
4384	253.63	140.8	5.84 5.83	1.708	0.131	1.115	0.348	5.87 5.89	5.57 5.71	4.85 4.84	4.83 4.76	4.52 4.60	3.70 3.66	3.60 3.55	3.15 3.26	1.56 1.40	0.34 0.38	0.35
4385	149.64	141.3	4.34 4.34	1.270	0.077	1.119	0.230	4.35 4.36	4.16 4.24	3.59 3.59	3.57 3.54	3.35 3.40	2.74 2.71	2.66 2.62	2.30 2.41	1.19 1.07	0.22 0.25	0.23
4386	47.57	142.4	1.91 1.89	0.558	0.025	1.127	0.141	1.89 1.90	1.81 1.84	1.55 1.55	1.54 1.56	1.45 1.47	1.19 1.18	1.15 1.14	1.00 1.06	0.50 0.46	0.15 0.17	0.14
4387	33.43	141.7	1.41 1.39	0.413	0.017	1.122	0.130	1.38 1.39	1.34 1.35	1.13 1.14	1.13 1.15	1.06 1.07	0.88 0.86	0.84 0.84	0.74 0.78	0.37 0.34	0.15 0.16	0.13
4388	135.06	180.6	4.89 4.88	1.430	0.070	1.430	0.249	4.92 4.92	4.65 4.77	4.09 4.08	4.07 4.02	3.79 3.88	3.11 3.07	3.02 2.97	2.56 2.71	1.29 1.15	0.23 0.27	0.25
4389	126.62	180.8	4.81 4.80	1.408	0.065	1.432	0.249	4.83 4.84	4.56 4.69	3.97 3.95	3.92 3.89	3.64 3.73	2.96 2.92	2.88 2.81	2.39 2.58	1.21 1.07	0.23 0.26	0.25

TABLE II.—Continued.

(b) Hydrogen

Run	$\dot{w}$, g/s	T_o, K	P_o, MPa	$P_{R,o}$	G_R	$T_{R,o}$	P_B, MPa	Pressure at pressure tap locations 1 to 10, MPa P_1	P_2	P_3	P_4	P_5	P_6	P_7	P_8	P_9	P_{10}	P_e, MPa
4398	14.12	290.9	1.99 1.97	1.538	0.038	8.815	0.167	1.96 1.98	1.87 1.91	1.64 1.64	1.64 1.63	1.47 1.53	1.25 1.23	1.22 1.18	0.97 1.09	0.54 0.47	0.17 0.18	0.17
4399	20.71	293.8	2.79 2.77	2.153	0.055	8.903	0.213	2.78 2.78	2.63 2.68	2.31 2.31	2.31 2.28	2.08 2.16	1.76 1.72	1.72 1.65	1.35 1.52	0.75 0.66	0.21 0.22	0.21
4400	27.50	295.5	3.58 3.57	2.765	0.074	8.955	0.261	3.56 3.58	3.38 3.45	2.99 2.97	2.98 2.93	2.68 2.79	2.26 2.21	2.21 2.12	1.72 1.95	0.95 0.83	0.24 0.26	0.26
4401	35.50	296.4	4.51 4.49	3.478	0.095	8.982	0.319	4.50 4.52	4.25 4.35	3.77 3.75	3.75 3.70	3.39 3.52	2.85 2.78	2.78 2.67	2.16 2.44	1.18 1.03	0.29 0.32	0.32
4402	40.34	296.2	5.07 5.05	3.911	0.108	8.976	0.355	5.06 5.09	4.78 4.89	4.25 4.22	4.22 4.15	3.81 3.96	3.20 3.12	3.12 3.00	2.42 2.73	1.31 1.15	0.32 0.36	0.36
4403	46.84	295.7	5.80 5.78	4.472	0.125	8.961	0.405	5.79 5.83	5.47 5.60	4.87 4.84	4.84 4.76	4.37 4.54	3.65 3.57	3.56 3.42	2.76 3.11	1.49 1.30	0.37 0.40	0.40
4404	123.10	28.6	6.32 6.33	4.873	0.329	0.867	0.335	6.35 6.38	5.98 6.11	4.61 4.62	4.59 4.49	4.16 4.22	2.82 2.77	2.66 2.62	2.13 2.27	0.91 0.81	0.34 0.34	0.34
4405	96.60	28.8	4.55 4.56	3.515	0.258	0.873	0.269	4.56 4.58	4.31 4.38	3.31 3.32	3.31 3.24	3.00 3.04	2.11 2.08	2.00 1.98	1.64 1.75	0.78 0.70	0.30 0.27	0.27
4406	71.59	28.4	3.02 3.01	2.329	0.192	0.861	0.232	3.00 3.02	2.86 2.89	2.21 2.23	2.23 2.18	2.02 2.05	1.49 1.49	1.43 1.42	1.21 1.29	0.64 0.58	0.24 0.23	0.23
4407	46.41	29.8	1.87 1.86	1.444	0.124	0.903	0.193	1.83 1.84	1.78 1.77	1.42 1.44	1.45 1.44	1.33 1.35	1.07 1.07	1.04 1.04	0.92 0.98	0.46 0.44	0.20 0.19	0.19
4408	123.33	28.2	6.08 6.09	4.691	0.330	0.855	0.323	6.10 6.13	5.72 5.86	4.37 4.37	4.35 4.24	3.90 3.97	2.62 2.57	2.47 2.44	1.95 2.09	0.85 0.75	0.33 0.33	0.32
4409	91.74	27.7	4.01 4.01	3.096	0.245	0.839	0.249	4.00 4.02	3.76 3.85	2.86 2.87	2.87 2.80	2.57 2.61	1.80 1.78	1.71 1.69	1.38 1.49	0.69 0.61	0.26 0.25	0.25
4410	66.92	27.9	2.61 2.60	2.018	0.179	0.845	0.214	2.59 2.60	2.45 2.49	1.88 1.90	1.90 1.87	1.71 1.74	1.27 1.26	1.21 1.20	1.02 1.09	0.54 0.50	0.23 0.21	0.21
4411	46.15	27.9	1.66 1.65	1.284	0.123	0.845	0.183	1.62 1.63	1.57 1.57	1.24 1.25	1.26 1.25	1.15 1.17	0.91 0.91	0.89 0.88	0.78 0.83	0.40 0.38	0.20 0.19	0.18
4412	116.34	32.8	6.11 6.13	4.718	0.311	0.994	0.323	6.15 6.17	5.78 5.92	4.50 4.50	4.49 4.38	4.06 4.13	2.83 2.78	2.69 2.66	2.18 2.33	1.07 0.93	0.32 0.33	0.32
4413	93.59	33.3	4.65 4.66	3.585	0.250	1.009	0.261	4.65 4.67	4.39 4.48	3.42 3.43	3.42 3.34	3.10 3.15	2.25 2.22	2.14 2.12	1.78 1.90	0.89 0.81	0.29 0.26	0.26
4414	71.87	33.0	3.32 3.32	2.563	0.192	1.000	0.226	3.30 3.32	3.14 3.19	2.47 2.48	2.49 2.44	2.27 2.29	1.72 1.70	1.65 1.64	1.41 1.50	0.72 0.66	0.23 0.23	0.23

TABLE II.—Continued.

(b) Concluded.

Run	$\dot{w}$, g/s	T_o, K	P_o, MPa	$P_{R,o}$	G_R	$T_{R,o}$	P_B, MPa	Pressure at pressure tap locations 1 to 10, MPa										P_e, MPa
								P_1	P_2	P_3	P_4	P_5	P_6	P_7	P_8	P_9	P_{10}	
4415	49.21	34.7	2.43 2.42	1.873	0.132	1.052	0.194	2.40 2.41	2.31 2.33	1.88 1.89	1.90 1.88	1.76 1.78	1.42 1.41	1.38 1.37	1.21 1.28	0.58 0.54	0.20 0.20	0.19
4416	111.06	36.7	6.15 6.17	4.745	0.297	1.112	0.310	6.19 6.21	5.83 5.97	4.62 4.62	4.61 4.50	4.19 4.25	3.01 2.96	2.87 2.83	2.35 2.50	1.16 1.02	0.29 0.32	0.31
4417	87.74	36.3	4.64 4.64	3.577	0.235	1.100	0.256	4.64 4.67	4.40 4.49	3.49 3.50	3.50 3.44	3.19 3.23	2.37 2.34	2.27 2.25	1.91 2.02	0.95 0.86	0.25 0.26	0.26
4418	61.00	37.1	3.22 3.22	2.487	0.163	1.124	0.213	3.20 3.23	3.07 3.11	2.48 2.50	2.50 2.46	2.30 2.33	1.81 1.79	1.74 1.73	1.51 1.59	0.74 0.68	0.22 0.22	0.21
4419	44.83	36.3	2.37 2.36	1.827	0.120	1.100	0.186	2.34 2.36	2.27 2.28	1.86 1.88	1.88 1.86	1.75 1.76	1.41 1.40	1.37 1.36	1.21 1.26	0.57 0.52	0.19 0.19	0.19
4420	21.55	36.4	1.64 1.62	1.262	0.058	1.103	0.144	1.61 1.61	1.58 1.57	1.35 1.36	1.38 1.38	1.30 1.30	1.11 1.12	1.09 1.09	0.97 1.05	0.45 0.43	0.16 0.16	0.14
4421	94.35	46.8	6.30 6.32	4.863	0.252	1.418	0.320	6.35 6.38	6.05 6.16	4.96 4.96	4.95 4.85	4.57 4.62	3.41 3.35	3.25 3.22	2.73 2.87	1.31 1.25	0.32 0.33	0.32
4422	68.96	47.2	4.87 4.88	3.755	0.184	1.430	0.256	4.90 4.91	4.67 4.75	3.88 3.89	3.88 3.82	3.61 3.64	2.79 2.76	2.68 2.66	2.30 2.42	1.24 1.33	0.25 0.27	0.26

(c) Hydrogen with backpressure control

Run	$\dot{w}$, g/s	T_o, K	P_o, MPa	$P_{R,o}$	G_R	$T_{R,o}$	P_B, MPa	Pressure at pressure tap locations 1 to 10, MPa										P_e, MPa
								P_1	P_2	P_3	P_4	P_5	P_6	P_7	P_8	P_9	P_{10}	
4423	47.74	47.5	3.73 3.73	2.875	0.128	1.439	0.208	3.72 3.74	3.59 3.63	3.01 3.03	3.03 2.98	2.83 2.85	2.26 2.24	2.18 2.17	1.91 2.00	1.15 1.13	0.20 0.22	0.21
4424	33.23	47.2	2.81 2.81	2.171	0.089	1.430	0.175	2.80 2.81	2.72 2.73	2.27 2.29	2.29 2.28	2.14 2.15	1.72 1.71	1.67 1.65	1.46 1.52	0.87 0.76	0.17 0.19	0.18
4425	23.42	48.0	2.19 2.18	1.688	0.063	1.455	0.156	2.16 2.17	2.11 2.11	1.75 1.76	1.76 1.75	1.64 1.66	1.31 1.30	1.27 1.26	1.10 1.16	0.52 0.48	0.16 0.17	0.16
4426	99.39	26.2	4.39 4.40	3.390	0.266	0.794	0.252	4.38 4.43	4.00 4.13	2.96 2.97	2.96 2.88	2.64 2.69	1.80 1.76	1.70 1.67	1.34 1.45	0.60 0.60	0.27 0.27	0.25
4427	97.84	25.9	4.40 4.40	3.394	0.262	0.785	0.557	4.40 4.42	4.05 4.19	3.04 3.05	3.03 2.97	2.71 2.76	1.86 1.83	1.76 1.74	1.40 1.52	0.66 0.64	0.55 0.45	0.56
4428	95.50	26.2	4.40 4.41	3.396	0.255	0.794	0.763	4.41 4.43	4.07 4.21	3.10 3.11	3.10 3.03	2.79 2.85	1.98 1.94	1.88 1.86	1.53 1.65	0.82 0.82	0.75 0.56	0.76

TABLE II.—Concluded.

(c) Concluded.

Run	$\dot{w}$, g/s	T_o, K	P_o, MPa	$P_{R,o}$	G_R	$T_{R,o}$	P_B, MPa	Pressure at pressure tap locations 1 to 10, MPa										P_e, MPa
								P_1	P_2	P_3	P_4	P_5	P_6	P_7	P_8	P_9	P_{10}	
4429	94.16	26.7	4.41 4.42	3.401	0.252	0.809	0.860	4.41 4.44	4.11 4.22	3.15 3.16	3.15 3.09	2.84 2.89	2.05 2.02	1.96 1.93	1.61 1.72	0.92 0.91	0.85 0.57	0.86
4430	92.44	27.7	4.41 4.42	3.402	0.247	0.839	0.887	4.41 4.44	4.14 4.22	3.16 3.17	3.16 3.10	2.85 2.91	2.07 2.04	1.98 1.96	1.64 1.76	0.95 0.95	0.88 0.57	0.89
4431	86.39	29.6	4.47 4.47	3.448	0.231	0.897	0.293	4.48 4.50	4.21 4.31	3.25 3.26	3.24 3.18	2.94 2.97	2.09 2.06	1.99 1.96	1.63 1.74	0.87 0.82	0.30 0.31	0.29
4432	86.87	30.4	4.47 4.47	3.447	0.232	0.921	0.702	4.48 4.50	4.22 4.31	3.25 3.26	3.25 3.20	2.95 2.99	2.11 2.08	2.01 1.99	1.66 1.77	0.91 0.87	0.63 0.40	0.70
4433	84.38	31.6	4.48 4.49	3.458	0.226	0.958	0.863	4.49 4.51	4.24 4.33	3.30 3.31	3.29 3.22	3.01 3.05	2.18 2.15	2.08 2.08	1.74 1.87	1.00 0.98	0.77 0.46	0.86
4434	79.40	34.0	4.50 4.51	3.470	0.212	1.030	1.243	4.51 4.53	4.28 4.37	3.43 3.44	3.43 3.38	3.17 3.19	2.43 2.40	2.34 2.32	2.03 2.13	1.35 1.33	1.25 0.54	1.24

TABLE III.—FLOW RATE AND PRESSURE DROP DATA FOR THREE-STEP LABYRINTH SEAL, TWO-THIRDS FULLY ECCENTRIC POSITION

TABLE III.—FLOW RATE AND PRESSURE DROP DATA FOR THREE-STEP LABYRINTH SEAL, TWO-THIRDS FULLY ECCENTRIC POSITION

[Where two values are given, the top value is for the 0° circumferential position (minimum clearance), and the bottom value is for the 180° circumferential position (maximum clearance).]

(a) Nitrogen

Run	$\dot{w}$, g/s	T_o, K	P_o, MPa	$P_{R,o}$	G_R	$T_{R,o}$	P_B, MPa	Pressure at pressure tap locations 1 to 10, MPa										P_e, MPa
								P_1	P_2	P_3	P_4	P_5	P_6	P_7	P_8	P_9	P_{10}	
4208	20.67	282.3	0.81	0.238	0.011	2.235	0.067	0.81	0.78	0.64	0.63	0.62	0.51	0.48	0.46	0.21	0.11	0.07
			0.80					0.79	0.74	0.66	0.69	0.60	0.51	0.50	0.42	0.22	0.11	
4209	29.41	287.1	1.15	0.336	0.015	2.273	0.068	1.15	1.10	0.92	0.90	0.88	0.72	0.68	0.64	0.29	0.11	0.07
			1.14					1.12	1.06	0.94	0.97	0.85	0.73	0.71	0.58	0.32	0.11	
4210	38.11	289.0	1.45	0.424	0.020	2.288	0.069	1.45	1.39	1.17	1.14	1.12	0.91	0.86	0.81	0.36	0.16	0.07
			1.44					1.43	1.34	1.20	1.21	1.08	0.92	0.90	0.73	0.40	0.12	
4211	45.51	289.8	1.69	0.496	0.023	2.295	0.069	1.70	1.63	1.37	1.34	1.31	1.06	1.01	0.94	0.42	0.13	0.07
			1.68					1.67	1.57	1.41	1.42	1.26	1.08	1.05	0.85	0.46	0.13	
4212	59.62	291.7	2.16	0.633	0.031	2.310	0.069	2.17	2.08	1.76	1.72	1.68	1.36	1.30	1.20	0.53	0.16	0.07
			2.15					2.15	2.02	1.81	1.81	1.62	1.38	1.35	1.08	0.59	0.15	
4213	85.97	294.3	3.02	0.885	0.044	2.330	0.069	3.04	2.91	2.48	2.43	2.36	1.89	1.82	1.68	0.73	0.22	0.07
			3.01					3.02	2.82	2.54	2.53	2.26	1.93	1.89	1.51	0.81	0.20	
4214	109.79	294.5	3.78	1.106	0.057	2.332	0.070	3.80	3.65	3.11	3.04	2.95	2.36	2.27	2.09	0.90	0.28	0.07
			3.77					3.78	3.54	3.18	3.17	2.84	2.41	2.36	1.87	1.01	0.26	
4215	124.01	293.4	4.22	1.234	0.064	2.323	0.070	4.24	4.07	3.47	3.40	3.30	2.63	2.53	2.33	1.00	0.32	0.07
			4.21					4.22	3.95	3.56	3.53	3.17	2.70	2.64	2.08	1.12	0.28	
4216	151.42	294.9	5.05	1.478	0.078	2.335	0.070	5.08	4.88	4.17	4.09	3.96	3.15	3.03	2.78	1.18	0.38	0.07
			5.04					5.07	4.73	4.27	4.22	3.80	3.23	3.15	2.48	1.32	0.34	
4217	176.50	295.1	5.78	1.693	0.091	2.336	0.070	5.82	5.60	4.79	4.69	4.54	3.60	3.46	3.17	1.34	0.44	0.07
			5.78					5.81	5.43	4.89	4.86	4.36	3.69	3.61	2.83	1.50	0.39	
4218	196.42	294.8	6.36	1.860	0.101	2.334	0.070	6.40	6.15	5.26	5.16	4.99	3.95	3.80	3.47	1.45	0.49	0.07
			6.35					6.38	5.97	5.38	5.35	4.80	4.05	3.96	3.10	1.64	0.43	

(b) Hydrogen

Run	$\dot{w}$, g/s	T_o, K	P_o, MPa	$P_{R,o}$	G_R	$T_{R,o}$	P_B, MPa	Pressure at pressure tap locations 1 to 10, MPa										P_e, MPa
								P_1	P_2	P_3	P_4	P_5	P_6	P_7	P_8	P_9	P_{10}	
4222	9.02	294.7	1.31	1.012	0.024	8.930	0.044	1.29	1.26	1.05	1.04	1.00	0.80	0.77	0.72	0.32	0.16	0.04
			1.30					1.29	1.20	1.09	1.10	0.96	0.83	0.80	0.66	0.35	0.14	
4223	9.06	294.8	1.32	1.016	0.024	8.933	0.045	1.29	1.27	1.06	1.05	1.01	0.81	0.78	0.73	0.32	0.16	0.04
			1.30					1.30	1.21	1.09	1.10	0.97	0.84	0.81	0.66	0.36	0.14	
4224	12.51	298.7	1.76	1.357	0.033	9.052	0.062	1.74	1.69	1.42	1.41	1.36	1.09	1.04	0.97	0.43	0.18	0.06
			1.74					1.74	1.63	1.47	1.47	1.30	1.12	1.09	0.88	0.48	0.15	
4225	19.58	303.2	2.61	2.014	0.052	9.188	0.109	2.59	2.52	2.13	2.10	2.02	1.61	1.55	1.43	0.63	0.22	0.11
			2.59					2.59	2.43	2.18	2.18	1.94	1.66	1.62	1.29	0.70	0.19	

TABLE III.—Continued.

(b) Continued.

Run	$\dot{w}$, g/s	T_o, K	P_o, MPa	$P_{R,o}$	G_R	$T_{R,o}$	P_B, MPa	Pressure at pressure tap locations 1 to 10, MPa										P_e, MPa
								P_1	P_2	P_3	P_4	P_5	P_6	P_7	P_8	P_9	P_{10}	
4226	38.55	305.8	3.90 3.88	3.010	0.103	9.267	0.194	3.89 3.90	3.78 3.64	3.20 3.27	3.15 3.26	3.04 2.90	2.40 2.48	2.32 2.41	2.13 1.91	0.92 1.02	0.30 0.26	0.19
4227	52.48	306.2	5.17 5.15	3.989	0.140	9.279	0.283	5.16 5.17	5.01 4.83	4.25 4.34	4.19 4.32	4.04 3.85	3.17 3.27	3.06 3.19	2.80 2.51	1.19 1.33	0.38 0.33	0.28
4228	54.38	304.4	6.53 6.51	5.040	0.145	9.224	0.383	6.54 6.54	6.34 6.11	5.38 5.49	5.30 5.46	5.11 4.88	4.01 4.13	3.86 4.02	3.51 3.14	1.47 1.65	0.48 0.41	0.38
4229	33.22	301.7	4.18 4.16	3.227	0.089	9.142	0.210	4.17 4.18	4.06 3.90	3.43 3.51	3.38 3.50	3.26 3.12	2.59 2.66	2.49 2.59	2.29 2.05	0.98 1.09	0.32 0.27	0.21
4238	127.38	27.5	6.11 6.12	4.716	0.341	0.833	0.225	6.14 6.15	5.93 5.74	4.36 4.42	4.23 4.35	4.02 3.91	2.59 2.64	2.45 2.48	2.12 2.00	0.72 0.80	0.33 0.31	0.22
4239	107.39	27.1	4.82 4.82	3.717	0.287	0.821	0.163	4.83 4.84	4.67 4.51	3.41 3.48	3.32 3.42	3.15 3.07	2.09 2.12	1.97 2.01	1.73 1.64	0.63 0.70	0.27 0.25	0.16
4240	88.84	26.9	3.66 3.66	2.824	0.238	0.815	0.129	3.66 3.67	3.53 3.41	2.59 2.64	2.53 2.60	2.40 2.34	1.64 1.67	1.56 1.58	1.38 1.31	0.55 0.62	0.23 0.21	0.13
4241	69.57	26.4	2.60 2.60	2.008	0.186	0.800	0.108	2.59 2.59	2.50 2.41	1.85 1.90	1.82 1.88	1.74 1.69	1.24 1.26	1.18 1.20	1.06 1.02	0.47 0.52	0.21 0.20	0.11
4242	49.80	26.8	1.69 1.68	1.304	0.133	0.812	0.087	1.67 1.67	1.62 1.56	1.24 1.27	1.23 1.28	1.17 1.15	0.90 0.91	0.86 0.87	0.80 0.78	0.38 0.40	0.19 0.19	0.09
4243	38.46	27.0	1.27 1.26	0.978	0.103	0.818	0.075	1.24 1.25	1.22 1.18	0.96 0.99	0.96 1.00	0.92 0.90	0.74 0.76	0.72 0.73	0.67 0.67	0.31 0.32	0.18 0.17	0.08
4244	113.81	34.7	6.03 6.04	4.652	0.304	1.052	0.210	6.06 6.07	5.87 5.70	4.44 4.52	4.34 4.44	4.14 4.04	2.84 2.89	2.70 2.75	2.41 2.29	0.95 1.08	0.32 0.29	0.21
4245	97.22	34.5	4.95 4.95	3.816	0.260	1.045	0.161	4.96 4.97	4.82 4.67	3.65 3.72	3.57 3.66	3.41 3.33	2.41 2.44	2.30 2.33	2.07 1.97	0.86 0.94	0.27 0.23	0.16
4246	68.34	35.9	3.43 3.43	2.647	0.183	1.088	0.123	3.43 3.43	3.34 3.24	2.60 2.65	2.56 2.64	2.46 2.41	1.86 1.88	1.79 1.81	1.65 1.59	0.70 0.76	0.23 0.21	0.12
4247	51.21	35.5	2.54 2.54	1.964	0.137	1.076	0.099	2.53 2.54	2.47 2.41	1.97 2.01	1.95 2.00	1.88 1.84	1.48 1.50	1.43 1.45	1.34 1.30	0.56 0.60	0.20 0.18	0.10
4248	38.90	34.3	1.92 1.92	1.481	0.104	1.039	0.079	1.90 1.91	1.87 1.82	1.52 1.55	1.51 1.57	1.46 1.44	1.18 1.20	1.14 1.15	1.05 1.01	0.46 0.47	0.19 0.17	0.08
4249	19.68	34.9	1.43 1.42	1.103	0.053	1.058	0.043	1.41 1.42	1.40 1.37	1.20 1.22	1.20 1.23	1.17 1.14	0.90 0.92	0.87 0.88	0.81 0.79	0.52 0.47	0.16 0.14	0.04
4250	125.41	28.1	6.08 6.08	4.690	0.336	0.852	0.186	6.12 6.12	5.90 5.72	4.33 4.41	4.21 4.33	4.00 3.88	2.58 2.62	2.43 2.47	2.11 1.98	0.74 0.82	0.30 0.27	0.19

TABLE III.—Continued.

(b) Continued.

Run	$\dot{w}$, g/s	T_o, K	P_o, MPa	$P_{R,o}$	G_R	$T_{R,o}$	P_B, MPa	Pressure at pressure tap locations 1 to 10, MPa										P_e, MPa
								P_1	P_2	P_3	P_4	P_5	P_6	P_7	P_8	P_9	P_{10}	
4251	106.89	28.1	4.86	3.748	0.286	0.852	0.133	4.87	4.71	3.44	3.34	3.18	2.10	1.99	1.74	0.66	0.24	0.13
			4.87					4.88	4.55	3.51	3.44	3.09	2.14	2.02	1.65	0.74	0.22	
4252	82.07	27.7	3.52	2.714	0.220	0.839	0.110	3.52	3.40	2.50	2.44	2.32	1.59	1.52	1.35	0.57	0.22	0.11
			3.52					3.52	3.28	2.55	2.52	2.26	1.62	1.54	1.29	0.63	0.20	
4253	97.43	39.2	5.53	4.265	0.261	1.188	0.203	5.56	5.40	4.18	4.09	3.92	2.80	2.68	2.42	1.01	0.31	0.20
			5.53					5.57	5.25	4.24	4.18	3.83	2.84	2.71	2.30	1.11	0.28	
4254	88.44	38.9	4.94	3.815	0.237	1.179	0.177	4.97	4.82	3.74	3.67	3.52	2.55	2.45	2.22	0.94	0.28	0.18
			4.95					4.97	4.69	3.80	3.76	3.44	2.59	2.48	2.12	1.02	0.25	
4255	65.46	39.0	3.67	2.830	0.175	1.182	0.126	3.67	3.57	2.82	2.77	2.67	2.02	1.95	1.79	0.76	0.23	0.13
			3.67					3.68	3.48	2.87	2.85	2.61	2.05	1.97	1.72	0.83	0.21	
4256	39.83	38.2	2.41	1.857	0.107	1.158	0.079	2.41	2.36	1.91	1.89	1.83	1.44	1.39	1.29	0.59	0.19	0.08
			2.40					2.41	2.30	1.94	1.95	1.78	1.45	1.39	1.24	0.61	0.17	
4257	13.50	38.2	1.64	1.264	0.036	1.158	0.040	1.63	1.62	1.44	1.45	1.42	1.30	1.28	1.26	0.40	0.15	0.04
			1.63					1.63	1.59	1.47	1.48	1.40	1.31	1.28	1.24	0.45	0.13	
4258	0.00	37.3	1.11	0.860	0.000	1.130	0.031	1.09	1.11	1.06	1.08	1.07	1.05	1.05	1.04	0.88	0.14	0.03
			1.11					1.10	1.09	1.08	1.10	1.04	1.06	1.03	1.03	0.86	0.14	
4259	61.56	49.8	4.68	3.609	0.165	1.509	0.165	4.70	4.60	3.73	3.67	3.55	2.70	2.60	2.39	1.08	0.28	0.16
			4.68					4.71	4.49	3.78	3.75	3.47	2.74	2.63	2.28	1.15	0.23	
4260	58.18	50.2	4.49	3.464	0.156	1.521	0.152	4.50	4.40	3.59	3.53	3.42	2.62	2.53	2.32	1.07	0.26	0.15
			4.50					4.52	4.31	3.64	3.61	3.34	2.65	2.55	2.22	1.15	0.22	
4261	26.40	50.2	2.47	1.907	0.071	1.521	0.068	2.46	2.41	1.97	1.95	1.89	1.48	1.43	1.32	0.52	0.18	0.07
			2.47					2.47	2.36	2.01	2.00	1.85	1.50	1.44	1.27	0.58	0.15	
4262	11.49	51.6	1.29	0.996	0.031	1.564	0.039	1.26	1.25	1.02	1.02	0.98	0.78	0.75	0.69	0.29	0.15	0.04
			1.28					1.27	1.22	1.05	1.07	0.96	0.79	0.76	0.68	0.31	0.13	
4263	91.51	27.1	4.16	3.210	0.245	0.821	0.170	4.17	4.02	2.94	2.86	2.72	1.82	1.73	1.52	0.59	0.28	0.17
			4.16					4.18	3.89	3.00	2.96	2.64	1.85	1.75	1.44	0.66	0.27	
4264	86.00	26.9	3.02	2.329	0.230	0.815	0.114	3.01	2.91	2.13	2.08	1.98	1.37	1.31	1.17	0.50	0.22	0.11
			3.01					3.02	2.81	2.18	2.18	1.92	1.40	1.33	1.12	0.55	0.21	
4265	71.11	26.6	2.29	1.766	0.190	0.806	0.093	2.28	2.20	1.63	1.61	1.53	1.10	1.06	0.95	0.44	0.20	0.09
			2.28					2.28	2.13	1.68	1.67	1.49	1.12	1.07	0.92	0.47	0.19	
4266	62.30	26.6	1.70	1.314	0.167	0.806	0.079	1.68	1.64	1.24	1.23	1.17	0.89	0.86	0.78	0.37	0.19	0.08
			1.70					1.69	1.58	1.28	1.28	1.14	0.90	0.86	0.77	0.39	0.18	
4267	44.28	26.9	1.31	1.012	0.118	0.815	0.067	1.28	1.26	0.98	0.98	0.94	0.75	0.72	0.67	0.31	0.18	0.07
			1.30					1.29	1.22	1.01	1.03	0.92	0.76	0.73	0.67	0.33	0.17	

TABLE III.—Continued.

(b) Continued.

Run	$\dot{w}$, g/s	T_o, K	P_o, MPa	$P_{R,o}$	G_R	$T_{R,o}$	P_B, MPa	Pressure at pressure tap locations 1 to 10, MPa										P_e, MPa
								P_1	P_2	P_3	P_4	P_5	P_6	P_7	P_8	P_9	P_{10}	
4268	19.96	26.9	0.93 0.92	0.721	0.053	0.815	0.055	0.91 0.91	0.90 0.87	0.73 0.76	0.74 0.78	0.72 0.70	0.58 0.59	0.56 0.57	0.52 0.51	0.24 0.24	0.17 0.16	0.06
4274	7.68	235.3	1.23 1.20	0.946	0.021	7.130	0.130	1.19 1.19	1.18 1.13	0.96 0.99	0.97 1.01	0.93 0.89	0.74 0.76	0.72 0.74	0.67 0.62	0.29 0.32	0.16 0.13	0.13
4275	11.32	261.9	1.71 1.68	1.320	0.030	7.936	0.145	1.67 1.68	1.64 1.59	1.37 1.41	1.37 1.44	1.32 1.26	1.05 1.08	1.01 1.04	0.95 0.86	0.41 0.45	0.17 0.14	0.14
4276	19.73	280.0	2.73 2.70	2.110	0.053	8.485	0.201	2.70 2.71	2.63 2.56	2.22 2.28	2.20 2.28	2.13 2.03	1.68 1.73	1.62 1.68	1.50 1.35	0.65 0.72	0.22 0.18	0.20
4277	31.42	290.4	4.09 4.04	3.154	0.084	8.800	0.284	4.06 4.07	3.94 3.84	3.35 3.43	3.31 3.41	3.20 3.05	2.53 2.59	2.43 2.52	2.24 2.00	0.96 1.06	0.30 0.25	0.28
4278	48.50	296.2	6.00 5.94	4.630	0.130	8.976	0.414	5.98 6.00	5.79 5.65	4.94 5.06	4.88 5.02	4.71 4.50	3.69 3.79	3.55 3.68	3.25 2.90	1.36 1.52	0.43 0.35	0.41
4279	69.64	27.7	2.85 2.82	2.200	0.186	0.839	0.242	2.83 2.85	2.73 2.66	2.05 2.10	2.02 2.09	1.93 1.88	1.38 1.40	1.32 1.34	1.20 1.14	0.54 0.58	0.27 0.25	0.24
4280	56.57	27.6	2.19 2.17	1.693	0.151	0.836	0.209	2.17 2.18	2.10 2.04	1.60 1.63	1.58 1.62	1.51 1.47	1.12 1.13	1.08 1.09	0.99 0.95	0.46 0.48	0.23 0.21	0.21
4281	55.91	27.7	1.73 1.70	1.335	0.150	0.839	0.187	1.70 1.71	1.66 1.60	1.28 1.31	1.27 1.31	1.22 1.19	0.94 0.95	0.91 0.92	0.85 0.83	0.40 0.41	0.21 0.19	0.19
4282	30.46	27.7	1.22 1.20	0.941	0.081	0.839	0.163	1.20 1.20	1.19 1.14	0.95 0.97	0.95 0.99	0.92 0.89	0.75 0.76	0.73 0.73	0.68 0.66	0.31 0.31	0.19 0.17	0.16
4283	29.45	28.3	1.02 1.00	0.789	0.079	0.858	0.155	0.99 0.99	0.98 0.95	0.81 0.83	0.82 0.85	0.79 0.77	0.64 0.64	0.62 0.62	0.57 0.55	0.29 0.28	0.18 0.16	0.16
4284	73.92	26.3	2.74 2.71	2.117	0.198	0.797	0.238	2.72 2.73	2.63 2.54	1.96 2.01	1.93 1.99	1.84 1.80	1.31 1.33	1.26 1.27	1.14 1.09	0.50 0.54	0.26 0.24	0.24
4286	36.08	26.0	1.59 1.56	1.226	0.097	0.788	0.179	1.55 1.56	1.52 1.46	1.16 1.19	1.16 1.21	1.11 1.08	0.85 0.86	0.82 0.82	0.76 0.74	0.36 0.38	0.20 0.18	0.18
4287	33.19	26.3	1.21 1.18	0.933	0.089	0.797	0.159	1.17 1.18	1.16 1.11	0.90 0.93	0.91 0.94	0.88 0.86	0.70 0.71	0.68 0.69	0.65 0.63	0.30 0.31	0.18 0.17	0.16
4288	40.07	26.3	1.10 1.09	0.853	0.107	0.797	0.156	1.07 1.08	1.06 1.02	0.84 0.86	0.85 0.88	0.82 0.80	0.67 0.68	0.65 0.65	0.62 0.60	0.30 0.29	0.18 0.16	0.16
4289	17.22	27.3	0.71 0.69	0.547	0.046	0.827	0.138	0.67 0.68	0.68 0.66	0.54 0.57	0.56 0.59	0.53 0.51	0.43 0.44	0.42 0.42	0.39 0.38	0.22 0.21	0.17 0.15	0.14
4290	102.88	25.6	4.49 4.46	3.468	0.275	0.776	0.279	4.49 4.50	4.31 4.18	3.16 3.22	3.08 3.18	2.92 2.85	1.92 1.95	1.81 1.84	1.60 1.50	0.57 0.63	0.30 0.28	0.28

TABLE III.—Continued.

(b) Continued.

Run	$\dot{w}$, g/s	T_o, K	P_o, MPa	$P_{R,o}$	G_R	$T_{R,o}$	P_B, MPa	Pressure at pressure tap locations 1 to 10, MPa										P_e, MPa
								P_1	P_2	P_3	P_4	P_5	P_6	P_7	P_8	P_9	P_{10}	
4291	83.99	25.3	3.34	2.579	0.225	0.767	0.214	3.33	3.20	2.34	2.29	2.18	1.48	1.40	1.25	0.49	0.24	0.21
			3.31					3.34	3.10	2.40	2.38	2.12	1.50	1.42	1.18	0.54	0.22	
4292	66.91	25.4	2.42	1.871	0.179	0.770	0.190	2.40	2.32	1.71	1.68	1.60	1.13	1.08	0.97	0.43	0.21	0.19
			2.40					2.41	2.24	1.75	1.74	1.56	1.14	1.09	0.93	0.47	0.20	
4293	50.90	25.7	1.66	1.282	0.136	0.779	0.168	1.63	1.58	1.19	1.18	1.13	0.84	0.81	0.75	0.36	0.19	0.17
			1.63					1.63	1.52	1.22	1.22	1.11	0.86	0.82	0.73	0.38	0.17	
4294	37.35	25.6	1.22	0.944	0.100	0.776	0.157	1.19	1.17	0.91	0.91	0.87	0.69	0.67	0.63	0.30	0.18	0.16
			1.20					1.20	1.12	0.93	0.96	0.85	0.70	0.67	0.62	0.31	0.16	
4295	133.40	25.9	6.45	4.975	0.357	0.785	0.297	6.47	6.22	4.57	4.45	4.22	2.66	2.50	2.16	0.66	0.33	0.30
			6.41					6.48	6.04	4.66	4.56	4.11	2.70	2.53	2.02	0.74	0.30	
4296	108.24	25.6	4.79	3.698	0.290	0.776	0.234	4.80	4.62	3.36	3.28	3.11	2.02	1.91	1.67	0.57	0.26	0.23
			4.77					4.81	4.47	3.44	3.37	3.03	2.05	1.93	1.56	0.63	0.23	
4297	83.65	25.4	3.29	2.535	0.224	0.770	0.190	3.26	3.14	2.30	2.25	2.14	1.45	1.38	1.23	0.48	0.22	0.19
			3.26					3.28	3.04	2.36	2.32	2.09	1.48	1.40	1.16	0.54	0.20	
4298	63.51	25.9	2.30	1.774	0.170	0.785	0.175	2.27	2.20	1.63	1.61	1.54	1.10	1.05	0.96	0.44	0.20	0.18
			2.27					2.28	2.12	1.68	1.66	1.50	1.12	1.07	0.92	0.47	0.18	
4299	75.63	23.8	2.52	1.942	0.202	0.721	0.218	2.50	2.40	1.76	1.73	1.64	1.13	1.08	0.97	0.40	0.24	0.22
			2.49					2.51	2.32	1.80	1.79	1.60	1.15	1.09	0.92	0.43	0.23	
4300	57.06	23.7	1.97	1.519	0.153	0.718	0.188	1.93	1.87	1.37	1.36	1.30	0.92	0.88	0.80	0.36	0.21	0.19
			1.94					1.94	1.80	1.42	1.41	1.26	0.93	0.89	0.76	0.39	0.20	
4301	46.37	24.1	1.54	1.189	0.124	0.730	0.166	1.50	1.47	1.09	1.09	1.04	0.77	0.74	0.68	0.33	0.19	0.17
			1.51					1.51	1.41	1.12	1.13	1.01	0.78	0.74	0.65	0.34	0.17	
4302	43.50	24.4	1.22	0.944	0.116	0.739	0.154	1.19	1.17	0.89	0.89	0.85	0.66	0.63	0.60	0.30	0.18	0.15
			1.20					1.20	1.12	0.92	0.93	0.83	0.67	0.64	0.58	0.30	0.17	
4303	91.70	26.0	3.82	2.951	0.245	0.788	0.197	3.82	3.67	2.69	2.64	2.50	1.68	1.59	1.41	0.57	0.22	0.20
			3.80					3.83	3.55	2.75	2.70	2.44	1.70	1.61	1.33	0.59	0.20	
4304	85.93	52.0	6.39	4.930	0.230	1.576	0.321	6.41	6.23	5.08	5.00	4.83	3.59	3.45	3.15	1.35	0.35	0.32
			6.36					6.43	6.12	5.16	5.10	4.74	3.63	3.48	2.99	1.45	0.29	
4305	63.04	49.8	4.79	3.696	0.169	1.509	0.252	4.79	4.67	3.83	3.78	3.66	2.81	2.71	2.51	1.25	0.28	0.25
			4.77					4.81	4.58	3.89	3.86	3.59	2.84	2.73	2.39	1.31	0.23	
4306	34.81	51.8	3.13	2.414	0.093	1.570	0.182	3.11	3.05	2.50	2.48	2.40	1.88	1.81	1.68	0.66	0.21	0.18
			3.11					3.12	2.98	2.55	2.54	2.36	1.89	1.82	1.60	0.72	0.16	
4307	20.05	51.1	2.01	1.551	0.054	1.548	0.152	1.98	1.95	1.60	1.59	1.54	1.21	1.17	1.09	0.44	0.18	0.15
			1.99					1.99	1.90	1.63	1.63	1.51	1.23	1.18	1.04	0.48	0.15	

TABLE III.—Continued.

(b) Concluded.

Run	$\dot{w}$, g/s	T_o, K	P_o, MPa	$P_{R,o}$	G_R	$T_{R,o}$	P_B, MPa	Pressure at pressure tap locations 1 to 10, MPa										P_e, MPa
								P_1	P_2	P_3	P_4	P_5	P_6	P_7	P_8	P_9	P_{10}	
4308	14.55	50.4	1.55 1.53	1.196	0.039	1.527	0.137	1.51 1.52	1.50 1.46	1.23 1.25	1.23 1.26	1.19 1.16	0.94 0.95	0.90 0.91	0.84 0.80	0.34 0.37	0.17 0.13	0.14
4309	10.19	51.4	1.17 1.15	0.904	0.027	1.558	0.130	1.13 1.14	1.13 1.09	0.92 0.94	0.92 0.96	0.89 0.87	0.70 0.71	0.68 0.69	0.63 0.61	0.26 0.28	0.17 0.12	0.13

(c) Hydrogen with backpressure control

Run	$\dot{w}$, g/s	T_o, K	P_o, MPa	$P_{R,o}$	G_R	$T_{R,o}$	P_B, MPa	Pressure at pressure tap locations 1 to 10, MPa										P_e, MPa
								P_1	P_2	P_3	P_4	P_5	P_6	P_7	P_8	P_9	P_{10}	
4230	33.30	301.7	4.19 4.17	3.237	0.089	9.142	0.286	4.18 4.19	4.07 3.91	3.44 3.52	3.39 3.51	3.28 3.13	2.59 2.67	2.50 2.60	2.30 2.06	0.99 1.10	0.39 0.33	0.29
4231	33.33	302.4	4.20 4.18	3.242	0.089	9.164	0.326	4.19 4.19	4.08 3.92	3.45 3.53	3.40 3.51	3.28 3.13	2.60 2.68	2.50 2.61	2.30 2.06	0.99 1.10	0.42 0.37	0.33
4232	33.30	302.1	4.21 4.20	3.250	0.089	9.155	0.443	4.20 4.21	4.09 3.93	3.46 3.54	3.41 3.52	3.29 3.14	2.61 2.68	2.51 2.62	2.31 2.07	1.00 1.11	0.53 0.49	0.44
4233	33.17	301.7	4.22 4.21	3.259	0.089	9.142	0.625	4.22 4.22	4.10 3.94	3.47 3.55	3.42 3.53	3.30 3.15	2.62 2.70	2.52 2.63	2.33 2.08	1.02 1.12	0.71 0.65	0.62
4234	33.10	301.3	4.24 4.22	3.269	0.089	9.130	0.798	4.23 4.23	4.11 3.96	3.48 3.56	3.43 3.55	3.32 3.17	2.64 2.71	2.54 2.64	2.34 2.10	1.10 1.14	0.88 0.82	0.80
4235	32.88	300.8	4.25 4.23	3.278	0.088	9.115	0.944	4.24 4.24	4.13 3.97	3.50 3.58	3.45 3.57	3.33 3.18	2.66 2.74	2.57 2.67	2.38 2.13	1.20 1.20	1.04 0.96	0.94
4236	32.51	300.5	4.26 4.25	3.289	0.087	9.106	1.143	4.26 4.26	4.14 3.99	3.53 3.61	3.48 3.60	3.36 3.22	2.71 2.78	2.62 2.72	2.43 2.20	1.35 1.33	1.21 1.16	1.14
4237	30.88	300.9	3.92 3.90	3.022	0.083	9.118	0.193	3.91 3.91	3.81 3.66	3.22 3.29	3.17 3.28	3.06 2.92	2.43 2.50	2.34 2.43	2.15 1.93	0.93 1.03	0.30 0.25	0.19
4310	96.35	26.5	4.14 4.10	3.191	0.258	0.803	0.298	4.13 4.15	3.98 3.86	2.94 3.00	2.87 2.95	2.73 2.65	1.84 1.87	1.75 1.76	1.56 1.45	0.61 0.66	0.33 0.30	0.30
4311	94.14	25.8	4.14 4.11	3.192	0.252	0.782	0.681	4.13 4.14	3.98 3.86	2.94 3.01	2.88 2.97	2.74 2.68	1.87 1.90	1.78 1.80	1.60 1.51	0.74 0.74	0.54 0.67	0.68
4312	90.16	25.9	4.15 4.12	3.204	0.241	0.785	0.955	4.14 4.16	4.00 3.89	3.04 3.10	2.97 3.06	2.85 2.79	2.05 2.07	1.96 1.98	1.80 1.71	1.00 1.00	0.55 0.94	0.96
4313	86.93	26.4	4.16 4.14	3.211	0.233	0.800	1.151	4.15 4.17	4.02 3.92	3.11 3.16	3.05 3.12	2.94 2.87	2.18 2.20	2.10 2.12	1.94 1.86	1.20 1.20	0.55 1.14	1.15
4314	79.86	28.4	4.18 4.16	3.226	0.214	0.861	1.461	4.17 4.19	4.05 3.96	3.22 3.28	3.17 3.24	3.07 3.02	2.39 2.41	2.32 2.34	2.18 2.10	1.50 1.50	0.55 1.45	1.46

4.16 4.19 3.96 3.28 3.24 3.02 2.41 2.34 2.10 1.50 1.45

TABLE III.—Continued.

(d) Helium

Run	$\dot{w}$, g/s	T_o, K	P_o, MPa	$P_{R,o}$	G_R	$T_{R,o}$	P_B, MPa	Pressure at pressure tap locations 1 to 10, MPa										P_e, MPa
								P_1	P_2	P_3	P_4	P_5	P_6	P_7	P_8	P_9	P_{10}	
4315	10.71	183.5	1.27 1.24	5.595	0.046	35.288	0.134	1.22 1.23	1.21 1.16	0.99 1.02	0.99 1.02	0.96 0.92	0.75 0.77	0.73 0.74	0.68 0.63	0.29 0.31	0.16 0.13	0.13
4316	10.08	192.5	1.26 1.23	5.555	0.043	37.019	0.129	1.22 1.22	1.19 1.13	0.97 1.00	0.97 1.02	0.94 0.90	0.74 0.76	0.72 0.73	0.66 0.63	0.28 0.31	0.15 0.12	0.13
4317	22.07	208.4	2.52 2.48	11.101	0.095	40.077	0.164	2.48 2.50	2.45 2.31	1.96 2.02	1.96 2.02	1.89 1.81	1.49 1.53	1.44 1.47	1.34 1.22	0.55 0.61	0.19 0.14	0.16
4318	15.68	213.0	1.72 1.69	7.577	0.067	40.962	0.145	1.68 1.69	1.68 1.58	1.36 1.39	1.35 1.39	1.31 1.25	1.02 1.05	0.99 1.01	0.92 0.85	0.38 0.42	0.18 0.13	0.14
4319	20.39	225.4	2.18 2.15	9.608	0.088	43.346	0.159	2.14 2.15	2.12 2.02	1.74 1.78	1.73 1.79	1.68 1.60	1.31 1.35	1.26 1.30	1.18 1.08	0.48 0.54	0.18 0.14	0.16
4320	26.50	236.9	2.88 2.84	12.665	0.114	45.558	0.188	2.85 2.86	2.79 2.68	2.29 2.34	2.27 2.34	2.20 2.11	1.72 1.76	1.66 1.71	1.54 1.40	0.63 0.70	0.21 0.16	0.19
4321	37.38	249.7	3.74 3.71	16.498	0.161	48.019	0.237	3.72 3.73	3.64 3.51	3.07 3.14	3.03 3.12	2.94 2.82	2.30 2.35	2.21 2.28	2.05 1.84	0.82 0.92	0.47 0.20	0.24
4322	44.52	258.6	4.31 4.27	18.996	0.191	49.731	0.274	4.29 4.30	4.18 4.05	3.54 3.62	3.50 3.58	3.39 3.25	2.64 2.71	2.54 2.62	2.34 2.10	0.94 1.06	0.29 0.24	0.27
4323	51.79	266.8	4.89 4.84	21.546	0.223	51.308	0.314	4.87 4.89	4.74 4.59	4.02 4.11	3.97 4.08	3.85 3.68	3.00 3.07	2.88 2.97	2.65 2.37	1.06 1.19	0.32 0.27	0.31
4324	59.18	273.4	5.45 5.41	24.022	0.254	52.577	0.357	5.44 5.45	5.28 5.12	4.50 4.59	4.43 4.55	4.29 4.11	3.34 3.42	3.21 3.31	2.94 2.63	1.18 1.32	0.36 0.30	0.36
4325	15.83	240.1	1.77 1.73	7.793	0.068	46.173	0.152	1.78 1.78	1.76 1.67	1.45 1.48	1.44 1.48	1.40 1.30	1.10 1.12	1.05 1.05	0.98 0.87	0.41 0.44	0.17 0.14	0.15
4326	11.80	245.8	1.31 1.29	5.793	0.051	47.269	0.135	1.27 1.28	1.26 1.20	1.04 1.07	1.03 1.08	1.00 0.96	0.79 0.81	0.76 0.78	0.71 0.66	0.30 0.33	0.16 0.13	0.14
4327	13.28	264.1	1.48 1.44	6.507	0.057	50.788	0.141	1.43 1.44	1.42 1.35	1.17 1.21	1.16 1.22	1.13 1.08	0.89 0.91	0.86 0.89	0.80 0.73	0.34 0.37	0.16 0.14	0.14
4328	18.78	268.9	2.00 1.97	8.828	0.081	51.712	0.161	1.96 1.97	1.93 1.85	1.61 1.66	1.60 1.65	1.55 1.48	1.22 1.25	1.17 1.21	1.09 0.99	0.46 0.51	0.18 0.15	0.16
4329	25.32	274.1	2.59 2.55	11.405	0.109	52.712	0.189	2.55 2.56	2.50 2.40	2.10 2.15	2.08 2.16	2.01 1.92	1.58 1.62	1.52 1.57	1.41 1.27	0.59 0.65	0.20 0.16	0.19
4330	29.05	276.7	2.90 2.86	12.775	0.125	53.212	0.206	2.87 2.88	2.80 2.70	2.36 2.42	2.33 2.41	2.26 2.16	1.78 1.82	1.70 1.76	1.58 1.42	0.66 0.73	0.22 0.18	0.21
4331	30.31	278.5	2.99 2.96	13.194	0.130	53.558	0.212	2.96 2.98	2.89 2.79	2.44 2.50	2.41 2.49	2.34 2.23	1.84 1.88	1.76 1.83	1.64 1.47	0.68 0.75	0.23 0.18	0.21

TABLE III.—Continued.

(d) Concluded.

Run	$\dot{w}$, g/s	T_o, K	P_o, MPa	$P_{R,o}$	G_R	$T_{R,o}$	P_B, MPa	Pressure at pressure tap locations 1 to 10, MPa										P_e, MPa
								P_1	P_2	P_3	P_4	P_5	P_6	P_7	P_8	P_9	P_{10}	
4341	9.62	280.4	1.06 1.04	4.674	0.041	53.923	0.121	1.04 1.04	1.02 0.97	0.83 0.86	0.83 0.88	0.81 0.78	0.64 0.65	0.61 0.64	0.57 0.52	0.24 0.27	0.13 0.12	0.12
4342	15.39	283.8	1.64 1.61	7.211	0.066	54.577	0.143	1.62 1.62	1.57 1.51	1.31 1.35	1.30 1.37	1.26 1.21	1.00 1.02	0.96 0.99	0.89 0.81	0.38 0.42	0.15 0.14	0.14
4343	23.42	289.6	2.36 2.33	10.396	0.101	55.692	0.179	2.34 2.35	2.27 2.20	1.91 1.96	1.89 1.97	1.83 1.76	1.45 1.48	1.39 1.44	1.29 1.16	0.54 0.60	0.18 0.16	0.18
4344	38.47	296.3	3.63 3.59	15.991	0.165	56.981	0.255	3.62 3.63	3.50 3.40	2.98 3.05	2.94 3.04	2.84 2.72	2.23 2.29	2.14 2.22	1.97 1.76	0.82 0.90	0.26 0.22	0.26
4345	54.77	300.5	4.92 4.88	21.687	0.235	57.788	0.345	4.92 4.93	4.75 4.61	4.06 4.14	4.00 4.11	3.87 3.70	3.02 3.10	2.89 3.00	2.66 2.37	1.09 1.20	0.34 0.30	0.34
4346	71.92	302.6	6.27 6.22	27.639	0.309	58.192	0.441	6.28 6.29	6.06 5.90	5.20 5.30	5.12 5.25	4.94 4.73	3.84 3.94	3.68 3.82	3.36 3.00	1.37 1.51	0.44 0.38	0.44
4347	48.24	300.4	4.39 4.35	19.335	0.207	57.769	0.304	4.38 4.39	4.24 4.11	3.62 3.69	3.56 3.67	3.45 3.30	2.70 2.76	2.58 2.69	2.38 2.13	0.98 1.08	0.30 0.26	0.30
4348	26.76	297.7	2.63 2.60	11.586	0.115	57.250	0.194	2.61 2.62	2.54 2.45	2.14 2.20	2.11 2.19	2.05 1.96	1.62 1.66	1.55 1.61	1.44 1.29	0.60 0.67	0.20 0.17	0.19
4349	14.40	296.3	1.52 1.49	6.692	0.062	56.981	0.142	1.50 1.50	1.46 1.40	1.22 1.25	1.21 1.26	1.17 1.12	0.93 0.95	0.89 0.93	0.83 0.75	0.36 0.39	0.15 0.14	0.14

(e) Helium with backpressure control

Run	$\dot{w}$, g/s	T_o, K	P_o, MPa	$P_{R,o}$	G_R	$T_{R,o}$	P_B, MPa	Pressure at pressure tap locations 1 to 10, MPa										P_e, MPa
								P_1	P_2	P_3	P_4	P_5	P_6	P_7	P_8	P_9	P_{10}	
4332	36.04	283.0	3.48 3.44	15.339	0.155	54.423	0.241	3.45 3.46	3.36 3.25	2.84 2.91	2.81 2.90	2.72 2.60	2.13 2.19	2.05 2.12	1.90 1.70	0.78 0.87	0.26 0.21	0.24
4333	35.95	282.9	3.49 3.45	15.370	0.154	54.404	0.457	3.46 3.47	3.37 3.26	2.85 2.92	2.82 2.90	2.73 2.61	2.14 2.20	2.06 2.13	1.91 1.71	0.80 0.88	0.46 0.41	0.46
4334	35.87	283.4	3.49 3.45	15.366	0.154	54.500	0.565	3.46 3.47	3.37 3.26	2.85 2.92	2.82 2.91	2.73 2.61	2.15 2.20	2.06 2.13	1.91 1.71	0.83 0.88	0.57 0.52	0.56
4335	35.75	284.3	3.49 3.46	15.396	0.154	54.673	0.683	3.47 3.48	3.37 3.26	2.86 2.93	2.83 2.92	2.74 2.62	2.16 2.21	2.08 2.15	1.93 1.73	0.89 0.91	0.69 0.64	0.68
4336	35.47	285.5	3.50 3.46	15.419	0.152	54.904	0.831	3.47 3.48	3.38 3.27	2.87 2.94	2.84 2.93	2.75 2.63	2.19 2.24	2.10 2.17	1.96 1.76	0.99 0.98	0.84 0.79	0.83
4337	34.98	286.3	3.52 3.48	15.511	0.150	55.058	1.035	3.49 3.50	3.40 3.29	2.90 2.98	2.88 2.96	2.79 2.67	2.24 2.29	2.16 2.23	2.02 1.83	1.16 1.14	1.04 [illegible]	1.04

TABLE III.—Concluded.

(e) Concluded.

Run	$\dot{w}$, g/s	T_o, K	P_o, MPa	$P_{R,o}$	G_R	$T_{R,o}$	P_B, MPa	Pressure at pressure tap locations 1 to 10, MPa										P_e, MPa
								P_1	P_2	P_3	P_4	P_5	P_6	P_7	P_8	P_9	P_{10}	
4338	34.37	286.8	3.54	15.581	0.148	55.154	1.212	3.51	3.42	2.94	2.91	2.83	2.30	2.23	2.09	1.32	1.22	1.21
			3.50					3.52	3.32	3.01	3.00	2.72	2.35	2.29	1.92	1.29	1.17	
4339	33.81	287.3	3.55	15.652	0.145	55.250	1.372	3.53	3.44	2.98	2.95	2.87	2.36	2.29	2.17	1.46	1.38	1.37
			3.52					3.54	3.34	3.05	3.03	2.76	2.41	2.35	2.00	1.44	1.34	
4340	36.38	287.8	3.49	15.374	0.156	55.346	0.244	3.46	3.37	2.85	2.82	2.73	2.14	2.06	1.90	0.79	0.25	0.24
			3.45					3.47	3.26	2.92	2.91	2.61	2.20	2.13	1.70	0.87	0.21	

TABLE IV.—DATA FOR GASEOUS HELIUM

[Inlet stagnation temperature, T_o, 280 K.]

Run	Reduced inlet stagnation pressure, $P_{R,o}$	Reduced differential pressure, $P_{R,o} - P'_{R,o}$	Reduced mass flux, G_R	Reduced inlet stagnation temperature, $T_{R,o}$	Equivalent flow coefficient, C	$C\psi_Q$	$P_{R,o}/10$
4341	4.674	2.67	0.041	53.92	0.058	0.0644	0.467
4342	7.211	5.2	.066	54.58	.061	.0676	.72
4343	10.40	2.4	.101	55.69	.065	.0724	1.04
4344	16.00	14.0	.165	57.0	.070	.0779	1.60
4345	21.70	14.7	.235	57.8	.074	.0823	2.17
4346	27.60	25.6	.309	58.0	.076	.0850	2.76
4347	19.30	19.3	.207	57.7	.073	.0815	1.93
4348	11.59	9.6	.115	57.2	.067	.0750	1.16
4349	6.69	4.7	.062	57.0	.063	.0700	.67

1. Report No.	2. Government Accession No.	3. Recipient's Catalog No.
NASA TP-1848		

4. Title and Subtitle	5. Report Date
Three-Step Labyrinth Seal for High-Performance Turbomachines	June 1987
	6. Performing Organization Code 505-62-21
7. Author(s) Robert C. Hendricks	8. Performing Organization Report No. E-3186
	10. Work Unit No.
9. Performing Organization Name and Address National Aeronautics and Space Administration Lewis Research Center Cleveland, Ohio 44135	11. Contract or Grant No.
	13. Type of Report and Period Covered Technical Paper
12. Sponsoring Agency Name and Address National Aeronautics and Space Administration Washington, D.C. 20546	14. Sponsoring Agency Code

15. Supplementary Notes

Data and information contained herein were released for general use in May 1977.

16. Abstract

A three-step labyrinth seal with 12, 11, and 10 labyrinth teeth per step, respectively, was tested under static (*nonrotating*) conditions. The configuration represented the seal for a high-performance turbopump (e.g., the space shuttle main engine fuel pump). The test data included critical mass flux and pressure profiles over a wide range of fluid conditions at concentric, partially eccentric, and fully eccentric seal positions. The seal mass fluxes (leakage rates) were lower over the entire range of fluid conditions tested than those for data collected for similar straight and three-step cylindrical seals, and this conformed somewhat to expectations. However, the pressure profiles for the eccentric positions indicated little, if any, direct stiffness for this configuration in contrast to significant direct stiffness reported for the straight and three-step cylindrical seals over the range of test conditions. Seal dynamics depend on geometric configuration, inlet and exit parameters, fluid phase, and rotation. The method of corresponding states was applied to the mass flux data, which were found to have a pressure dependency for helium. Data for helium corresponded to the parahydrogen and nitrogen data but required an empirical correction for reduced pressure. In comparison with the straight and three-step cylindrical seals the three-step labyrinth seal offers the poorest dynamic stability and the lowest forces for restoring an out-of-balance dynamic shaft to the concentric position.

17. Key Words (Suggested by Author(s))	18. Distribution Statement
Seals; Turbomachines, Fluid mechanics; Space shuttle main engine; Dynamics; Instability	Unclassified – unlimited STAR Category 34

19. Security Classif. (of this report)	20. Security Classif. (of this page)	21. No of pages	22. Price*
Unclassified	Unclassified	74	A04